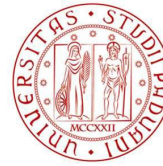


REPUBLIC OF CAMEROON
REPUBLIQUE DU CAMEROUN



DEPARTMENT OF CIVIL ENGINEERING
DEPARTEMENT DE GENIE CIVIL

MINISTRY OF HIGHER EDUCATION
MINISTERE DE L'ENSEIGNEMENT SUPERIEUR



UNIVERSITÀ
DEGLI STUDI
DI PADOVA

DEPARTMENT OF CIVIL, ARCHITECTURAL
AND ENVIRONMENTAL ENGINEERING

**SEISMIC RESPONSE OF A STEEL
COMPOSITE BRIDGE CONSIDERING A FRAME
SCHEME: CASE OF A CONCEIVED THREE
SPANS FRAME BRIDGE**

*Master thesis / Mémoire de fin d'études
In order to obtain a / En vue de l'obtention du
Master in Engineering in Civil Engineering / Diplôme d'Ingénieur de Génie Civil*

Presented by / Présenté par

MBA NZOKOU Steve De Valère
Student number: 16TP21182

Supervised by / Supervisé par

Prof. Eng. Carmelo MAJORANA
Full Professor of Structural Mechanics – University of Padova, DICEA, Italy

Co-supervised by / Co-supervisé par

Dr. Eng. Guillaume Hervé POH'SIE
*Assistant Professor of Structural
Engineering, ENSTP - Ydé*

Dr. Eng. Emanuele MAJORANA
*Assistant Professor of Structural
Engineering, University of Padova,
DICEA, Italy*

Defended on July 20, 2022 in front of the jury composed of:

President: Pr. NKENG George ELAMBO
Examiner: Dr. WOUNBA Jean François
Reporter: Dr. POH'SIE Guillaume Hervé

Academic year / Année académique
2020/2021

DEDICATION

To my mother

FOTSING MATSINDJOU Marcelle Blanche

ACKNOWLEDGMENTS

This thesis is the result of combined direct and indirect contributions of numerous individuals whose names may not all be mentioned. Their contributions are wholeheartedly appreciated and indebtedly acknowledged. Nonetheless, it is with respect and pleasure that I address my thanks to:

- The President of the jury, **Prof. NKENG George ELAMBO** for the honour of accepting to preside this jury;
- The Examiner of the jury, **Dr. Jean François WOUNBA** for accepting to make criticisms aimed at ameliorating this work;
- The Director of the National Advanced School of Public Works (NASPW), **Prof. NKENG George ELAMBO** and **Prof. Eng. Carmelo MAJORANA** of the University of Padua, Italy who are the principal supervisors of this Master's in Engineering (MEng) curricula at NASPW in partnership with the University of Padua;
- The Head of the Department of Civil Engineering, **Prof. MBESSA Michel** for his tutoring, advice and availability;
- My supervisors **Prof. Eng. Carmelo MAJORANA**, **Dr. Eng. Emanuele MAJORANA** and **Dr. Eng. Guillaume Hervé POH'SIE** for the guidance, criticisms and availability throughout the making of this work;
- The **teaching staff** of the **NASPW** and the **University of Padua** for their quality teaching and motivational skills;
- The **administrative staff** of the **NASPW** for their sense of professionalism,
- My parents, **MBA Joseph** and **FOTSING MATSINDJOU Blanche Marcelle** and my aunt **FOTSING KENGNE Apolline Beatrice** who offered unconditional love, invaluable educational facilities, guidance and support;
- My junior brother **Christ Nathanael** and my junior sisters **Ange Lucas** and **Emilie Carelle** for the moments of joy, happiness and for their love and affection since my childhood;
- The whole **FOTSING** families for the moral, social and financial support;
- My friends **Ariel BITCHEBE**, **Delano WOUNBA**, **Barnabas INROMBE** for all the great, moral support and special time spent together.

LIST OF ABBREVIATIONS

AASHTO	American Association of State Highway and Transportation Officials
ADRS	Accelerate Displacement Response Spectrum
ATC	Applied Technology Council
CP	Collapse Prevention
CQC	Complete Quadratic Equation
EC	Eurocode
ERS	Earthquake Resisting Systems
ESDOF	Equivalent Single Degree of Freedom
FEMA	Federal Emergency Management Agency
IO	Immediate Occupancy
LS	Life Safety
MDOF	Multiple Degree of Freedom
NEHRP	National Earthquake Hazards Reduction Program
PGA	Peak Ground Acceleration
RSA	Response Spectrum Analysis
SDOF	Single Degree of Freedom
SLS	Serviceability Limit State
SRSS	Square Root of Sum of the Squares
SSI	Soil-Structure Interaction
TS	Tandem System
UDL	Uniform Distributed Load
ULS	Ultimate limit state

LIST OF SYMBOLS

α	Post-elastic stiffness
β_{eff}	Effective damping
γ_d	Dynamic factors
γ_{M2}	Partial safety factor
$\gamma_{R,p}$	Factor to reflect local uncertainties of the structure
γ_s	ULS factor
γ_v	Partial factor
$\Delta\alpha_j$	Horizontal force increment
$\Delta F_{i,j}$	Horizontal load increments
ε	Thermal coefficient
ε_{cd}	Dry shrinkage strain
ε_{ca}	Autogeneous shrinkage
ζ_i	Shape factor
$\theta_{p,E}$	Plastic rotation demand
$\theta_{p,u}$	Plastic rotation capacity
μ_d	Ductility demand factor
$\bar{\lambda}$	Slenderness ratio
ξ_{eq}	Equivalent damping
ρ	Air density
ρ_t	Creep coefficient
ρ_0	Reference reinforcement ratio
σ_c	Stress in concrete

$\sigma_{up,slab}$	Stress at slab upper section
$\sigma_{low,slab}$	Stress at slab lower section
$\sigma_{up,steel}$	Stress at steel upper section
$\sigma_{low,steel}$	Stress at steel lower section
σ_s	Stress in steel
τ_b	Shear stress per meter
χ	Reduction factor
ψ_L	Creep multiplier
a_g	Design ground acceleration
A_c	Slab area
A_{id}	Area of ideal mixed section
A_{net}	Net cross section area
A_v	Resisting shear area
b_{eff}	Effective width
c_{dir}	Directional factor
c_f	Force coefficient
c_o	Orography coefficient
c_r	Roughness coefficient
c_{season}	Season factor
d	Diameter of the shank of the stud
d_E	Design demand displacement
d_{Ee}	Demand displacement
d_{tot}	Total depth of the structural element
$E_{c,eff}$	Reduced modulus of elasticity for concrete

E_{cm}	Concrete elastic modulus
f_u	Specified ultimate tensile strength of the material of the stud
F_w	Wind force
f_{yk}	Characteristic yield stress
g	Gravitational acceleration
$G1$	Structural loads
$G2$	Non-structural loads
h_s	Overall nominal height of the stud
i	Radius of gyration
I_v	Turbulence intensity
J_{cr}	Moment of inertia of the cracked section
J_{id}	Moment of inertia of ideal mixed section
J_{un}	Moment of inertia of the gross section of the uncracked pier
k_t	Turbulence factor
L_{cr}	Buckling length
M_{Ed}	Design value of the bending moment
$M_{pl,Rd}$	Plastic moment resistance
M_{Rd}	Design ultimate moment
n_L	Modular ratio at infinite time
n_0	Modular ratio for the short-term loading
N_{Ed}	Design value of the compression force
$N_{b,Rd}$	Buckling resistance
$N_{pl,Rd}$	Plastic shear resistance
P_{Rd1}	Stud resistance

P_{Rd2}	Concrete resistance
q	Behaviour factor
q_p	Peak velocity pressure
r	Air density
S_a	Spectral acceleration
S_{a0}	Elastic spectrum acceleration with 5% viscous damping
$S_{a\beta}$	Elastic spectrum acceleration with viscous damping
S_d	Spectral displacement
$S_d(T)$	Design spectrum
$S_e(T)$	Elastic response spectrum
T	Period
T_B	Lower limit of period of the constant spectral acceleration branch
T_C	Upper limit of the period of the constant spectral acceleration branch
T_D	Value defining the beginning the constant displacement response range of the spectrum
$T_{e,max}$	Maximum uniform bridge temperature
$T_{e,min}$	Minimum uniform bridge temperature
T_{eff}	Effective period
T_{max}	Maximum shade air temperature
T_{min}	Minimum shade air temperature
T_o	Initial bridge temperature
v_b	Basic wind velocity
$v_{b,o}$	Characteristic speed of the site
$V_{b,Rd}$	Shear buckling resistance
V_{Ed}	Design value of the shear force

v_m	Mean wind velocity
$V_{pl,Rd}$	Design plastic shear resistance
$W_{low,slab}$	Resistance modulus relative to slab lower section
$W_{low,steel}$	Resistance modulus relative to steel lower section
$W_{up,slab}$	Resistance modulus relative to slab upper section
$W_{up,steel}$	Resistance modulus relative to steel upper section
y_{id}	Coordinate y of gravity centre
z_0	Roughness length

ABSTRACT

The main objective of this work was to analyse the response of a steel composite frame bridge against a seismic action of PGA equal to 1.39g. To achieve this, a literature review was done in order to have a view on some bridge structural typologies, seismic failures mechanisms and methods of analysis. The methodology used, consisted in defining the procedures, loading and analysis with the European standard and FEMA regulations. The case study which is a three spans frame bridge was designed statically. The static loads acting on the bridge have been evaluated in order to perform static analysis and verifications have been done according to Eurocodes norms. The method used in the seismic design varied as to whether the nonlinearity of the materials is considered and can be static or dynamic. From this method, the nonlinear static analysis was put into practice. The modelling of the structure was done, using the software Midas Civil 2022 (version 1.2). Other aspects associated to the analysis was explored, such as the modelling of the inelastic behaviour of structural elements, mass and adopted static load pattern. The ductile capacity of the structure was analysed in the form of the capacity curve, which reproduces the variation of deformability with the increment of lateral loads, exploring the behaviour of the structure. From this plot, conclusions were drawn regarding the possible oversizing of the structure. With the response spectrum and the capacity curve, the performance point and the performance level of the structure was obtained. Then an additional analysis considering the ductile behaviour of the superstructure was carried out, in order to verify the importance of the influence of the girders in the seismic response. The results showed that the bridge in the longitudinal direction were able to develop more ductile mechanisms compare to the transverse direction. For the earthquake in question, the structure was almost entirely in the elastic branch at the performance point. When considering a ductile superstructure prior to an essentially elastic superstructure, it was noticed that in the longitudinal direction, the bridge has collapsed due to the failure of the girders, the piers was still having a residual stiffness to sustain actions after the capacity displacement was reached. The plastic hinges were formed in the top and bottom of the piers and at the connection between the piers and girders, which illustrated the various critical regions of the bridge.

Keywords: Frame bridge, nonlinear behaviour, response spectrum, seismic demand, pushover analysis, capacity curve, plastic hinge, performance point.

RESUME

L'objectif principal de ce travail était d'analyser la réponse d'un pont à portiques en acier contre une action sismique avec une accélération maximale du sol égal à 1.39g. Pour ce faire, une recherche bibliographique a été effectuée afin d'avoir une vue sur certaines typologies structurelles de ponts, les mécanismes de défaillances sismiques et les méthodes d'analyse. La méthodologie utilisée, a consisté à définir les procédures, le chargement et l'analyse avec la norme Eurocode et les règlements FEMA. L'étude de cas, qui est un pont à trois travées, a été conçue de manière statique. Les actions statiques agissant sur le pont ont été évaluées afin d'effectuer une analyse statique et des vérifications ont été faites selon les normes Eurocodes. La méthode utilisée pour l'analyse sismique varie selon que la non-linéarité des matériaux est prise en compte et peut être statique ou dynamique. A partir de cette méthode, l'analyse statique non-linéaire a été mise en pratique. La modélisation de la structure a été réalisée à l'aide du logiciel Midas Civil 2022 (version 1.2). D'autres aspects associés à l'analyse ont été explorés, tels que la modélisation du comportement inélastique des éléments structurels, la masse et le modèle de charge statique adopté. La capacité ductile de la structure a été analysée sous la forme de la courbe de capacité, qui reproduit la variation de la déformabilité avec l'incrément des charges latérales, explorant le comportement de la structure. A partir de ce tracé, des conclusions ont été tirées concernant le surdimensionnement éventuel de la structure. Avec le spectre de réponse et la courbe de capacité, le point de performance et le niveau de performance de la structure ont été obtenus. Ensuite, une analyse supplémentaire considérant le comportement ductile de la superstructure a été effectuée, afin de vérifier l'importance de l'influence des poutres dans la réponse sismique. Les résultats ont montré que le pont dans la direction longitudinale était capable de développer des mécanismes plus ductiles que dans la direction transversale. Pour le séisme en question, la structure était presque entièrement dans la branche élastique au point de performance. En considérant une superstructure à comportement ductile avant une superstructure à comportement essentiellement élastique, il a été remarqué que, dans la direction longitudinale, le pont s'est effondré en raison de la rupture des poutres et les piles avaient encore une rigidité résiduelle pour soutenir les actions après que le déplacement de capacité ait été atteint. Les rotules plastiques se sont formées au sommet, au bas des piles et à la connexion entre les piles et les poutres, ce qui illustre les différentes régions critiques du pont.

Mots clés : Pont portiques, comportement non linéaire, spectre de réponse, demande sismique, analyse pushover, courbe de capacité, rotule plastique, point de performance.

LIST OF FIGURES

Figure 1.1. Batchenga – Ntui bridge (direct-info.net)	6
Figure 1.2. Bridge over the highway between Padova and Venezia (Google maps)	7
Figure 1.3. Aerial view of the bridge over the highway in Italy (Google maps)	7
Figure 1.4. Multi-girder composite bridges, Lagentium Viaduct (steelconstruction.info).....	8
Figure 1.5. Seismic behaviour (Kolias et al., 2008)	10
Figure 1.6. Ductile Substructure system allowing Plastic Hinges (midasbridge.com)	11
Figure 1.7. Allowable Earthquake-Resisting System (AASHTO Guide Specification for Seismic Bridge Design).....	12
Figure 1.8. Simple SDOF structure with applied incrementally increasing lateral forces (midasbridge.com).....	16
Figure 1.9. Pushover curve from the SDOF system (midasbridge.com).....	17
Figure 1.10. Equivalent secant effective stiffness and performance point definitions (Davi, 2014).....	18
Figure 1.11. Moment-curvature analysis and distribution over the pier’s height, from EC8-2 (Kolias et al., 2008)	22
Figure 1.12. General flowchart for Nonlinear Static Procedure (S. R.Bento, 2004).....	23
Figure 1.13. Response Spectrum Conversion (ATC-40, 1996).....	25
Figure 1.14. Capacity Curve (Applied Technology Council, 1996)	26
Figure 1.15. Idealized Force-Displacement Curves (Applied Technology Council, 2005) ...	26
Figure 1.16. Capacity Curve transformed into a Capacity Spectrum (Applied Technology Council, 1996)	27
Figure 1.17. Bilinear representation of capacity spectrum (Applied Technology Council, 2005)	28
Figure 1.18. Bilinear representation of capacity spectrum(Applied Technology Council, 2005)	30
Figure 1.19. Idealized force-displacement curve for nonlinear static analysis (Applied Technology Council, 2005).....	31
Figure 1.20. 1995 Kobe earthquake (ENSTP, 2021).....	36
Figure 1.21. Insufficient confinement of columns (Northridge, California 1994).....	37
Figure 1.22. Insufficient number of stirrups for shear (Hanshin expressway, Kobe, 1995) ..	37
Figure 2.1. Preliminary design data (SETRA, 2010)	40
Figure 2.2. Correlation between minimum/maximum shade air temperature and minimum/maximum uniform bridge temperature component (EN 1991-1-5, 2011).....	44
Figure 2.3. Effective width of composite deck.....	50
Figure 2.4. Influence length diagram.....	50

Figure 2.5. Mixed section with local axis (Self-made).....	51
Figure 2.6. Force-displacement or moment-rotation curve for a hinge definition used in Midas Civil (plastic deformation curve).....	66
Figure 3.1. Longitudinal view of the bridge model.....	69
Figure 3.2. Isometric view of the bridge model	69
Figure 3.3. Steel frame composite bridge.....	70
Figure 3.4. Transversal section of the deck.....	71
Figure 3.5. Bridge elevation	71
Figure 3.6. Locations of stress computation.....	80
Figure 3.7. Isometric view (Mode 1).....	93
Figure 3.8. Plan View (Mode 1).....	93
Figure 3.9. Isometric view (Mode 5).....	93
Figure 3.10. Elevation view (Mode 5).....	94
Figure 3.11. Seismic zonation of Italy (Conference & Engineering, 2004).....	96
Figure 3.12. Design response spectrums	97
Figure 3.13. Steel bilinear model	100
Figure 3.14. Steel trilinear model	100
Figure 3.15. FEMA hinge model.....	101
Figure 3.16. Capacity curve obtained for the uniform shape distribution in the longitudinal direction (FEMA)	102
Figure 3.17. Capacity curve obtained for the uniform shape distribution in the transverse direction (FEMA)	103
Figure 3.18. Capacity curve obtained for the modal shape distribution in the longitudinal direction (FEMA)	103
Figure 3.19. Capacity curve obtained for the uniform shape distribution in the transverse direction (FEMA)	104
Figure 3.20. Plastic hinges at step 15	106
Figure 3.21. Plastic hinges at step 17	106
Figure 3.22. Plastic hinges at step 23	107
Figure 3.23. Plastic hinges at step 36	107
Figure 3.24. Plastic hinges at step 36	107
Figure 3.25. Plastic hinges at step 45	108
Figure 3.26. Plastic hinges at step 32	108
Figure 3.27. Plastic hinges at step 43, type B.....	109
Figure 3.28. Plastic hinges at step 43, type IO	109
Figure 3.29. Final plastic hinges pattern	109
Figure 3.30. Performance point for uniform loading in the longitudinal direction.....	111

Figure 3.31. Performance point for uniform loading in the transverse direction	112
Figure 3.32. Performance point for modal loading in the longitudinal direction.....	113
Figure 3.33. Performance point for modal loading in the transverse direction	114
Figure 3.34. Localization of the performance point (case study) accordingly to performance level (ATC-40, 1996)	115
Figure 3.35. Plastic hinges at step 10	116
Figure 3.36. Plastic hinges at step 15	117
Figure 3.37. Plastic hinges at step 16	117
Figure 3.38. Plastic hinges at step 29	117
Figure 3.39. Plastic hinges at step 39	118
Figure 3.40. Final plastic hinge pattern	118
Figure 3.41. Capacity curve for the uniform loading	119
Figure 3.42. Capacity curve for the modal loading	119
Figure 3.43. Performance point for the uniform loading.....	120
Figure 3.44. Performance point for the modal loading	121

LIST OF TABLES

Table 2.1. Multipliers for the characteristic values of variable loads (EN 1991-2, 2003)	41
Table 2.2. Characteristic values of load model 1 (EN 1991-2, 2003)	41
Table 2.3. Values of adjustment factors	42
Table 2.4. Assessment of groups of traffic loads (EN 1991-2, 2003)	42
Table 2.5. Temperature differences for bridge decks type 2: composite decks (EN 1991-1-5, 2011)	45
Table 2.6. Shrinkage components	46
Table 2.7. FEMA 450 and EC8-1 correspondence	47
Table 2.8. Partial safety factors for ULS combination	49
Table 2.9. Multipliers for the characteristic values of variable loads	49
Table 2.10. Geometric characteristics of mixed-section	51
Table 2.11. Stress calculation	52
Table 2.12. Maximum width-to-thickness ratios for compression parts (EN 1993-2, 2011)	53
Table 3.1. Characteristics of concrete	72
Table 3.2. Characteristics of steel reinforcement	72
Table 3.3. Material of structural steels elements	73
Table 3.4. Girder geometry	74
Table 3.5. Pier's geometry	74
Table 3.6. Self-weight of structural elements	75
Table 3.7. Self-weights of non-structural elements	75
Table 3.8. Shrinkage computation	75
Table 3.9. Load values for group 1a	76
Table 3.10. Coefficients of wind	76
Table 3.11. Wind load computation	77
Table 3.12. Temperature load calculation	77
Table 3.13. Loads combinations	78
Table 3.14. Loads description	78
Table 3.15. Mixed-section characteristics at $t=0$	79
Table 3.16. Mixed-section characteristics at $t=\infty$	79
Table 3.17. Stress verification at section 1	81
Table 3.18. Stress verification at section 2	82
Table 3.19. Stress verification at section 3	83
Table 3.20. Stress verifications at section 1 (phase 2)	84

Table 3.21. Stress verifications at section 2 (phase 2).....	85
Table 3.22. Stress verifications at section 2 (phase 2).....	86
Table 3.23. Web classification	87
Table 3.24. Flanges classification.....	87
Table 3.25. Verification of shear resistance	88
Table 3.26. Buckling resistance of section 2	88
Table 3.27. Pier section classification	88
Table 3.28. Bending resistance of the piers.....	89
Table 3.29. Resistance to compression.....	89
Table 3.30. Buckling resistance verification	89
Table 3.31. Shear verifications	89
Table 3.32. Classification of transversal cross beam sections.....	90
Table 3.33. Bending resistance of the cross beams	90
Table 3.34. Frequency and periods of the first 15 modes.....	91
Table 3.35. Modal participation ratios.....	91
Table 3.36. Seismic zonation criteria and reference horizontal peak ground acceleration (Conference & Engineering, 2004)	95
Table 3.37. Seismic parameters.....	96
Table 3.38. Design seismic displacement.....	98
Table 3.39. Performance point for uniform loading in the longitudinal direction	111
Table 3.40. Performance point for uniform loading in the transverse direction	111
Table 3.41. Performance point for modal loading in the longitudinal direction	112
Table 3.42. Performance point for modal loading in the transverse direction	113

TABLE OF CONTENTS

DEDICATION	i
ACKNOWLEDGMENTS.....	ii
LIST OF ABBREVIATIONS	iii
LIST OF SYMBOLS.....	iv
ABSTRACT	ix
RESUME	x
LIST OF FIGURES.....	xi
LIST OF TABLES	xiv
TABLE OF CONTENTS	xvi
GENERAL INTRODUCTION	1
CHAPTER 1: LITERATURE REVIEW.....	3
Introduction.....	3
1.1 Steel	3
1.1.1 Steel typologies	3
1.1.2 Properties of steel.....	4
1.1.3 Applications of steel.....	5
1.2 Steel-concrete composite deck road bridges.....	5
1.3 Bridge structural typology	6
1.3.1 Rigid-frame bridges	6
1.3.2 Beam bridges.....	7
1.4 Seismic design of bridges	8
1.4.1 Basic principles of the bridge seismic design according to Eurocode 8-28	
1.4.2 Seismic load resisting systems.....	10
1.4.3 Methods of analysis	14
1.4.4 Pushover analysis methodology.....	22
1.4.5 Bridges seismic damages	34

Conclusion.....	38
CHAPTER 2: METHODOLOGY.....	39
Introduction.....	39
2.1 Conception.....	39
2.1.1 Codes.....	39
2.1.2 Preliminary design	40
2.1.3 Loads actions.....	40
2.2 Static design methodology.....	49
2.2.1 Effective width of mixed section	50
2.2.2 Geometric mixed section characteristics.....	50
2.2.3 Ultimate limit state.....	52
2.3 Numerical modelling	58
2.3.1 Steel composite frame bridge modelling	58
2.3.2 Midas Civil description.....	58
2.4 Seismic study	59
2.4.1 Response spectrum analysis.....	59
2.4.2 Results obtained from Midas Civil	61
2.5 Pushover analysis.....	62
2.5.1 Pushover analysis model in Midas Civil.....	62
2.5.2 Pushover global control definition.....	63
2.5.3 Pushover Load Cases	63
2.5.4 Nonlinear behaviour definition of the elements.....	64
Conclusion.....	67
CHAPTER 3: RESULTS AND INTERPRETATIONS.....	68
Introduction.....	68
3.1 Presentation of the case study	68
3.1.1 Bridge geometry and structural solution.....	68
3.1.2 Statistical data	71

3.2	Structural analysis of the steel frame bridge.....	73
3.2.1	Preliminary design of structural elements.....	73
3.2.2	Loads computation.....	74
3.2.3	Load combinations.....	78
3.2.4	Verification at Ultimate Limit State.....	79
3.3	Eigen-value analysis	90
3.4	Seismic analysis.....	94
3.4.1	Response spectrum analysis.....	95
3.4.2	Pushover analysis.....	99
3.4.3	Performance point.....	110
3.4.4	Analysis of the bridge considering the ductile superstructure	115
	Conclusion.....	121
	GENERAL CONCLUSION.....	123
	BIBLIOGRAPHY	125
	WEBOGRAPHY.....	127
	ANNEXES	I
	ANNEX A: System deformation capacity of steel substructures (AASHTO GUIDE)	I
	Annex A.1 Five regions of expected performance and damage for steel.....	I
	Annex A.2 Areas of potential inelastic deformations in steel substructure.....	I
	ANNEX B: Seismic response with bilinear hinge type.....	II
	Annex B.1 Sequential plastic hinge formation in the longitudinal direction	II
	Annex B.2 Sequential plastic hinge formation in the transverse direction.....	III
	Annex B.5 Performance point in the longitudinal direction.....	IV
	Annex B.6 Performance point in the transverse direction.....	IV
	ANNEX C: Seismic response with trilinear hinge type	V
	Annex C.1 Sequential plastic hinge formation in the longitudinal direction	V
	Annex C.2 Sequential plastic hinge formation in the longitudinal direction	VI

Annex C.5 Performance point in the longitudinal direction.....	VII
Annex C.6 Performance point in the transverse direction.....	VII
ANNEX D: Seismic source regions in Cameroon (Open Journal of Earthquake Research, 2014)	VIII

GENERAL INTRODUCTION

In recent decades, the world has experienced several medium to large earthquakes, which have affected several countries, causing very large human and material losses. The level of performance of some structures during these earthquakes was low, and beyond that the level of structural damage was very high. This has resulted in the need to determine and assess the damage in the structures more than ever, the insufficiency of classical linear elastic methods encouraged researchers to develop new generations of seismic analysis and design methods, among which pushover analysis.

Pushover analysis is a nonlinear static analysis design to study the vulnerability of existing structures to earthquake. It is based on the time tracking of plastic formation of plastic hinges in a structure subjected to increasing vertical and lateral loading (earthquake) until collapse. The various results obtained allow the vulnerability of the structure to be assess. In the majority of recent seismic codes, in Europe and in the USA, the inelastic response of structures is determined by using pushover methods, such as the capacity spectrum method, the N2 method, the displacement coefficient method.

One of the major concerns of today's society is the preservation of human life and, consequently, the integrity of the structures sustaining them. As such, due to the great importance of bridges, it is essential to ensure that they can resist seismic actions, absorbing the energy that is transmitted through the ground without collapsing and allowing damages to be easily repaired.

The key objective of this thesis is to investigate the behaviour of a steel composite frame bridge under seismic loads using a pushover analysis with the software MIDAS/Civil. More precisely, it concerns the definition and formulation of the pushover method, as well as the application of the pushover method techniques, proposed in the international codes for the determination of inelastic responses of bridges, resulting from seismic motion.

In order to achieve this objective, this thesis is divided in three main axes hereafter outlined. The first chapter is focused on a general view on bridge structural typologies, seismic failures mechanisms and methods of analysis. The second chapter is focused on methodology. Here, the approach used in loads determination and static verifications shall be discussed. Next, a presentation of seismic analysis procedure will be done, as well as method used to define plastic hinges on frame bridge for illustration of failure mechanisms. At the end, in the third chapter which is the presentation of our results and their interpretations, the case study

will be detailed first. Secondly, static analysis and corresponding verifications will follow. The third point concerns the effects of seismic loads on steel frame bridge, and a comparative analysis will be done for different loading scenarios considered. Finally, girders collapse scenario will be checked, performance level and critical regions of the bridge will be evaluated.

CHAPTER 1: LITERATURE REVIEW

Introduction

Bridges are important structures in modern highway and transportation systems. Bridge engineering is a field of engineering dealing with the surveying, plan, design, analysis, construction, management, and maintenance of bridges that support or resist loads. Structural conception of bridges is strictly related to function, aesthetics and economics than in any other type of structures (Smith et al., 1986). Therefore, bridges give the impression of being simple structures whose seismic response could be easily predicted. Seismic calculation of bridge structures in active seismic areas is a significant part of the overall calculations with the aim of proving the mechanical resistance and stability. Seismic bridge design is of special importance because its serviceability during and after the earthquake depends on it. This chapter is meant for a thorough explanation of the theory underneath these concepts to ease the understanding of subsequent works. As such, the chapter starts by discussing the steel typologies right up to its application in bridge engineering passing through its properties. The next part discusses the structure and typology of a steel-concrete composite deck road bridges. Then comes the section on bridge structural typology to help understand the load transfer path and suitable range of application of various bridges structural form. Procedure of the seismic calculation and damage of bridge structures are discussed at the end of this chapter.

1.1 Steel

1.1.1 Steel typologies

Steel can be separated into low alloy and high alloy steel. More so, it can be further distinguished into low alloy with varying carbon contents, tool steel and stainless steel.

1.1.1.1 Plain carbon (low alloy) steel

Plain carbon steel is an alloy of iron and carbon with carbon content ranging from 0.15% to 1.5% with no more than 0.5% of silicon and 1.5% of manganese (Gorenc et al., 2012).

1.1.1.2 Tool steel

Tool steel is a variety of steel with a carbon content between 0.7% and 1.5%. They are adequate to be made into tools due to their distinctive hardness, abrasion resistance, their ability to hold a cutting edge, and/or their resistance to deformation at elevated temperatures. Also, tool steel with higher ratios of vanadium is more resistant to corrosion.

1.1.1.3 Stainless steel

Stainless steel differs from carbon steel by the high amount of chromium present. With about 18% of chromium, stainless steel does not readily corrode, rust or stain with water as ordinary steel does. Despite the name, it is not fully stain-proof, most notably under low oxygen, high-salinity, or poor circulation environments. They are used where both the properties of steel and corrosion resistance are required.

1.1.2 Properties of steel

1.1.2.1 Chemical properties

Steel is an extremely versatile material available in a very wide range of properties and chemical compositions to suit every field of technology (BRANKO E. et al., 2012). Carbon makes steel harder than pure iron due to the carbon atoms which makes it more difficult for dislocations in the iron crystal lattice to slide past each other. Also, steel contains additional elements, either as impurities or added to provide desirable properties. Most steel contains manganese, phosphorus, sulphur, silicon, and trace amounts of aluminium, oxygen, and nitrogen.

1.1.2.2 Physical properties

The amount of steel variation does not look significant, because carbon never makes up more than 1.5% of steel. Thus, most steels have a density of about 7,850 kg/m³, making them 7.85 times denser than water. Also, their melting point of 1,510°C is higher than that of most metals and their coefficient of linear expansion, at 20°C, of 11.1µm/m°C makes them more resistant to changing size with changes in temperature.

1.1.2.3 Mechanical properties

Steel's mechanical properties are obtained through a combination of chemical composition, heat treatment and manufacturing processes. The main constituent of steel is iron, but the addition of very small quantities of other elements can have a significant effect on the properties of the steel. The strength of steel can be increased by the addition of alloys such as manganese, niobium and vanadium. The addition of these alloys can also greatly affect other properties, such as ductility, toughness and weldability (BSCA Limited, 2010).

Thus, the main mechanical properties of steel are:

- Strength;
- Toughness;
- Ductility;

- Weldability;
- Durability.

1.1.3 Applications of steel

Steel is a versatile and effective material able to carry loads in tension, compression and shear. Its high strength-to-weight ratio implies a minimum structural weight of superstructures and thus minimises the cost of substructures. Also, steel's low self-weight positively impacts the cost of transporting and handling its components.

Thus, steel is used as beams, steel frames, columns, bars, plate girders in warehouses, aircraft hangers, bridges, residential and commercial buildings so as to provide economic solutions to the demands of safety, shallow construction depth, rapid construction, and minimal maintenance and flexibility in future use. Steel structures are also widely used in the mining, transportation, ship and aeronautics sectors. Steel scores well on all the sustainability measures and offers a broad range of benefits addressing the economic, environmental, and social priorities of sustainability.

In the world, the first structural steel railroad bridge was the Eads bridge, constructed in 1874 in St. Louis, Missouri. In Cameroon, the first major bridge was built by the Germans in 1911.

1.2 Steel-concrete composite deck road bridges

Steel-Concrete composite road bridges provide an efficient and cost-effective form of bridge construction. By utilising the tensile strength of steel in the main girder and the compressive strength of concrete in the slab, the bending resistance of the combined materials is greatly increased and larger spans are made possible. Steel-Concrete composite road bridges are used as alternatives to concrete road bridges because of their ability to adapt their geometry to design constraints, possibility of reusing some of the materials in the structure and the added value they provide due to their attractive appearance (Sarraf et al., 2013). Steel-Concrete composite road bridges are very important due to the fact that they help connect one part of a country to another and support the network of product transportation that is vital to each nation. Figure 1.1 shows an example of Steel-Concrete composite road bridge found in the Republic of Cameroun.



Figure 1.1. Batchenga – Ntui bridge (direct-info.net)

1.3 Bridge structural typology

Although bridges can be classified by different methods, the bridge classification according to its structural form is still the common way. This is necessary because the structural form is the most important factor that affects the whole service life of the bridge, including design, construction, repair, and maintenance. Bridges with different structural forms have their load transfer path and suitable range of application. In general, bridges can be classified into beam bridges, rigid-frame bridges, truss bridges, arch bridges, cable-stayed bridges, and suspension bridges. In the following parts, frame bridge and beam bridges will be presented.

1.3.1 Rigid-frame bridges

A rigid-frame bridge consists of superstructure supported on vertical or slanted monolithic legs (columns), in which the superstructure and substructure are rigidly connected to act as a unit and are economical for moderate medium-span lengths. The use of rigid-frame bridges began in the early 20th century.

Rigid-frame bridges are superstructure-substructure integral structures with the superstructure which can be considered as a girder. Bridges of superstructure-substructure integral structure include brace rigid-frame bridges, V-leg rigid-frame bridges, and viaducts in urban areas. The connections between superstructure and substructure are rigid connections which transfer bending moment, axial forces, and shear forces. A bridge design consisting of a rigid frame can provide significant structural benefits but can also be difficult to design and construct. Moments at the center of the deck of a rigid-frame bridge are smaller than the corresponding moments in a simply supported deck. Therefore, a much shallower cross section at mid-span can be used. Additional benefits are that less space is required for the approaches and structural details for where the deck bears on the abutments are not necessary (Portland

Cement Association, 1936). However, as a statically indeterminate structure, the design and analysis are more complicated than that of simply supported or continuous bridges.

Example of steel frame bridge, especially the bridge over the highway between Padova and Venezia in Italy on figure 1.2 and figure 1.3.



Figure 1.2. Bridge over the highway between Padova and Venezia (Google maps)



Figure 1.3. Aerial view of the bridge over the highway in Italy (Google maps)

1.3.2 Beam bridges

Beam bridges are the most common, inexpensive, and simplest structural forms supported between abutments or piers. In its most basic form, a beam bridge is just supported at each end by piers (or abutments). The weight of the beam and other external load need to be resisted by the beam itself, and the internal forces include the bending moment and shear force. When subjected a positive bending moment, the top fibers of a beam are in compression while the bottom fibers are in tension. This is more complex than a cable only in tension or an arch mainly in compression. Therefore, only materials that can work well for both tension and compression can be used to build a beam bridge. Obviously, both plain concrete and stone

are not good materials for a beam because they are strong in compression, but weak in tension. Though ancient beam bridges were mainly made of wood, modern beam bridges can also be made of iron, steel, or concrete with the aid of prestressing. An example of continuous girder bridge that made of steel and concrete is shown in figure 1.4.



Figure 1.4. Multi-girder composite bridges, Lagentium Viaduct (steelconstruction.info)

Sometimes, the beam bridges are also classified into slab bridges, beam bridges and girder bridges. The slab bridge refers to spans without support below the deck, beam bridges represent bridges with only longitudinal support below the deck and girder bridges refer to bridges with both longitudinal and transverse structural members under the deck. However, all these three categories are classified as the same type because of their similar load transfer mechanisms (Smith et al., 1986).

1.4 Seismic design of bridges

1.4.1 Basic principles of the bridge seismic design according to Eurocode 8-2

The calculation philosophy of the seismic resistant bridges according to the Eurocodes is based on the demand that, during the period of bridge exploitation after the occurrence of earthquake of the predicted intensity, the bridge must not collapse (ultimate limit state) and that the damage (serviceability limit state) must not influence the traffic (Kolias et al., 2008). Eurocode 8-2 gives recommendations for the seismic calculation of bridges with a description of basic principles and rules which follow the basic demands of the seismic calculations presented in Eurocode 8-1. These rules are destined for construction girder bridges supported by abutments and vertical or nearly vertical piers, arch and frame bridges, and are not recommended for suspension bridges, highly curved bridges, bridges with significant longitudinal grade and skew bridges. Eurocode 8-2 also incorporates some basic rules and

principles for constructing special bridges and seismic protection of the bridges by the use of isolation devices for the purpose of reducing the seismic response.

In designing the seismic resistant structures according to the European standards aimed to assure integrity and serviceability of the bridge structure during the earthquake with foreseen intensity, special attention should be focussed on aseismic shaping of bridges. Namely, seismic conditions, especially in the areas of higher seismic intensity, are often the decisive factor for choosing the type of structure, the load-bearing system, the connections between superstructure and substructure, dimensioning of elements and reinforcement, material consumption, detailing, etc.

In seismic active areas the bridge superstructure should be designed as a continuous deck, that is to say as a statically highly indeterminate system. That means that the superstructure should have as few expansion joints as possible. As superstructure is leaned on substructure, the stiffness of abutments and piers influence the seismic forces redistribution. The dispositions of the bridges with equal pier heights are more favourable because of a more even redistribution of the seismic forces on the supporting elements which is the equalization of pier dimensions and the quantity of built-in reinforcement and equable distribution of stresses in the subsoil. Namely, the short very stiff piers as well as very high flexible piers should be avoided or expelled from the seismic forces acceptance system using flexible bearings. The first should be expelled due to the ability of accepting a greater part of the total seismic force, and the second due to the very high deformability. The ductile behaviour of bridge structure is ensured by the equalization of pier height and by making it possible to have a greater number of supporting elements to take part in the longitudinal and transverse bridge direction seismic forces acceptance with simultaneous opening of the plastic hinges in the majority of piers. The plastic hinges in piers (which are foreseen in the bottom parts) should be ensured according to the foreseen pier deformation by adequate reinforcement taking the damage into consideration which must not affect the traffic on the bridge. The eventuality of damage occurrence should be foreseen in easily accessible places due to the easy detection and repair. The opening of the plastic hinges in the bridge superstructure is not allowed. The plastic hinges will not open in the piers flexibly connected to the bridge superstructure and in the piers with the smaller stiffness compared with the other bridge piers. The bridge foundations should stay undamaged upon seismic actions (MICHAEL N. et al., 2012).

The behaviour of the bridge during an earthquake can be designed by the adequate disposition of the elastomeric bearings upon which the bridge superstructure is leaned on abutments and piers. The flexibility of the elastomeric bearings (increasing its height) causes

the prolongation of the fundamental period of the bridge and the reduction of the seismic force. At the same time, displacements of the structure are increased which causes a need for placing bigger and more expensive expansion joints or increases the number of bridge dilatations. To reduce the displacements of the structure it is possible to direct the dissipation of the seismic energy to the abutments and piers with seismic dampers. Furthermore, for leaning the superstructure on the substructure over the movable bearings it is necessary to assure the satisfactory width of the superstructure overlapping in order to prevent the falling of the bridge superstructure during extreme movements. In that case, the structure should be additionally assured by designing seismic boundary stone on the piers, i.e., by appropriate design and reinforcement of the breast abutment wall. The combination of all the aforementioned points would be the most effective in high seismic areas (F. Naeim and J. M. Kelly, 1999).

1.4.2 Seismic load resisting systems

Generally, Eurocode 8-2 recommends that the bridge shall be designed in such a way that its behaviour under the design seismic action is either ductile, or limited ductile/essentially elastic, depending on the seismicity of the site, on whether seismic isolation is adopted for its design, or any other constraints which may prevail. This behaviour (ductile or limited ductile) is characterised by the global force-displacement relationship of the structure, shown schematically in figure 1.5.

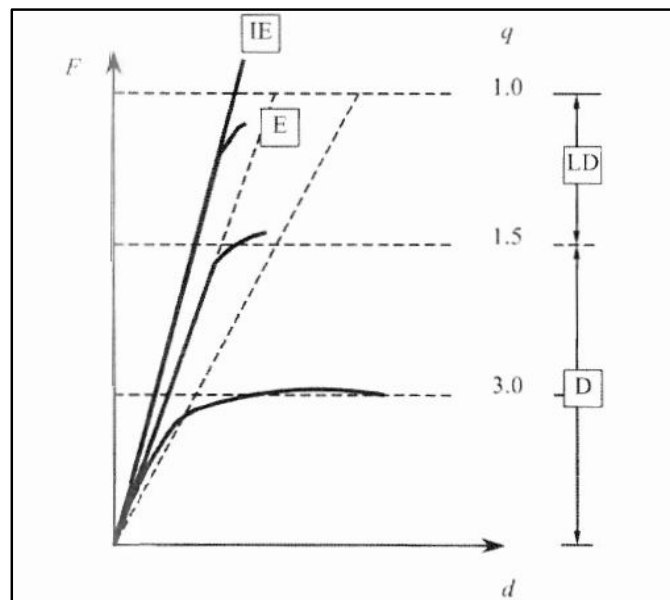


Figure 1.5. Seismic behaviour (Kolias et al., 2008)

- q – Behaviour factor;
- IE – Ideal elastic;

- E – Essentially elastic;
- LD – Limited ductile;
- D – Ductile;

1.4.2.1 Ductile seismic behaviour of bridges

In regions of moderate to high seismicity, it is usually preferable both for economic and safety reasons, to design a bridge for ductile behaviour (ductile yielding of elements to reduce the overall forces resisted by the bridge), i.e., to provide it with reliable means to dissipate a significant amount of the input energy under severe earthquakes (Eurocode 8, 2000). This is accomplished by providing for the formation of an intended configurations of flexural plastic hinges or by using isolating devices. These hinges normally form in the piers and act as the primary energy dissipating components. Plastic hinges are primarily energy dispersing elements that occur in the event of a strong earthquake. The economic savings and design protection to other elements due to plastic hinges highly outweigh the cons of dealing with repairable damages. A configuration of plastic hinges is shown on figure 1.6.

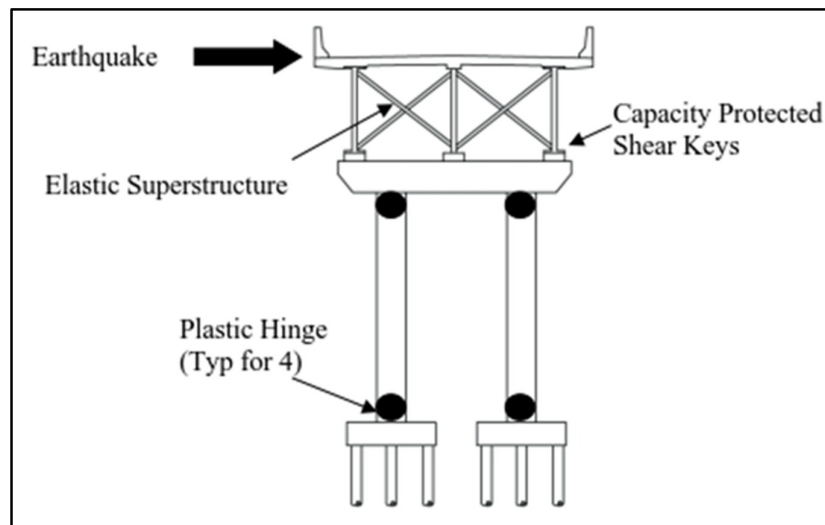


Figure 1.6. Ductile Substructure system allowing Plastic Hinges (midasbridge.com)

A plastic hinge is a section of an element where plastic bending occurs. Plastic hinges are developed when a section has exceeded its elastic capacity and has entered plastic behaviour. It should be noted that they are not true hinges and will continue to have lateral resistance up to a certain point. The plastic hinge forms after a section reach yield capacity and will be able to accommodate increased displacements under plastic behaviour, which can be a considerable amount just before the collapse (Aboubakr, 2018).

Plastic hinges are commonly considered energy-damping devices that allow increased displacement of the bridge via plastic rotation. It is permitted in various design codes,

including those using the traditional Force-Based method of design. The formation of the hinges allows plastic deformation, which in turn reduces the peak elastic seismic design force needed to be resisted by the bridge.

Although plastic hinge formation causes irreversible deformations, they are only allowed for strong seismic events with a low probability of exceedance.

In bridges design for ductile behaviour, the regions of plastic hinges shall be verified to have adequate flexural strength to resist the design seismic action effects. The shear resistance of the plastic hinges, as well as both the shear and flexural resistances of all other regions, shall be design to resist the capacity design effect. For bridges of ductile behaviour, capacity design shall be use to ensure that an appropriate hierarchy of resistance exists within the various structural components. This is to ensure that the intended configuration of plastic hinges will form and that brittle failure modes are avoided (Eurocode 8, 2000).

As far as is reasonably practicable, the location of plastic hinges should be selected at points accessible for inspection and repair. It is shown in figure 1.7, an example of an earthquake resisting systems (ERS).

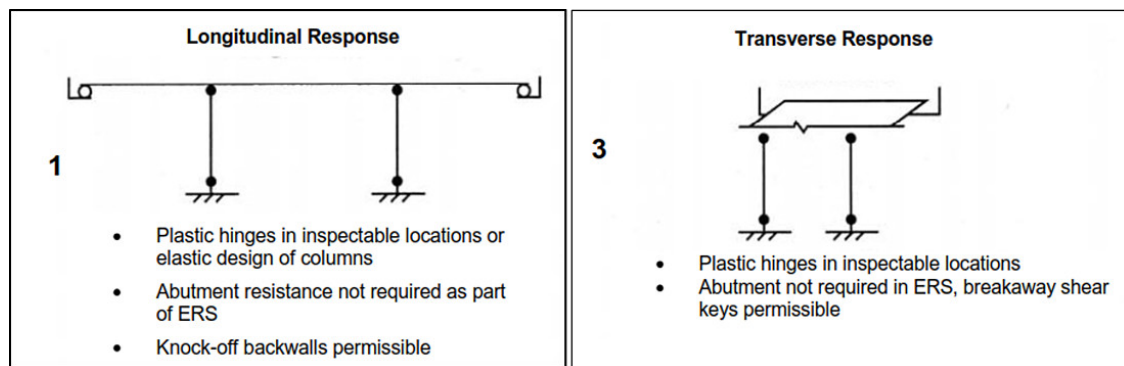


Figure 1.7. Allowable Earthquake-Resisting System (AASHTO Guide Specification for Seismic Bridge Design)

1.4.2.2 Limited-ductile seismic behaviour of bridges

It is the seismic design for strength instead of ductility. Part 2 of Eurocode 8 gives the option to design a bridge to resist the seismic action through strength alone, without explicitly resorting to ductility and energy dissipation capacity. As design seismic forces are derived with a value of the behaviour factor, q , possibly greater than 1.0, structures designed for strength and little engineered ductility and energy dissipation capacity are termed ‘limited ductile’, in lieu of ‘non-ductile’ (Kolias et al., 2008).

In structures with limited-ductile behaviour, a yielding region with signification reduction in secant stiffness need not appear under the design seismic action. In terms of force-

displacement characteristics, the formation of a force plateau is not required, while deviation from the ideal elastic behaviour provides some hysteretic energy dissipation. Such behaviour corresponds to a value of the behaviour factor $q \leq 1,5$.

1.4.2.3 Seismic isolation

Seismic isolation is used as a common way to reduce the seismic action to the structure and to prevent the structural damage. Two systems can be used: isolators and dampers. Isolators are flexible devices which reduce the stiffness of the structure and the period of the structure becomes longer. Dampers reduce seismic load according to the principle of energy dissipation.

Elastomeric bearings are frequently used as isolators to lengthen a natural period of bridges, especially viaducts. They are situated between the superstructure and columns. They have a great bearing capacity and stiffness in the vertical direction and less shear stiffness in the horizontal direction which implies the reduction of the total structural stiffness in the longitudinal and transversal direction, as well as reduction of the seismic load. An earthquake causes large horizontal displacements and deformation of the bearings. Therefore, the choice of the bearings has significant influence on the obtained results (Naeim and Kelly, 1999).

Several methods can be used for the analysis of seismically isolated bridges. The type of analysis can be linear or non-linear, while the dynamic model is single-degree of freedom or multi-degree of freedom. Eurocode 8-2 proposes the following methods for analysis of bridges: fundamental mode method, response spectrum method, alternative linear methods (power spectrum analysis, time series analysis) and nonlinear time domain analysis.

The corresponding dynamic equation in the analysis of seismic isolated bridges includes mass, damping and stiffness matrix, time, acceleration, velocity, displacement and load vectors. The change of the damping matrix, the stiffness matrix and the load vector over time depends on the applied accelerogram. The change of stiffness matrix in isolated bridges depends, not only on accelerogram, but also on the changing of elastomeric bearings stiffness. This change depends on the force in elastomeric bearings. The damping matrix in isolation systems also additionally changes due to the velocity in the bearings. The use of nonlinear models in seismic analysis of isolated bridges is necessary to obtain relevant results especially for complex bridges with large spans, the stiffness changes, dilatations, etc.

The fundamental mode method gives equivalent static seismic forces which are derived from the inertia forces corresponding to the fundamental natural period of the structure in the direction under consideration. The method includes simplifications regarding the shape of the

first mode and the estimation of the fundamental period. The method can be applied in all cases in which the dynamic behaviour of the structure can be sufficiently approximated by a single dynamic degree of freedom model.

The response spectrum method can provide an acceptable approximation if the appropriate approximation of the elastomeric bearings is applied. However, the typical behaviour of elastomeric bearings is elastoplastic (Naeim and Kelly, 1999) so it is difficult to model their characteristics by a linear model. In addition, the modulus of elasticity is different in the vertical and horizontal directions, which should be considered in numerical modelling.

1.4.3 Methods of analysis

The elastic analysis uses a linear stress-strain relationship but incorporates a correction factor (R) to permit better consideration of the nonlinear characteristics of the response.

The fundamental mode method quantifies the total seismic action in inertial forces, given by the product of the vibrating mass by the maximum seismic acceleration, which is obtained from a spectrum of inelastic accelerations for the period of vibration of an equivalent system of one degree of freedom with the same condensed stiffness and mass properties of the structure under analysis. This analysis is permitted for structures which do not have irregular structural systems. All the restrictions should be checked before applying this type of approach because it assumes continuity of the structure and distributes seismic forces along all elements of the bridge and is based on the fundamental mode of vibration in either longitudinal or transverse direction (Davi, 2014).

In the response spectrum method, the structure is not represented as one degree of freedom system (SDOF), but rather several SDOFs representing the various modes of vibration of the structure, making this procedure more accurate than the previous one. Structure, even being regular and having a symmetrical distribution of mass and rigidity, present several modes of vibration that can have greater or lesser influence in its global dynamic behaviour.

Therefore, the seismic response must attend to all the modes that influence it, combining them according to a consideration of the relative importance embodied, quantified by the modal mass they effectively mobilize. This combination of the responses of the various systems of one degree of freedom uses the method of modal combination to obtain the states of tension and deformation experienced by the structure.

In the other way, nonlinear analysis predicts the nonlinear behaviour of a structure under seismic loads. It allows to identify potential weak areas in the structure and can

demonstrate how progressive failure in bridges really occurs and identify the mode of final failure.

In a static inelastic analysis, known as pushover analysis, a structural model directly incorporating the nonlinear load-deformation characteristics of the elements is “pushed over” by a monotonically increasing lateral load representing inertia forces in an earthquake until a predetermined value or state is reached. From this analysis results a capacity curve that represents the variation of the total lateral seismic shear demand, “V” of the structure, with the lateral deflection of the bridge at the deck level. The intersection between this curve and a demand curve result in the performance point, and the project performance objectives can be judged by evaluating where the performance point falls on the capacity curve.

Time history analysis is a nonlinear dynamic analysis that reproduces the dynamic behaviour of the structures more correctly and provide a realistic internal force. This approach considers nonlinear damping, stiffness, load deformation behaviour of members including soil, and mass properties. The structure is subjected to forces based on accelerograms, often recorded in historical earthquakes, simulating a real seismic event, or synthetically generated. A nonlinear system is approximated as a series of linear systems and the response is calculated for a series of small equal intervals of time Δt and equilibrium is established at the beginning and end of each interval. The computational and time-consuming demands of these analyses are very high, which is why they are not so common and mostly used only for bridges of high importance and in zones susceptible to earthquakes as a tool to verify a design obtained from other simpler calculation methods (Davi, 2014).

1.4.3.1 Static nonlinear analysis (pushover analysis, EC8-2 approach)

Design of structures evolved over time, passing from a perception in which the goal was to avoid collapse to the one that incorporates different levels of performance. The concept of “strength” is no longer understood as a guarantee of better performance, if the strength is increased without a corresponding increase in the ductility of the structure, the performance of the structure in the event of an earthquake could be worse. The structure must be designed according to its "importance" and performance required by the code or the owner of the project. Pushover analysis allows, for a given seismic action, to estimate its performance and check if it meets the desired one. However, in order to perform the pushover analysis, it is necessary to know all the elements of the structure and the behaviour curves of the materials, so this type of analysis is used to validate the previous design. Pushover analysis consists in a static nonlinear analysis of the structure under monotonically increased horizontal loads, representing the effect of a horizontal seismic component. The main objectives of the analysis

are the estimation of the sequence and the final pattern of plastic hinge formation, the estimation of the redistribution of internal forces following the formation of plastic hinges, and the assessment of the force-displacement curve of the structure (“capacity curve”) and of the deformation demands of the plastic hinges up to the ultimate constitutive materials strain limits.

In the basic approach described in EC8-2 informative annex H, horizontal forces are distributed according to the initial elastic fundamental mode shape, and the displacement demand evaluation of the reference point (chosen at the centre of mass of the deck) is based on the code elastic response spectrum for five percent damping.

Main criticisms that can be addressed on this basic pushover analysis approach consist in the facts that it does not take into account some dynamic or nonlinear behaviour aspects of prime importance such as higher modes effects, structural softening, modification of the vibration modes and damping increase with post-yield plastic deformations and damage.

The analysis of the structure via pushover analysis assumes that structures oscillate predominantly in the lower modes of vibrations during seismic events, which reduces a multi-degree of freedom system (MDOF) to an equivalent single-degree-of-freedom system (ESDOF). To better help in understanding the concept of pushover analysis, consider an SDOF system with an incrementally increased lateral force according to the figure 1.8.

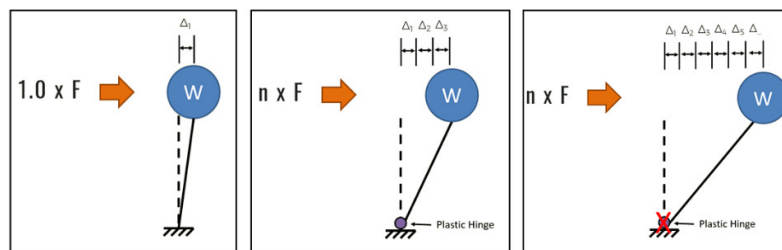


Figure 1.8. Simple SDOF structure with applied incrementally increasing lateral forces (midasbridge.com)

Incrementally increasing the lateral force causes the structure to undergo the following stages:

- Force is initially applied, and structure behaves elastically;
- Force is multiplied by a factor of ‘n’ wherein the base of the column reaches yield capacity, and a plastic hinge is formed;
- The unchanged force multiplied by ‘n’ produces additional displacements until the loss of lateral strength of the plastic hinge is achieved.

The pushover analysis records these stages, and a corresponding pushover curve is produced (figure 1.9).

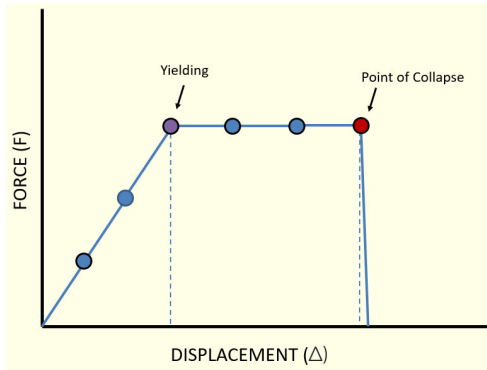


Figure 1.9. Pushover curve from the SDOF system (midasbridge.com)

To apply this type of analysis the following steps must be taken (Applied Technology Council, 2005):

- Define the mathematical model with the nonlinear force deformation relationship for the various components/elements;
- Define a suitable lateral load pattern and use the same pattern to define the capacity of the structure;
- Define the seismic demand in the form of an elastic response spectrum;
- Evaluate the performance of the bridge.

It should be noted that a static nonlinear (pushover) analysis leads to realistic results in structures, the response of which to the horizontal seismic action in the direction considered can be reasonably approximated by a generalized one degree of freedom system. Assuming the influence of the pier masses to be minor, the above condition is always met in the longitudinal direction of approximately straight bridges. The condition is also met in the transverse direction, when the distribution of the stiffness of piers along the bridge provides a more or less uniform lateral support to a relative stiff deck. This is the most common case for bridges where the height of the piers decreases towards the abutments or does not present intense variations. When, however, the bridge has one exceptionally stiff and unyielding pier, located between groups of regular piers, the system cannot be approximated in the transverse direction by a single-degree-of-freedom and the pushover analysis may not lead to realistic results (Informative annex H, Eurocode8-2, 2005).

1.4.3.2 Alternative pushover analysis (performance point approach)

As recognized to be a very powerful tool for seismic performance evaluation of structures, the static nonlinear pushover analysis has become a new trend due to its simplicity compared with the conventional dynamic time-history analysis procedure (see below). In recent years, considerable research effort has therefore been put to develop some extensions and improvements of pushover analysis methods (Applied Technology Council, 1996). Most of them are based on the performance point concept which consists in intersecting the performance curve by the demand acceleration-displacement (or force displacement) spectrum, by considering the equivalent secant effective stiffness instead of the initial, as represented on figure 1.10.

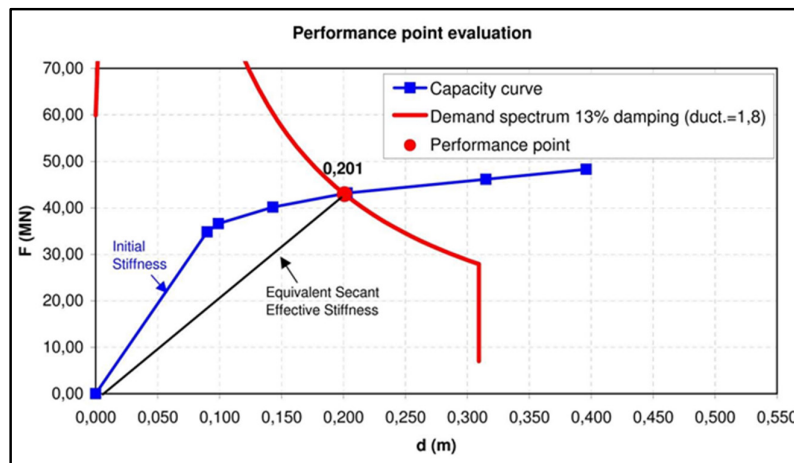


Figure 1.10. Equivalent secant effective stiffness and performance point definitions (Davi, 2014)

Main differences between used alternative pushover analysis compared with basic EC8-2 approach pushover analysis are the followings:

- Equivalent multimodal shape based on spectral deformation response in order to account for higher modes contribution;
- Re-evaluation of equivalent mode shape at each load increment;
- Performance point approach accounting for structural softening with post-yield plastic response (equivalent effective secant stiffness);
- Equivalent displacement derived for general dynamic analysis theory instead of centre of mass of the deck reference point displacement;
- Equivalent damping ξ_{eq} evaluated from Takeda model as described by Otani (1981) and Kowalsky and Ayers (2002) and expressed by Equation 1.1 from reached ductility demand μ_d .

$$\xi_{eq} = 0.05 + \frac{1}{\pi} \left(1 - \frac{1 - 0.03}{\sqrt{\mu_d}} - 0.03\sqrt{\mu_d} \right) \geq 0.05 \quad (1.1)$$

1.4.3.3 Nonlinear dynamic time-history analysis

Dynamic response of structures can also be obtained through direct numerical integration of nonlinear differential equations of motion using specialized structural analysis programs. The seismic input then consists of ground motion time-histories (accelerograms). It has to be noted that for new bridges design, Eurocode 8-2 requires that at least three pairs of accelerograms shall be used, selected from recorded events with magnitudes, source distances, and mechanisms consistent with those that define the design seismic action at the location of the bridge. This method can be used only in combination with a standard response spectrum analysis to provide insight into the post-elastic response and comparison between required and available local ductility demands. Generally, the results of the nonlinear analysis shall not be used to relax requirements resulting from the response spectrum analysis (see below). However, in the cases of bridges with isolating devices or irregular bridges, lower values estimated from a rigorous time-history analysis may be substituted for the results of the response spectrum analysis.

1.4.3.4 Linear static analysis (fundamental mode method)

In the fundamental mode method, equivalent static seismic forces are derived from the inertia forces corresponding to the fundamental mode and natural period of the structure in the direction under consideration, using the relevant ordinate of the site dependent design spectrum. The method also includes simplifications regarding the shape of the first mode and the estimation of the fundamental period.

The fundamental mode method quantifies the total seismic action in inertial forces, given by the product of the vibrating mass by the maximum seismic acceleration, which is obtained from a spectrum of inelastic accelerations for the period of vibration of an equivalent system of one degree of freedom with the same condensed stiffness and mass properties of the structure under analysis. This analysis is permitted for structures which do not have irregular structural systems. All the restrictions should be checked before applying this type of approach because it assumes continuity of the structure and distributes seismic forces along all elements of the bridge and is based on the fundamental mode of vibration in either longitudinal or transverse direction (MICHAEL et al., 2012).

Depending on the particular characteristics of the bridge, this method may be applied using three different approaches for the model, namely:

- The rigid deck model, only applied, when, under the seismic action, the deformation of the deck within a horizontal plane is negligible compared to the horizontal displacements of the pier tops. This condition is always met in the longitudinal direction of approximately straight bridges with continuous deck.
- The flexible deck model, which is used when equation 1.2 is not satisfied:

$$\frac{\Delta_d}{d_a} \leq 0,20 \quad (1.2)$$

Where Δ_d and d_a are respectively the maximum difference and the average of the displacements in the transverse direction of all pier tops under the transverse seismic action, or under the action of a transverse load or similar distribution.

- The individual pier model in which the seismic action in the transverse direction of the bridge is resisted mainly by the piers, without significant interaction between adjacent piers.

Notice that when the rigid or the flexible deck model is used in the transverse direction of a bridge, torsional effects may be estimated by applying a static torsional moment.

This method may be applied in all cases in which the dynamic behaviour of the structure can be sufficiently approximated by a single dynamic degree of freedom model.

1.4.3.5 Force-based modal spectral analysis associated with behaviour factor q

This type of analysis method is nowadays probably still the most commonly used approach for seismic design of structures in most regions of the world subjected to earthquake hazard.

The first step consists in proceeding to elastic modal analysis in order to obtain eigenvalues (natural periods of vibration) and eigenvectors (natural mode shapes) according to well-known structural dynamic theories (Ray & Joseph, 2002). Elastic forces are then evaluated from elastic estimates of structure natural periods together with code design acceleration spectrum for five percent damping. Most significant modes responses are finally combined together using a quadratic combination in order to get the global dynamic elastic response of the structure. In this approach, the effective cracked stiffness of the piers is evaluated from design ultimate moment M_{Rd} using EC8-2 informative annex C method 2, whereas following EC8-2 requirements, the uncracked bending stiffness and 50% of the uncracked torsional stiffness are considered for the prestressed concrete deck.

When the bridge geometry fits some regularity consideration in terms of piers height, mass distribution, limited skew and curvature, simplified method based on fundamental mode

only can be alternatively used. Depending on the particular characteristics of the bridge, this method may be applied using different approaches for the model, namely Rigid Deck Model, Flexible Deck Model (Rayleigh Method) or Individual Pier Model as described in Eurocode 8-2.

In order to account for favourable plastic energy dissipation and hysteretic damping, force demands in the structure are uniformly reduced from the elastic level by dividing by the code specified force-reduction factor, usually called behaviour factor q , the value of which depends on the assumed ductility capacity of the structure.

When derived from the pre-divided by q code design acceleration spectrum, displacement levels need to be re-multiplied by the displacement ductility factor μ_d , the value of which depends of the fundamental period range (equal-displacement, equal-energy or equal-force) of the structure in the considered horizontal direction, according to EC8-2 requirements and Newmark general principles (Carr, 1994). In most cases of typical bridges, equal-displacement rule can be applied and $\mu_d=q$.

1.4.3.6 Displacement-based modal spectral analysis

Inspired from Newmark's equal-displacement rule presented above, many research efforts have been made in recent years into the development of direct displacement based seismic analysis methods. Those methods are based on the observation that displacements (and related material strains) are better indicators of damage potential than are forces.

Starting from the same general modal spectral analysis has described above, the displacement based modal spectral analysis used in this study uses displacements derived from elastic response spectrum as the starting point demand parameter. Force demands are then derived from those displacements by adjusting their values on the effective performance curves of the resisting piers. This alternative spectral analysis thus requires a preliminary step that consists in deriving the performance Force-displacement curves of the piers from materials stress-strain relationships (including concrete transverse confinement effect) and sections bi-linearized moment-curvature curves, as illustrated on figure 1.11.

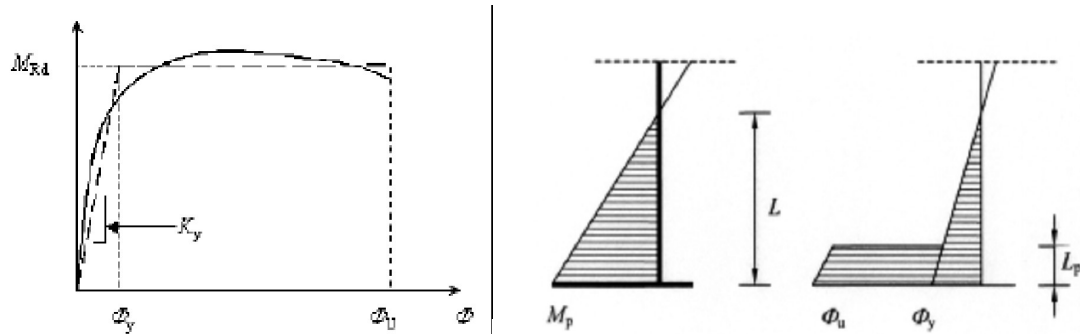


Figure 1.11. Moment-curvature analysis and distribution over the pier's height, from EC8-2 (Kolias et al., 2008)

1.4.4 Pushover analysis methodology

Design of structures evolved over time, passing from a perception in which the goal was to avoid collapse to the one that incorporates different levels of performance. The concept of strength is no longer understood as a guarantee of better performance, if the strength is increased without a corresponding increase in the ductility of the structure, the performance of the structure in the event of an earthquake could be worse. The structure must be designed according to its importance and performance required by the code or the owner of the project. Pushover analysis allows, for a given seismic action, to estimate its performance and check if it meets the desired one. However, in order to perform the pushover analysis, it is necessary to know all the elements of the structure and the behaviour curves of the materials, so this type of analysis is used to validate the previous design.

A brief description of the pushover has been made previously. In this chapter, it will be discussed how this nonlinear static analysis is performed and the various proposals that exist for its realization. The nonlinear designation is due to the fact that various elements are modelled using a nonlinear mathematical model.

To apply this type of analysis the following steps must be taken that are also represented in the figure 1.12 (Giuseppe et al., 2004):

- Define the mathematical model with the nonlinear force deformation relationship for the various components/elements;
- Define a suitable lateral load pattern and use the same pattern to define the capacity of the structure;
- Define the seismic demand in the form of an elastic response spectrum; -
Evaluate the performance of the building.

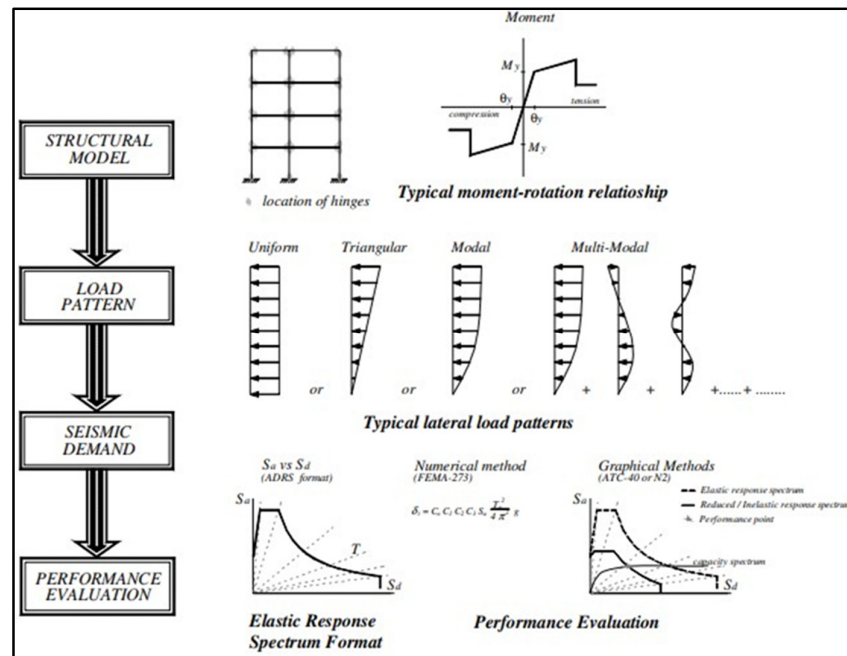


Figure 1.12. General flowchart for Nonlinear Static Procedure (S. R.Bento, 2004).

Mathematical model for the elements can be based on the experimental results or in numerical analysis.

Some of the methodologies that were developed for this type of analysis are:

- The Displacement Coefficient Method (FEMA-273 updated to FEMA-440), (Applied Technology Council, California, 2005);
- The Capacity Spectrum Method (ATC-40 updated to FEMA-440), (Applied Technology Council, California, 2005);
- The N2 Method (EC8).

FEMA 273 NEHRP Guidelines for the Seismic Rehabilitation of Buildings and ATC 40 Seismic Evaluation and Retrofit of Concrete Building were the first earthquake guidelines, developed by American Civil Engineers, on the application of nonlinear analysis. Later improvements have been proposed in FEMA 440. In Europe, in turn, the N2 method is implemented in the Eurocode. These methods differ on the clarity of theoretical base and simplicity of the application, but all are based on an explicitly or implicitly defined equivalent system of SDOF.

1.4.4.1 Lateral load

The choice of the load to be applied is very important for the results. These load patterns should represent the likely distribution of inertia forces in a seismic design. According to FEMA and EC8, at least two load patterns should be used:

- Uniform pattern with lateral forces proportional to mass, independent of their elevation (uniform response acceleration);
- Modal pattern with lateral forces proportional to the modal lateral force distribution according to elastic analysis in the direction under consideration.

Using an invariant load pattern is possible and representative of reality when the structural response is mainly influenced by the first mode and has only one yielding mechanism. Using this type of load may not allow to consider correctly the inertia forces redistribution in the structure. Some other types of load patterns were proposed in ATC-40 that intends to consider this factor (Applied Technology Council, 2005):

- For each increment beyond yielding, adjust the forces to be consistent with the changing deflected shape;
- Similar to the point above but include the effects of the higher modes of vibration in determining yielding in individual structural elements while plotting the capacity curve for the building in terms of first mode lateral forces and displacements.

1.4.4.2 Methodology proposed in FEMA 440

The procedure for the static nonlinear seismic analysis consists in verifying the capacity of the structure to withstand a certain seismic displacement, and can be divided in two parts:

- Definition of the capacity curve (pushover analysis)
- Calculation of the demand displacement through one of the following procedures:

a) Capacity spectrum method (equivalent linearization)

A step-by-step procedure for the method is described in the following lines:

- **Define the initial response spectrum, S_a vs. T , with initial damping β_i (normally 5%);**
- **Modify, if required, the selected spectrum, as appropriate, for soil-structure interaction (SSI).** This involves both potential reduction in spectral ordinates for kinematic interaction and a modification in the system damping;
- **Convert the response spectrum to S_a vs. S_d format;**

The response spectrum in forms of S_a versus period T is converted to S_a versus S_d by the following relations:

$$S_d = \frac{T_i^2}{4 \times \pi^2} S_{ai} \times g \quad (1.3)$$

Where:

- S_d is spectral displacement;
- T_i is period;
- S_{ai} is spectral acceleration;
- g is gravitational acceleration.

This transformation is represented graphically in figure 1.13.

“Every point on a response spectrum curve has associated with it a unique spectral acceleration, spectral velocity, S_v , spectral displacement, S_d and period, T . To convert a spectrum from the standard S_a vs T format to ADRS format, it is necessary to determine the value of S_d , for each point on the curve (S_{ai}, T_i) (Craig D. et al., 1996).”

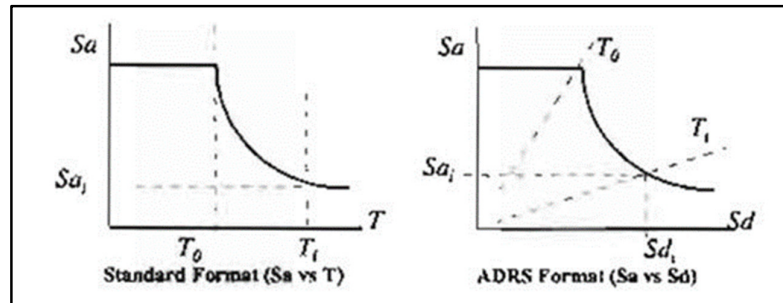


Figure 1.13. Response Spectrum Conversion (ATC-40, 1996)

Attention is called to the fact that in these graphics, each period of the structure can be represented by radial lines parting from the origin.

- **Generate the capacity curve of the structure;**

The goal is to represent the capacity of the structure in the form of the capacity curve by plotting the base shear force versus the deck displacement as represented in the figure 1.14.

The capacity of the structure depends on the strength and deformation capabilities of the structure and in order to correctly evaluate the behaviour in post-elastic regime, a nonlinear analysis is required.

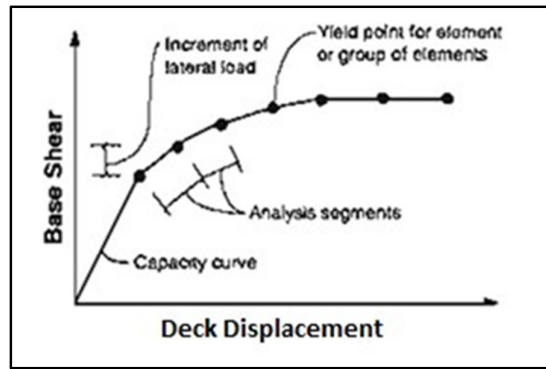


Figure 1.14. Capacity Curve (Applied Technology Council, 1996)

In order to obtain the capacity curve, uniform and modal lateral loads distribution are applied as mentioned before. The capacity curve shall be represented also as an idealized bilinear representation in order to calculate the yield strength and yield displacements, and the effective lateral stiffness and post yield slope, α represented in figure 1.15.

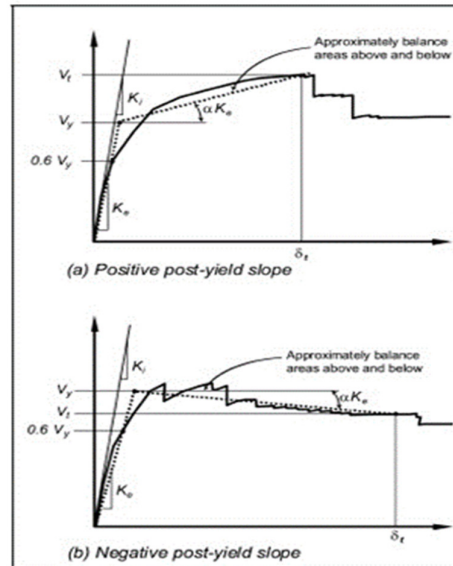


Figure 1.15. Idealized Force-Displacement Curves (Applied Technology Council, 2005)

- **Convert capacity curve to (S_a , S_d) format;**

The capacity curve in forms of shear force vs. deck displacement can be converted to an equivalent SDOF S_a vs. S_d graph by the following relations:

$$S_a = \frac{V/W}{\alpha} \quad (1.4)$$

$$S_d = \frac{\Delta}{PF \times \phi_1} \quad (1.5)$$

Where:

- V is the base shear force;
- W is the structural dead weight plus (if required) live load;
- α is the modal mass coefficient for the first natural mode;
- ϕ_1 is the amplitude of mode 1;
- PF is the modal participation factor for the first natural mode.

$$\alpha_1 = \frac{(\sum_{i=1}^N \frac{w_i \times \phi_{i1}}{g})^2}{(\sum_{i=1}^N \frac{w_i}{g}) (\sum_{i=1}^N \frac{(w_i \phi_{i1})^2}{g})} \quad (1.6)$$

$$PF_1 = \left(\frac{\sum_{i=1}^N \frac{w_i \times \phi_{i1}}{g}}{\sum_{i=1}^N \frac{w_i \times \phi_{i1}^2}{g}} \right) \quad (1.7)$$

Where:

- α_1 is modal mass coefficient for the first natural mode.
- PF_1 amplitude of mode 1 at level i.

This transformation is represented graphically in figure 1.16.

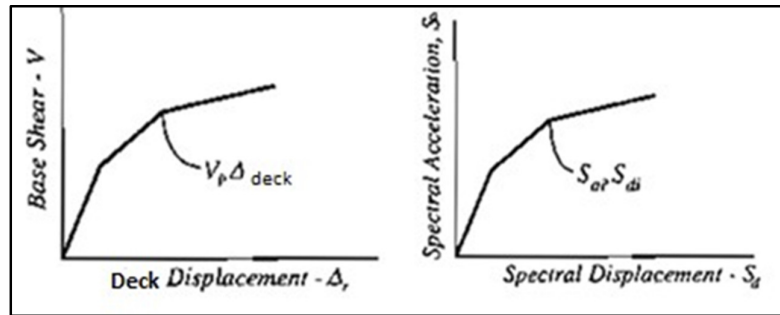


Figure 1.16. Capacity Curve transformed into a Capacity Spectrum (Applied Technology Council, 1996)

- **Select an initial performance point (max. acceleration a_{pi} and displacement d_{pi});**

This can be done by the equal-displacement approximation or any other point based on engineering judgement. The equal-displacement rule states that for long-period structures (e.g., $T > 1s$) the inelastic spectral displacement is the same as that which would occur if the structure remained perfectly elastic. For short-period (e.g., $T < 0.5s$) this can lead to significant differences but is a valid method to choose the initial trial performance point.

- Calculate the initial period, T_0 , and the yield displacements and acceleration, d_y and a_y ;

These can be obtained by superimposing the capacity curve with a bilinear representation (figure 1.17) and equalling the areas between them.

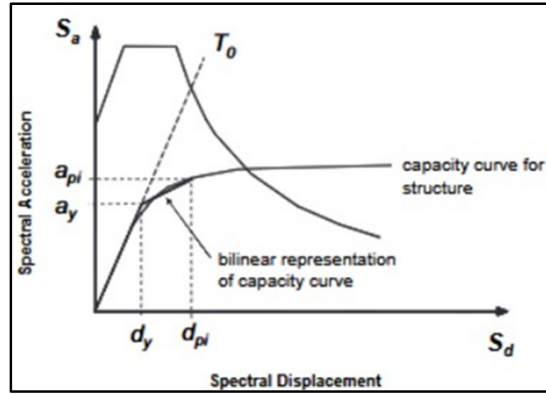


Figure 1.17. Bilinear representation of capacity spectrum (Applied Technology Council, 2005)

- Calculate the values of post-elastic stiffness α and ductility μ ;

$$\alpha_1 = \frac{\frac{a_{pi} - a_y}{d_{pi} - d_y}}{\left(\frac{a_y}{d_y}\right)} \quad (1.8)$$

$$\mu = \frac{d_{pi}}{d_y} \quad (1.9)$$

- Using the calculated values for post-elastic stiffness, α , and ductility, μ , calculate the corresponding effective damping β_{eff} and effective period T_{eff}

In the procedure of finding the performance point, the response spectrum has to be modified in order to consider the energy dissipation during the hysteretic cycles that lead to damage in the structure (e.g., the formation of plastic hinges).

This is done by an equivalent linear method (equivalent linearization), which consists in calculating the equivalent period (T_{eff}) and damping (β_{eff}) of the system, which are greater than the initial period and damping. With the formation of plastic hinges, the stiffness of the structure decreases, which in turn leads to increased T and damping. Both values are calculated from the maximum ductility ratio, μ . The main differences among equivalent linearization methods in the literature stem from the functions used to compute the equivalent period and equivalent damping ratio.

The FEMA 440 provides formulas for calculating T_{eff} and β_{eff} that depends on ductility and energy dissipation behaviour (Applied Technology Council, 2005).

The FEMA440 also proposes simplified equations, in case of doubts on which model to use, that are independent on the hysteretic model or α value.

- **Obtain the performance point**

The FEMA440 defines 3 procedures to obtain the PP, one of the procedures used will be presented:

- Procedure A (direct integration):

With the effective damping, obtain the adjusted ADRS to β_{eff} .

To obtain the adjusted ADRS to β_{eff} :

$$S_{a\beta} = \frac{S_{a0}}{B(\beta_{eff})} \quad (1.10)$$

Where:

$S_{a\beta}$ is the elastic spectrum acceleration with viscous damping β_{eff} ,

S_{a0} is the elastic spectrum acceleration with 5% viscous damping,

$B(\beta_{eff})$ is the reduction factor given by: $\frac{4}{6 - \ln \beta_{eff} \text{ (in \%)}}$

Intersect the radial effective period, T_{eff} , with the adjusted ADRS to obtain the estimated maximum displacement, d_i . The maximum acceleration, a_i , is the one corresponding to d_i on the capacity curve as shown in figure 1.18.

Then, Compare d_i with the previous (or initial) assumption. If it is within tolerances, the PP is found, otherwise repeat the process from point 6.

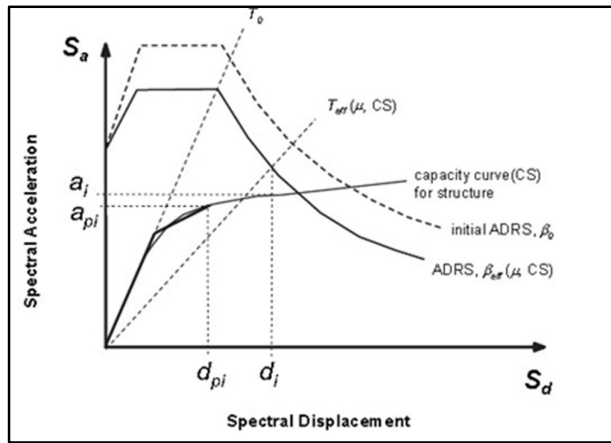


Figure 1.18. Bilinear representation of capacity spectrum (Applied Technology Council, 2005)

b) Coefficient method

The displacement coefficient method provides a direct numerical process for calculating the displacement demand.

The target displacement, which is the same as performance point, is obtained from the following equation:

$$\delta_t = C_0 C_1 C_2 C_3 S_a \frac{T_e^2}{4\pi^2} g \tag{1.11}$$

Where:

- T_e is the effective fundamental period of the bridge in the direction under consideration:

$$T_e = T_i \sqrt{\frac{K_i}{K_e}}, \text{ where:}$$

- T_i is the elastic fundamental period in the direction under consideration;
- K_i is the elastic lateral stiffness in the direction under consideration;
- K_e is the effective lateral stiffness in the direction under consideration (figure 1.19)

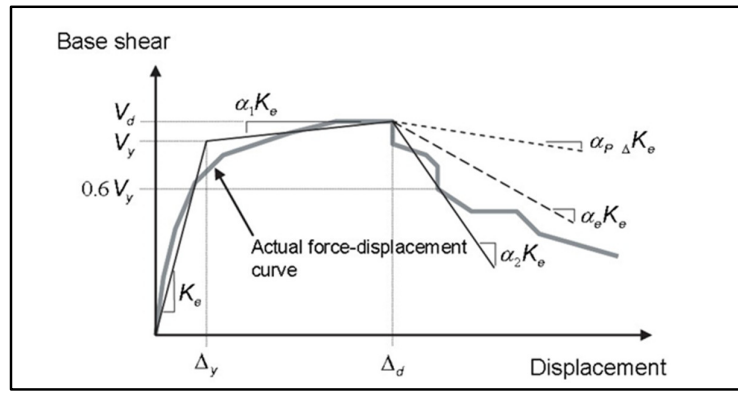


Figure 1.19. Idealized force-displacement curve for nonlinear static analysis (Applied Technology Council, 2005)

- C_0 is a modification factor to relate spectral displacement of an equivalent SDOF system to the deck displacement of the MDOF, which can be taken as the first modal participation factor at the level of the control node or the modal participation factor at the level of the control node calculated using a shape vector corresponding to the deflected shape of the building at the target displacement.
- C_1 is a modification factor to relate the maximum inelastic displacements to the displacements calculated for linear elastic response.

$$C_1 = 1 + \frac{R - 1}{\alpha T_e^2} \quad (1.12)$$

$$\text{if } T_e > 1s \rightarrow C_1 = 1.0$$

$$\text{if } T_e < 0.2s \rightarrow C_1 = 1 + \frac{R-1}{\alpha \times 0.2^2}$$

where:

- R is the strength ratio

$$R = \frac{S_a}{V_y/W} C_m \quad (1.13)$$

Where:

- S_a is response spectrum acceleration, at the effective fundamental period and damping ratio of the structure in the direction under consideration;
- V_y is the yield strength indicated in the above image;
- W is the effective seismic weight;

- C_m is the effective mass factor taken as the effective model mass calculated for the fundamental mode;
- α is equal to 130, 90 and 60 for site classes B, C and D;
- C_2 is a modification factor to represent the effect of pinched hysteretic shape, stiffness degradation, and strength deterioration on the maximum displacement response.

$$C_2 = 1 + \frac{1}{800} \left(\frac{R-1}{T} \right)^2 \quad (1.14)$$

$$\text{if } T_e > 0.7s \rightarrow C_2 = 1.0$$

$$\text{if } T_e < 0.2s \rightarrow C_2 = 1 + \frac{1}{800} \left(\frac{R-1}{T} \right)^2$$

In nonlinear procedures or in structures with non-degrading systems, C_2 may be taken as 1.0.

(The C_3 coefficient was removed in the FEMA440, and a limit on the strength ratio R was defined.)

1.4.4.3 The N2 Method

The designation of the method as “N2” results from the fact that a nonlinear (N) analysis is involved where two (2) mathematical models are applied.

The key points of the method that is defined in the Eurocode EN 1998-1:2004 are:

- Conversion of the MDOF structure into a SDOF system using a transformation factor;
- Determination of the idealized elasto-perfectly plastic force-displacement relationship (capacity curve);
- Determination of the target displacement using the period and spectral acceleration of the idealized SDOF system.

This method is of application for structures whose behaviour is not significantly affected by higher modes than the fundamental mode in each direction. This condition is deemed to be fulfilled when the fundamental period is smaller than $4T_c$ (T_c is the upper limit of the period of the constant spectral acceleration branch) and $2,0s$.

The procedure is defined in point 4.3.3.4.2.1 in EN 1998-1: 2004. The most relevant definitions are described in the following points. The purpose of the analysis is to:

- Verify the ductility of the structure (ratio α_u/α_1)

Where:

- α_u is the value by which the horizontal seismic design action is multiplied, in order to form plastic hinges in a number of sections sufficient for the development of overall structural instability, while all other design actions remain constant. The factor α_u may be obtained from a nonlinear static (pushover) global analysis;
- α_1 is the value by which the horizontal seismic design action is multiplied, in order to first reach the flexural resistance in any member in the structure, while all other design actions remain constant.
 - Estimate the expected plastic mechanisms and damage distribution;
 - Assess existing structures;
 - Offer an alternative to the behaviour factor q-based analysis.

In the Annex H of Eurocode EN 1998-2:2005, specific rules for the pushover analysis of bridges are given.

The target displacement is calculated as defined in Annex B of EN 1998-1:2004, with the following procedure:

- The multiple-degree-of-freedom structure (MDOF) is transformed into an equivalent SDOF system:

$$m^* = \sum m_i \phi_i = \sum F_i \quad (1.15)$$

$$F^* = \frac{F_b}{\Gamma} \quad (1.16)$$

$$d^* = \frac{d_n}{\Gamma} \quad (1.17)$$

Where:

- m_i is the mass of the different elements (ex: piers).
- ϕ_i is the normalized displacement of the deck. Usually, $\phi_n = 1$
- ϕ_n is the normalized displacement of the control node.
- $F_i = m_i \phi_i$ is the normalized lateral force
- F_b is the base shear force
- d_n is the control node displacement of the MDOF
- Γ is the transformation factor:

$$\Gamma = \frac{m^*}{\sum m_i \phi_i^2} = \frac{\sum F_i}{\sum \left(\frac{F_i^2}{m_i} \right)} \quad (1.18)$$

- Determination of the idealized elasto-perfectly plastic force-displacement relationship:

The initial stiffness of the idealized system is determined by equalling the areas under the actual and the idealized bilinear force-displacement curve. This process is iterative, starting with the assignment of an initial value to deformation d_m^* and consequently F_y . Then it is possible to calculate the deformation energy (E_m^*) and the yield displacement (d_y^*).

- Determination of the period of the idealized equivalent SDOF system, considering the energy dissipation during the formation of the plastic mechanism.

$$T^* = 2\pi \sqrt{\frac{m^* d_y^*}{F_y^*}} \quad (1.19)$$

This period is analogue to the effective period calculated in the FEMA440 method. The difference lies that the FEMA440 method uses implicit formulas relating the type of hysteretic cycles (and the associated A-H constants) and the structure ductility, whereas in the EC method the formulation relies on the deformation energy E_m .

- Determination of the target displacement of the equivalent SDOF system.

To obtain the displacement target it is necessary to transform the response spectrum in the format (S_e, T) to format (S_e, d), applying following relation:

$$d^* = S_e(T) \left(\frac{T}{2\pi} \right)^2 \quad (1.20)$$

(This formulation is analogue to the determination of the effective ADRS using the effective damping in the FEMA440 method).

1.4.5 Bridges seismic damages

Analysing the bridge seismic damages and their reasons is an important way for us to establish the correct seismic design method and develop effective earthquake resisting methods. According to the reference materials and earthquake damage examples, the bridge seismic damages can be classified as follows:

1.4.5.1 Over-displacement of superstructures

The over-displacement of superstructures refers to the seismic damages caused by the longitudinal and lateral displacement/torsion of bridge superstructure, which were commonly occurred around expansion joint (Li, 2020). The expression form of one of these seismic damages were dislocation and extrusion between girders, and another form was the unseating of superstructures, caused by the large displacement exceeds the bearing surface of piers and abutments. Girder-bearing relative slippage were much more common than girder falling in seismic area. Because of the absence of horizontal restraint between girders and piers, relative displacements would easily occur when the horizontal seismic force exceed the friction and shear capacity of the bearings.

The unseating of bridge superstructure is one of the most serious earthquake damages of girder bridges. The statistical data showed that girder-falling in vertical direction were much more than horizontal direction (almost five to six times). Because of the much bigger energy would be produced by the impact between the girder-falling in vertical direction and the walls of piers than by the shaking of girder on the pier-top. Most of the seismic damages of superstructures were occurred both at once.

Under the joint action of earthquake dynamic effect and landslide, the girder seismic damages are mainly girder body displacement and girder falling. The displacement of the girder body is mainly represented by a displacement in the longitudinal bridge, displacement in the transverse bridge, and plane rotation. Because the girder body is directly supported on the bridge piers, only the rubber bearings are connected with each other, and there is basically no horizontal constraint (Dai et al., 2019). When the horizontal seismic force exceeds the friction force or bearing shear capacity of bearing, relative displacement between girder and pier will occur. The displacement of the girder is also related to the height of the pier. The anti-pushing rigidity of the high pier is small, and the displacement is large under horizontal seismic force. When the girder displacement exceeds the support range, it will cause girder falling. In all seismic damages, girder falling is the most serious earthquake damage, which will directly lead to traffic disruption.

For earthquake damage of girder falling, the longitudinal girder falling accounts for the vast majority. The reasons for the girder of falling are that the overall integrity of the simply supported girder bridge is relatively poor, and the girders of many bridges in the earthquake zone are supported in a relatively small length. The form and arrangement of the bearings are not reasonable. There is no longitudinal displacement constraint; the lateral limit

stop is weak (Monteiro et al., 2008). The figure 1.20 shows a typical damage of superstructures.



Figure 1.20. 1995 Kobe earthquake (ENSTP, 2021)

1.4.5.2 Seismic damages of substructures

The piers are the principal component to support the superstructure of the bridge. The seismic damage to bridge piers mainly includes fracture and deformation, the specific performances include: the bridge piers displacement, tilt, bending and shear failure of pier bottom and pier body, the collapse of the top of the pier to form a plastic hinge, shear failure of the cross beam, cover beam cracking, block failure etc. Pier damage occurs mostly at the root and top, lateral stirrups of the piers that are collapsed or sheared are generally less, the sudden change in the stiffness of the pier body is prone to earthquake damage. Masonry piers are more damaged than reinforced concrete piers.

In the Wenchuan earthquake, the piers of the simply-supported girder bridge in the disaster area are in the form of reinforced concrete double-column circular pier, double-column rectangular pier, single-column rectangular pier, and single-column circular pier. Seismic damage survey data show that the double-column pier is preferable to the single-column pier, and the rectangular pier performs better than the circular pier. Pier's earthquake damage is shown in figure 1.21 and figure 1.22.



Figure 1.21. Insufficient confinement of columns (Northridge, California 1994)



Figure 1.22. Insufficient number of stirrups for shear (Hanshin expressway, Kobe, 1995)

Abutment is the supporting part on both sides of the bridge. Generally, abutment is built on the plain fill or the bank of the river or on the hillside. It's the support structure built with mortar flag stone or reinforced concrete, which is the direct part of the bridge to resist the earthquake. Abutment seismic damage mainly includes cracking at the wall of the gravity abutment, rib cracking at the ribbed slab abutment, cracking at the back wall and ear wall, abutment tilt, displacement, cracking at the conical slope etc. Masonry gravity abutment has poor seismic capability, which is easy to damage and hard to repair in an earthquake.

Causes of the abutment damage are mainly the interaction between girder and abutment, foundation slip and subsidence. The subgrade of abutment is generally high, and three facing empties. The stiffness of the abutment and the soil below is different. The foundation soil is prone to deformation and damage under the earthquake load. The strength and deformation of the abutment cannot meet the requirements of the earthquake force, and make the abutment damage. In the earthquake, serious damage of the subgrade and foundation is the main reason for the collapse of a bridge; this is also the important factor why the bridge is difficult to repair after the earthquake. The destruction of the foundation is closely related to the failure of the subgrade, and the destruction of almost all subgrade will cause the

destruction of the foundation. Foundation seismic damage is mainly manifested in displacement, tilt, subsidence, and fracture and buckling instability (Dai et al., 2019).

1.4.5.3 Damages of structure for support and connection

Seismic damage of the bearing is common in an earthquake. The adjacent beams collide with each other and the girder appears longitudinal and lateral displacement generally all happened after the destruction of the bearing. The bearing is subjected to great shear force and deformation during a strong earthquake. The reasons for the widespread failure of the bearing are that the mechanics characteristic of the bearing under the action of the earthquake is special, the seismic requirements of the bearing are not fully considered in the design, and the structural measures are insufficient, some bearing forms and materials are defective. Earthquake damage of the bearing mainly manifests as the bearing displacement, the pulling out of the anchor bolt, the snipping, the dropping of the movable bearing, and the construction damage of the bearing itself.

In addition to the earthquake damage to the main parts mentioned above, there are some non-structural seismic damages, including the failure of the joints, the destruction of the expansion joints, destruction of the handrail guardrails, and the failure of the block, etc. Although these parts of the damage will not cause the bridge to collapse, it will also greatly aggravate the seismic damage of the bridge, so the bridge seismic design and bridge construction should be given recognition and appropriate treatment (Dong et al., 2004).

Conclusion

Throughout this chapter, understanding the theories and concepts that surround the seismic response of a bridge was the aim. Thus, steel as the main material component of the bridge study was first discussed, explaining how important its properties, especially the mechanical ones, are for different applications and how to deal with possible defects. The structure of steel-concrete composite deck was discussed, then bridge structural typology was illustrated. An overview of the seismic design of bridges was assess at the end to present the different resisting systems, methods of analysis and associate to it an illustrative presentation of the bridge seismic damages. Hence for a proper study of the seismic response, the type of analysis has to be meaningfully chosen. The next chapter will give in details the methodology used for investigation in this work.

CHAPTER 2: METHODOLOGY

Introduction

In the previous chapter, bibliographic research was presented which permits us to have a global understanding of the objective of this work. The main point of this part is to describe the methodology involved in the investigations of the seismic response of a steel composite bridge considering a frame scheme. The methodology is the part of the study that establishes the research procedure after the definition of the problem, so as to achieve the set objectives. The content of this chapter is divided in five main parts. The first part of this work will explain the conception through the codes used, the preliminary design done, actions applied and combinations used, followed by a general static analysis and design of our case study, then an explanation of the numerical modelling will be made. Thirdly a seismic study will be assessed and at last the pushover analysis methodology will be described.

2.1 Conception

For analysis required in this thesis, a steel bridge with frame scheme will be conceived for traffic highway purposes and the norm applied is the British standard of European code of construction. The structural conception is detailed in the oncoming section via the application of specific norms and loads.

2.1.1 Codes

A good construction project respects a specific norm depending on where the construction is done. Worldwide, there are many types of norms among which the Chinese code, the Turkish code, the American code, European norm, etc. Eurocode is the standardised code recommended by the European Committee for Standardization. Depending on the site of construction, on the material used and the type of structure to be done, different parts of Eurocodes are used. For this theoretical case study, the parts of Eurocodes used are:

- Eurocode 0: Basis of structural design;
- Eurocode 1: Actions on the structures, part 1: general actions, part 2: traffic loads on bridges;
- Eurocode 3: Design of steel structures, part 1-1: general rules and rules for buildings, part 1-5: plated structural elements, part 1-8: design of joints, part 2: steel bridges;

- Eurocode 4: Design of composite steel and concrete structures, part 2: general rules and rules for bridges;
- Eurocode 8: Design of structures of earthquake resistance, part 1: general rules, seismic action rules for building, part 2: bridges.

FEMA 440 regulations is used also in the seismic analysis.

2.1.2 Preliminary design

In order to have sections of structural elements, a preliminary design will be done according to some principles. In order to obtain the dimensions of the various elements, the preliminary design data of a twin-girder directly supporting cross beam bridges will be performed (SETRA, 2010). The dimensions of the stiffeners shall be assumed regarding the literature documentations and an iterative procedure will be applied to determine the section of the steel piers starting from the section obtained for the plate girders. Figure 2.1 illustrates the different requirements to assess the preliminary design.

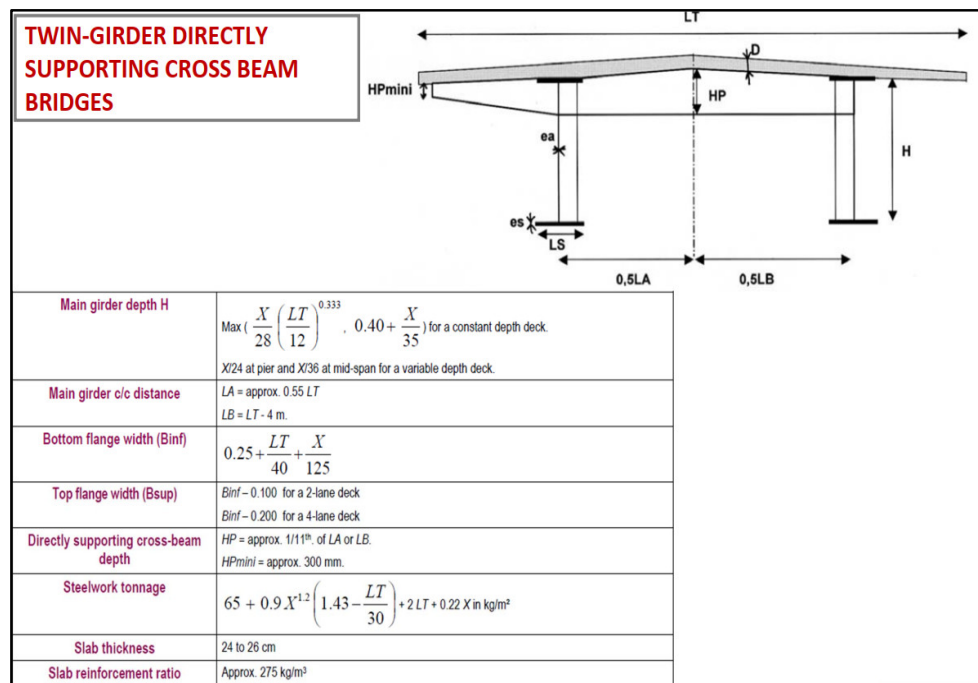


Figure 2.1. Preliminary design data (SETRA, 2010)

2.1.3 Loads actions

2.1.3.1 Static load actions

Different types of actions act on the bridge. Regarding our study, focus will be put on permanent and variable loads. Permanent loads are represented by $G_{k,j}$ and $Q_{k,i}$ express variable loads.

a) Permanent loads

Permanent loads can either be structural or non-structural.

- Structural loads (G_1): self-weight of slab, girders, piers, etc.
- Non-structural loads (G_2): barriers, road pavement, street lamps, etc.

b) Live loads

The live load on the bridge is moving load throughout bridge length. The moving loads are vehicles, pedestrians, etc.

(i) Number of lanes

The number and the width of notional lanes result from table 2.1(EN 1991-2, 2003).

Table 2.1. Multipliers for the characteristic values of variable loads (EN 1991-2, 2003)

Carriageway width w	Number of notional lanes	Width of a notional lane w_l	Width of the remaining area
$w < 5,4 \text{ m}$	$n_l = 1$	3 m	$w - 3 \text{ m}$
$5,4 \text{ m} \leq w < 6 \text{ m}$	$n_l = 2$	$\frac{w}{2}$	0
$6 \text{ m} \leq w$	$n_l = \text{Int}\left(\frac{w}{3}\right)$	3 m	$w - 3 \times n_l$
NOTE For example, for a carriageway width equal to 11m, $n_l = \text{Int}\left(\frac{11}{3}\right) = 3$, and the width of the remaining area is $11 - 3 \times 3 = 2 \text{ m}$.			

(ii) Traffic loads

For the complete analysis of the vertical forces, the traffic load model 1 (LM1) has been considered. This load model is constituted of a tandem load (TS) and a uniformly distributed load (UDL), (EN 1991-2, 2003). The class of the bridge is class 2. Table 2.2 recaps the values to consider for loads due to traffic.

Table 2.2. Characteristic values of load model 1 (EN 1991-2, 2003)

Location	Tandem system <i>TS</i>	UDL system
	Axle loads Q_{ik} (kN)	$\overline{[E\sigma]} q_{ik}$ (or q_{ik}) (kN/m ²) $\overline{[E\sigma]}$
Lane Number 1	300	9
Lane Number 2	200	2,5
Lane Number 3	100	2,5
Other lanes	0	2,5
Remaining area (q_{ik})	0	2,5

Correction factors $\alpha_{Q_{ik}}$, $\alpha_{q_{ik}}$, α_{qr} to be considered are shown in table 2.3:

Table 2.3. Values of adjustment factors

α_{Q1}	$\alpha_{Qi} (i \geq 2)$	α_{q1}	$\alpha_{qi} (i \geq 2)$	α_{qr}
0.9	0.8	0.7	1.0	1.0

The load group gr1a from table 2.4 was adopted. It is displayed in equation 2.1.

$$gr1a = TS_k + UDL_k + q * f_k \tag{2.1}$$

Where q^*_{fk} represents the uniformly distributed load on footways and cycle tracks.

Table 2.4. Assessment of groups of traffic loads (EN 1991-2, 2003)

Load type	CARRIAGEWAY						FOOTWAYS AND CYCLE TRACKS
	Vertical forces			Horizontal forces			Vertical forces only
Reference	4.3.2	4.3.3	4.3.4	4.3.5	4.4.1	4.4.2	5.3.2-(1)
Load system	LM1 (TS and UDL systems)	LM2 (Single axle)	LM3 (Special vehicles)	LM4 (Crowd loading)	Braking and acceleration forces ^a	Centrifugal and transverse forces ^a	Uniformly Distributed load
Groups of Loads	gr1a	Characteristic values					Combination value ^b
	gr1b		Characteristic value				
	gr2	Frequent values			Characteristic value	Characteristic value	
	gr3 ^d						Characteristic value ^c
	gr4				Characteristic value		Characteristic value
gr5	See annex A		Characteristic value				
Dominant component action (designated as component associated with the group)							
^a May be defined in the National Annex (for the cases mentioned). ^b May be defined in the National Annex. The recommended value is 3 kN/m ² . ^c See 5.3.2.1-(2). One footway only should be considered to be loaded if the effect is more unfavourable than the effect of two loaded footways. ^d This group is irrelevant if gr4 is considered.							

c) Wind load

The general expression of wind force F_w acting on a structure or a structural component can be determined directly by using equation 2.2.

$$F_w = c_s \cdot c_d \cdot c_f \cdot q_p(z_e) \cdot d_{tot} \tag{2.2}$$

Where:

$q_p(z_e)$ is the peak velocity pressure at reference height z_e ;

d_{tot} is the total depth of the structural element z_e ;

$c_s \cdot c_d$ is the structural factor;

c_f is the force coefficient.

The peak velocity pressure at height z is expressed by equation 2.3:

$$q_p(z) = \frac{1}{2} \cdot (1 + 7 \cdot I_v(z)) \cdot \rho \cdot v_m^2(z) = c_e(z) \cdot q_b \quad (2.3)$$

Where:

ρ is the air density;

$v_m(z)$ is the mean wind velocity at height z and is given by equation 2.4;

$$v_m(z) = c_r(z) \cdot c_o(z) \cdot v_b \quad (2.4)$$

$c_r(z)$ is the roughness coefficient;

$c_o(z)$ is the orography coefficient;

v_b is the basic wind velocity given by equation (2.6);

$I_v(z)$ is the turbulence intensity and can be obtained from equation (2.5).

$$I_v(z) = \frac{k_l}{c_o(z) \cdot \ln(z/z_0)} \quad (2.5)$$

k_l is the turbulence factor;

z_0 is the roughness length.

$$v_b = c_{dir} * c_{season} * v_{b,0} \quad (2.6)$$

c_{dir} is the directional factor;

c_{season} is the season factor.

Roughness length and coefficients depends on terrain category and parameters. The procedure to find values of different coefficients is detailed in (*EN 1991-1-4*).

The wind used for design will be wind acting on a loaded bridge.

d) Temperature load

Temperature load has two components.

(i) Uniform temperature component

It depends on the minimum and maximum temperature which a bridge will achieve. Having the minimum shade air temperature (T_{min}) and maximum shade air temperature (T_{max}) for the site, minimum and maximum uniform bridge temperature components $T_{e,min}$ and $T_{e,max}$ can be derive by using the graph on figure 2.2.

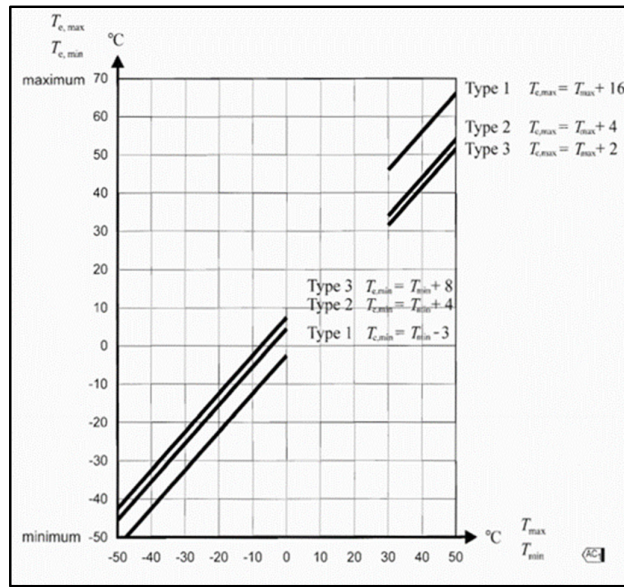


Figure 2.2. Correlation between minimum/maximum shade air temperature and minimum/maximum uniform bridge temperature component (EN 1991-1-5, 2011)

The initial bridge temperature T_0 is important for calculating contraction down to the minimum uniform bridge temperature component and expansion up to the maximum uniform bridge temperature component.

Thus the characteristic value of the maximum contraction range of the uniform bridge temperature component, $\Delta TN, con$ should be taken as :

$$\Delta TN, con = T_0 - T_{e,min} \quad (2.7)$$

And the characteristic value of the maximum expansion range of the uniform bridge temperature component, $\Delta TN, exp$ should be taken as :

$$\Delta TN, exp = T_{e,max} - T_0 \quad (2.8)$$

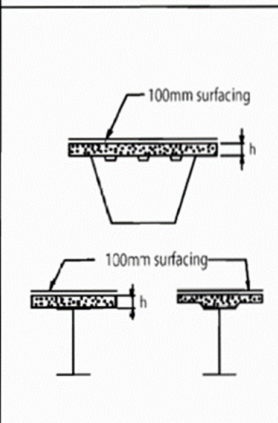
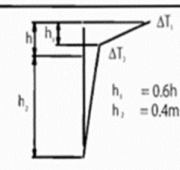
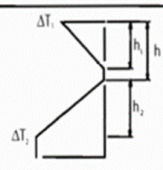
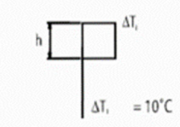
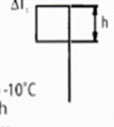
The overall range of the uniform bridge temperature component is :

$$\Delta TN = T_{e,max} - T_{e,min} \quad (2.9)$$

(ii) Vertical nonlinear component

The vertical temperature gradient applied on bridge deck was defined according to table 2.5 in (EN 1991-1-5, 2011).

Table 2.5. Temperature differences for bridge decks type 2: composite decks (EN 1991-1-5, 2011)

Type of Construction	Temperature Difference (ΔT)																									
	(a) Heating	(b) Cooling																								
 <p>2 Concrete deck on steel box, truss or plate girders</p>	<p>Normal Procedure</p>  <table border="1"> <thead> <tr> <th>h</th> <th>ΔT_1</th> <th>ΔT_2</th> </tr> <tr> <th>m</th> <th>°C</th> <th>°C</th> </tr> </thead> <tbody> <tr> <td>0.2</td> <td>13</td> <td>4</td> </tr> <tr> <td>0.3</td> <td>16</td> <td>4</td> </tr> </tbody> </table>	h	ΔT_1	ΔT_2	m	°C	°C	0.2	13	4	0.3	16	4	<p>Normal Procedure</p>  <table border="1"> <thead> <tr> <th>h</th> <th>ΔT_1</th> <th>ΔT_2</th> </tr> <tr> <th>m</th> <th>°C</th> <th>°C</th> </tr> </thead> <tbody> <tr> <td>0.2</td> <td>-3.5</td> <td>-8</td> </tr> <tr> <td>0.3</td> <td>-5.0</td> <td>-8</td> </tr> </tbody> </table>	h	ΔT_1	ΔT_2	m	°C	°C	0.2	-3.5	-8	0.3	-5.0	-8
	h	ΔT_1	ΔT_2																							
m	°C	°C																								
0.2	13	4																								
0.3	16	4																								
h	ΔT_1	ΔT_2																								
m	°C	°C																								
0.2	-3.5	-8																								
0.3	-5.0	-8																								
<p>Simplified Procedure</p>  <p>$\Delta T_1 = 10^\circ\text{C}$</p>	<p>Simplified Procedure</p>  <p>$\Delta T_1 = -10^\circ\text{C}$ $h_1 = 0,6h$ $h_2 = 0,4m$</p>																									
<p>Note: For composite bridges the simplified procedure given above may be used, giving upper bound thermal effects. Values for ΔT in this procedure are indicative and may be used unless specific values are given in the National Annex.</p>																										

The load (T_k) due to differential thermal variation (between slab and metal beams) is expressed by equation (2.10):

$$T_k = A_c \cdot \varepsilon \cdot E_{cm} \tag{2.10}$$

Where:

- A_c is the slab area ;
- ε is a thermal coefficient ;
- E_{cm} is the concrete elastic modulus with $E_{cm} = 22000 \cdot (f_{cm}/10)^{0.3}$.

Because an effective section of the bridge is studied, it is necessary to apply the corresponding temperature load. The force T_{beam} that will be considered is:

$$T_{beam} = T_k/n \quad \text{Where } n \text{ is the number of girders.} \tag{2.11}$$

e) Shrinkage effect

In steel-concrete composite bridges, the slab is restrained by steel beam. The shear connectors resist the force arising out of shrinkage, by inducing a tensile force on the slab (global effect). This reduces the apparent shrinkage of composite structure with respect to the free shrinkage of concrete. Shrinkage effect is combined to the creep effect; the latter is evaluated at infinite time.

(i) Creep

The effects of creep are taken into account by reducing concrete elastic modulus E_{cm} thus increasing the modular ratio.

Modular ratio at infinite time n_L is given by equation (2.12).

$$n_L = n_0(1 + \psi_L \rho_t) \tag{2.12}$$

Where:

- n_0 is the modular ratio E_s/E_{cm} for the short-term loading;
- ρ_t is the creep coefficient depending on the age t of concrete and the age t_0 at loading;
- ψ_L is the creep multiplier depending on the type of loading; to be taken as 1,1 for permanent loads; 0,55 for primary and secondary effects of shrinkage; 1,5 for pre-stressing by imposed deformations.

In order to determine the creep coefficient $\rho(t, t_0)$, following data was assumed or computed:

- Relative humidity RH=70%
- Reference zero time $t_0= 3$ days
- Fictitious dimension $h=2A_c/u$

(ii) Shrinkage

Total shrinkage at infinite is calculated through equation 2.13.

$$\varepsilon_{cs}(\infty) = \varepsilon_{ca}(\infty) + \varepsilon_{cd}(\infty) \tag{2.13}$$

Expressions of shrinkage strain components are reported in table 2.6.

Table 2.6. Shrinkage components

$\varepsilon_{ca} = 2.5. (f_{ck} - 10). 10^{-6}$	(2.14)
$\varepsilon_{cd}(\infty) = k_h. \varepsilon_{c0}$	(2.15)
$\varepsilon_{c0} = 0.85. ((220 + 110. \alpha_{ds1}). e^{(-\alpha_{ds2}. f_{cm}/f_{cm0})). 10^{-6}. \beta_{RH}$	(2.16)
$\beta_{RH} = 1.55. (1 - \left(\frac{RH}{RH_0}\right)^3)$	(2.17)

Where:

- $\varepsilon_{cd}(\infty)$ is the dry shrinkage strain at infinite
- $\varepsilon_{ca}(\infty)$ is the autogenous shrinkage

Shrinkage of concrete is taken into account by applying an axial force at slab ends. It is given by equation (3.23).

$$N_{c,r\infty} = \varepsilon_{cs}(\infty) \cdot E_{c,eff} \cdot A_c \quad (2.18)$$

Where $E_{c,eff}$ is the reduced modulus of elasticity for concrete and obtained from equation (3.24).

$$E_{c,eff} = \frac{E_{cm}}{1 + \rho(\infty, t_0)} \quad (2.19)$$

Because an effective section of the bridge is studied, the corresponding temperature load will be applied. The force N_{beam} that will be considered is taken from equation (3.25).

$$N_{beam} = N_{c,r\infty} / n \quad (2.20)$$

Where n is the number of beams.

f) Seismic action

Seismic load result from earthquake and the earthquake motion at a given point on the earth surface is represented by an elastic acceleration response spectrum which is defined as the relationship between the ground motion and the period of vibration during an earthquake.

Soil classes A, B, C and D in accordance with EC8-1, have the following correspondence to the relevant classes of NEHRP 2000 (FEMA-450, 2003).

Table 2.7. FEMA 450 and EC8-1 correspondence

EC8-1	A	B	C	D
NEHRP 2000	B (and A)	C	D	E

Soil class E consists of alluvium 5 to 20m thick underlain by stiffer material ($v_s \geq 800$ m/s).

For the horizontal components of the seismic action, the elastic response spectrum $S_e(T)$ is defined by the following expressions (see Fig. 2.4):

$$0 \leq T \leq T_B: S_e(T) = a_g S \left[1 + \frac{T}{T_B} (\eta 2.5 - 1) \right] \quad (2.21)$$

$$T_B \leq T \leq T_C: S_e(T) = a_g \eta S 2.5 \quad (2.22)$$

$$T_C \leq T \leq T_D: S_e(T) = a_g \eta S 2.5 \left[\frac{T_C}{T} \right] \quad (2.23)$$

$$T_D \leq T \leq 4sec: S_e(T) = a_g \eta S 2.5 \left[\frac{T_C T_D}{T^2} \right] \quad (2.24)$$

Where:

- $S_e(T)$ is the elastic response spectrum
- T : is the vibration period of a linear single degree of freedom system
- a_g : is the design ground acceleration on type A ground ($a_g = \gamma_1 a_{gR}$)
- T_B : is the lower limit of period of the constant spectral acceleration branch
- T_C : is the upper limit of the period of the constant spectral acceleration branch
- T_D : is the value defining the beginning the constant displacement response range of the spectrum
- S : is the soil factor that depends on the ground type
- η : is the correction factor given by $\eta = \sqrt{10 / (5 + \xi)}$
- ξ : is the viscous damping ratio

The values of T_B , T_C , T_D for each ground type and shape of spectrum used depends on the country in concern.

2.1.3.2 Load combinations

As recommended in EN 1990, the following rules have been considered for the combination of loads with respect to static loads applied in a structure.

a) Fundamental combination

This combination is used for Ultimate Limit State (ULS) associated to determining of structure resistance and is given by equation 2.25:

$$\sum_j \gamma_{G,j} * G_{k,j} + \gamma_{Q,1} * Q_{k,1} + \sum_{i>1} \gamma_{Q,i} * \psi_{0,i} * Q_{k,i} \quad (2.25)$$

Where the coefficients $\gamma_{G,j}$ and $\gamma_{Q,i}$ are partials factors which minimize the loads which tend to reduce the solicitations and maximise the ones that increase them. The recommended values preconized by the Eurocode 0 for the partial safety factors are given in table 2.8.

Table 2.8. Partial safety factors for ULS combination

Partial factor	Favorable	Unfavorable
$\gamma_{G,j}$	1.35	1.00
$\gamma_{Q,1}$	1.50	0.00
$\gamma_{Q,i}$	1.50	0.00

b) Characteristic combination (rare)

Usually used for non-reversible Serviceability Limit States (SLS), this combination (2.26) has to be used in the verifications with the allowable stress method:

$$\sum_j G_{k,j} + P + Q_{k,1} + \sum_{i>1} \psi_{0,i} * Q_{k,i} \tag{2.26}$$

c) Frequent combination

Frequent combination (2.27) is recommended for reversible SLS:

$$\sum_j G_{k,j} + P + \psi_{1,1} * Q_{k,1} + \sum_{i>1} \psi_{2,i} * Q_{k,i} \tag{2.27}$$

d) Quasi-permanent combination

Generally used for long-term effects, it is given by equation 2.28:

$$\sum_j G_{k,j} + P + \sum_{i \geq 1} \psi_{2,i} * Q_{k,i} \tag{2.28}$$

The values recommended for the reduction factors are given in table 2.9.

Table 2.9. Multipliers for the characteristic values of variable loads

	Temperature load	Wind load	Traffic load	
			TS	UDL
ψ_0	0.6	0.6	0.75	0.4
ψ_1	0.5	0.2	0.75	0.4
ψ_2	0.5	0	0	0

2.2 Static design methodology

The static analysis will pass through stress verification at bottom and top of girder and at slab level. Investigation in the steel pier mainly subjected to compression will also be done.

2.2.1 Effective width of mixed section

The effective width of a mixed section depends on the position on bridge (edge, middle, supports, etc.). Equation (2.29) gives expression of b_{eff} and figure 2.3 shows the effective width.

$$b_{eff} = b_0 + b_{e1} + b_{e2} \tag{2.29}$$

Where: $b_{ei} = \min(L_e/8 ; b_i)$ (2.30)

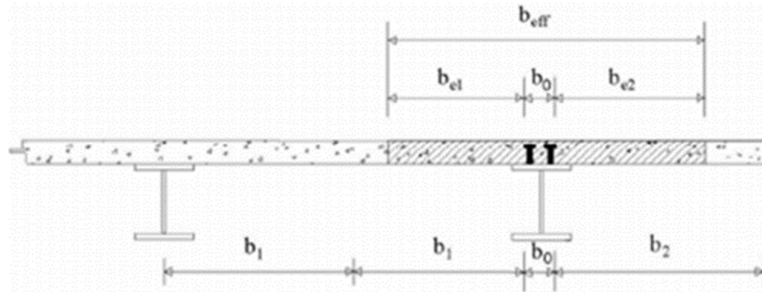


Figure 2.3. Effective width of composite deck

At the end support sections; equation 2.31 as formula of b_{eff} and equation (2.32) for value of β_i are used.

$$b_{eff} = b_0 + \beta_1 b_{e1} + \beta_2 b_{e2} \tag{2.31}$$

where: $\beta_i = (0.55 + 0.025 \cdot \frac{L_e}{b_{eff,i}}) \leq 1.0$ (2.32)

The value of influence length (L_e) can be obtained from Figure 2.4.

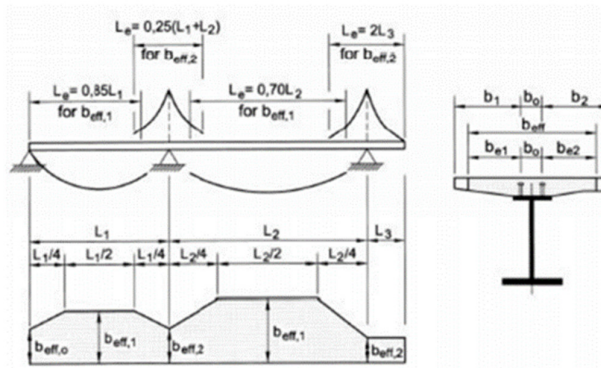


Figure 2.4. Influence length diagram

2.2.2 Geometric mixed section characteristics

The characteristics of mixed-section were calculated with respect to Figure 2.5, using the displayed local axis.

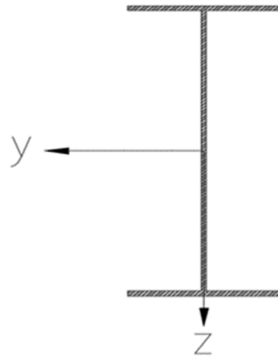


Figure 2.5. Mixed section with local axis (Self-made)

Geometric characteristics are summarized in table 2.10.

Table 2.10. Geometric characteristics of mixed-section

Steel-concrete homogenization coefficient at short-term	$n_0 = \frac{Es}{E_{cm}}$	(2.33)
Area of ideal mixed section	$A_{id} = A_{steel} + \frac{A_{slab}}{n_0} \quad \text{where} \quad A_{slab} = b_{eff} \cdot h_{slab}$	(2.34)
Coordinate y of gravity centre	$y_{id} = \frac{\sum A_i \cdot y_i + (A_{slab} \cdot y_{slab} / n_0)}{A_{id}}$	(2.35)
Moment of inertia of ideal mixed section	$J_{id} = J_{steel} + \frac{b_{eff} \cdot h_{slab}^3}{n_0} + \frac{A_{slab}}{n_0} (y_{id} - y_{slab})^2 + A_{steel} (y_{id} - y_s)^2$	(2.36)
Resistance modulus relative to slab upper section	$W_{up,slab} = \frac{J_{id} \cdot n_0}{y_{id} - h_{tot}} \quad \text{where} \quad h_{tot} = \sum h_i + h_{slab}$	(2.37)
Resistance modulus relative to slab lower section	$W_{low,slab} = \frac{J_{id} \cdot n_0}{y_{id} - y_{slab}}$	(2.38)
Resistance modulus relative to steel upper section	$W_{up,steel} = \frac{J_{id}}{(y_{id} - h_{steel})} \quad \text{where} \quad h_{steel} = \sum h_i$	(2.39)
Resistance modulus relative to steel lower section	$W_{low,steel} = \frac{J_{id}}{y_{id}}$	(2.40)

At time $t=\infty$, n_0 is replaced by n_L for long-term effects (phase 2).

2.2.3 Ultimate limit state

2.2.3.1 Stresses computation

To check the sections of the main beams, the stresses deriving from the application of the loads in the various phases must be found. These stresses are calculated considering the geometric and inertia characteristics relating to the analysed phase and their expressions are reported in table 2.11.

Table 2.11. Stress calculation

Stress at slab upper section	$\sigma_{up,slab} = \frac{N}{A_{id} \cdot n_0} + \frac{M}{W_{up,slab}}$	(2.41)
Stress at slab lower section	$\sigma_{low,slab} = \frac{N}{A_{id} \cdot n_0} + \frac{M}{W_{low,slab}}$	(2.42)
Stress at steel upper section	$\sigma_{up,steel} = \frac{N}{A_{id}} + \frac{M}{W_{up,steel}}$	(2.43)
Stress at steel lower section	$\sigma_{low,steel} = \frac{N}{A_{id}} + \frac{M}{W_{low,steel}}$	(2.44)

At time $t=\infty$, n_0 is replaced by n_L for long-term effects (phase 2).

For each section, allowable stresses for steel and concrete are given equations (2.45) and (2.46) respectively:

$$\sigma_{steel} < \sigma_{all} = f_{yk}/1.05 \tag{2.45}$$

$$\sigma_{slab} < f_{cd} = \frac{0.85f_{ck}}{1.5} \text{ or } f_{ctd} = \frac{0.15f_{ck}}{1.5} \text{ for parts in compression and } \tag{2.46}$$

tension respectively.

2.2.3.2 Classification of section

Table 2.12 permits us to classify sections depending on maximum solicitations obtained from static analysis.

Table 2.12. Maximum width-to-thickness ratios for compression parts (EN 1993-2, 2011)

Internal compression parts			
		Axis of bending	
		Axis of bending	
Class	Part subject to bending	Part subject to compression	Part subject to bending and compression
1			
	$c/t \leq 72\varepsilon$	$c/t \leq 33\varepsilon$	when $\alpha > 0,5$: $c/t \leq \frac{396\varepsilon}{13\alpha - 1}$ when $\alpha \leq 0,5$: $c/t \leq \frac{36\varepsilon}{\alpha}$
2			
	$c/t \leq 83\varepsilon$	$c/t \leq 38\varepsilon$	when $\alpha > 0,5$: $c/t \leq \frac{456\varepsilon}{13\alpha - 1}$ when $\alpha \leq 0,5$: $c/t \leq \frac{41,5\varepsilon}{\alpha}$
3			
	$c/t \leq 124\varepsilon$	$c/t \leq 42\varepsilon$	when $\psi > -1$: $c/t \leq \frac{42\varepsilon}{0,67 + 0,33\psi}$ when $\psi \leq -1^*$: $c/t \leq 62\varepsilon(1 - \psi)\sqrt{(-\psi)}$
$\varepsilon = \sqrt{235/f_y}$	f_y	235	275
	ε	1,00	0,92
			355
			420
			460
			0,75
			0,71

*) $\psi \leq -1$ applies where either the compression stress $\sigma \leq f_y$ or the tensile strain $\varepsilon_y > f_y/E$

2.2.3.3 Shear verification

The maximum shear under previous load combinations will be considered. A look at plastic resistance of sections to vertical shear, shear buckling resistance will be done. It will be checked if there is no interaction between moment and shear.

a) Plastic resistance

For verifying the design plastic shear resistance $V_{c,Rd}$ the criterion expressed by equation (2.47) for a critical point of the cross section may be used :

$$V_{Ed} \leq V_{pl,Rd} = A_v \frac{f_y}{\gamma_a \sqrt{3}} \tag{2.47}$$

Where:

V_{Ed} is the design value of the shear force;

A_v is the resisting shear area.

b) Shear buckling resistance

The shear buckling resistance $V_{b,Rd}$ of steel web is taken from equation (2.48).

$$V_{b,Rd} = V_{bw,Rd} + V_{bf,Rd} \leq \frac{\eta f_{yw} h_w t}{\sqrt{3} \gamma_{M1}} \quad (2.48)$$

In which the contribution from the web is given by equation (2.49).

$$V_{bw,Rd} = \frac{\chi f_{yw} h_w t}{\sqrt{3} \gamma_{M1}} \quad (2.49)$$

$V_{bf,Rd}$ is the contribution from the flanges and η is taken as 1,00.

c) Interaction between shear and moment

To attest that there is no interaction between shear (V_{Ed}) and bending moment M_{Ed} , the criterion in equation (2.50) has to be verified:

$$V_{Ed} \leq 0.5 \min\{V_{pl,Rd}; V_{b,Rd}\} \quad (2.50)$$

2.2.3.4 Studs design

Shear connectors shall be capable of preventing separation of the concrete element from the steel element. To prevent it, they will be designed under previous designed shear T_{Ed} .

The design shear resistance of a stud is given by equation (2.51):

$$P_{Rd} = \min \left\{ \begin{array}{l} P_{Rd1} = \frac{0.8 f_u \pi d^2 / 4}{\gamma_v} \\ P_{Rd2} = \frac{0.29 \alpha d^2 \sqrt{f_{ck} E_{cm}}}{\gamma_v} \end{array} \right. \quad (2.51)$$

Where:

$$\alpha = 0.2 \left(\frac{hs}{d} + 1 \right) \text{ for } 3 \leq hs/d \leq 4 \quad \text{or } \alpha = 1 \text{ for } h/d > 4$$

P_{Rd1} is the stud resistance;

P_{Rd2} is the concrete resistance;

d is the diameter of the shank of the stud, $16 \text{ mm} \leq d \leq 25 \text{ mm}$;

f_u is the specified ultimate tensile strength of the material of the stud;

h_s is the overall nominal height of the stud;

γ_v is the partial factor and the recommended value is 1,25.

Considering ULS and dynamic load the stud will be designed with value from equation (2.52).

$$\overline{P_{Rd}} = \frac{P_{Rd}}{\gamma_s \gamma_d} \quad (2.52)$$

Where $\gamma_s = \gamma_d = 1.5$ are ULS and dynamic factors respectively.

To obtain the number of studs per meter, it is necessary to get first the shear stress per meter. It is taken from equation (2.53).

$$\tau_b = \frac{V_{Ed} \cdot S}{J_{id}} \quad \text{with } S = \frac{A_{slab}}{n_o} (y_{slab} - y_{id}) \quad (2.53)$$

Where:

τ_b is the shear stress per meter;

V_{Ed} is the design shear force;

S is the static moment of the mixed section;

J_{id} is the moment of inertia of the mixed section.

The number of studs per meter is then:

$$n_s = \frac{\tau_b}{\overline{P_{Rd}}} \quad (2.54)$$

2.2.3.5 Buckling resistance

Members which are subjected to axial compression should satisfy equation (2.54).

$$\frac{N_{Ed}}{N_{b,Rd}} \leq 1,0 \quad (2.54)$$

Where $N_{b,Rd}$ is the design buckling resistance of the compression member. It is expressed by equation 2.55.

$$N_{b,Rd} = \frac{\chi \cdot A_{eff} \cdot f_y}{\gamma_{M1}} \quad (2.55)$$

$$\bar{\lambda} = \frac{L_{cr}}{i} \frac{1}{\lambda_1} \quad (2.56)$$

Where:

- $\bar{\lambda}$ is the slenderness ratio;
- χ is the reduction factor;
- L_{cr} is the buckling length in the buckling plane considered;
- i is the radius of gyration about the relevant axis.

2.2.3.6 Steel Pier verification

Verifications will be done according to *EN 1993-1.1*. Classification of pier will be done according to table 2.14. Following that, resistance to compression has to be checked. The design value of the compression force N_{Ed} at each cross-section shall satisfy equation (2.57).

$$\frac{N_{Ed}}{A_{eff}} + \frac{M_y}{W_y} \leq \frac{f_y}{\gamma_{M0}} \quad (2.57)$$

Since steel member are slender, compression is mainly associated with buckling, hence the resistance check must take into account this effect. For members subjected to axial compression, the design value of the compressive force N_{Ed} at each cross-section shall satisfy the following inequation:

$$N_{Ed} \leq N_{c,Rd} \quad (2.58)$$

$N_{c,Rd}$ is the minimum between:

$$N_{pl,Rd} = \frac{A \cdot f_y}{\gamma_{M0}} \quad (2.59)$$

$$N_{o,Rd} = \frac{A_{eff} \cdot f_y}{\gamma_{M1}} \quad (2.60)$$

A_{eff} is the effective area that accounts the effects of local buckling. The first formula (2.59) is related to the class 1, 2 or 3 and the second formula is related to elements in 4th class only, for which $A_{eff} < A$.

These formulas are related to strength of the compressed element (when buckling is prevented). The buckling resistance will be evaluated on the same way as explained in the previous section.

For cross-section strength, it must be verified that:

$$\frac{M_{Ed}}{M_{c,Rd}} \leq 1 \quad (2.61)$$

Where:

$$\text{For class 1 or 2 cross sections, } M_{c,Rd} = \frac{W_{pl} \cdot f_y}{\gamma_{M0}} \quad (2.62)$$

$$\text{For class 3 cross sections, } M_{c,Rd} = M_{el,Rd} = \frac{W_{el,min} \cdot f_y}{\gamma_{M0}} \quad (2.63)$$

$$\text{For class 4 cross sections, } M_{c,Rd} = \frac{W_{eff,min} \cdot f_y}{\gamma_{M0}} \quad (2.64)$$

The shear action verification will be evaluated on the same way as explained in the previous section.

2.2.3.7 Cross beams verifications

The shear action and bending verification will be evaluated the same way as explained in the previous section. Also, regarding the verification due to compression will be done in the same way.

For members in axial tension the design value of the tensile force, the design value of the tensile force N_{Ed} at each cross-section should satisfy the following equation:

$$N_{Ed} \leq N_{t,Rd} \quad (2.65)$$

Where $N_{t,Rd}$ is the minimum between:

- Design plastic resistance of gross cross section

$$N_{pl,Rd} = \frac{A \cdot f_y}{\gamma_{M0}} \quad (2.66)$$

Where:

A is the gross cross section area;

f_y is the yield strength of steel;

γ_{M0} is the partial safety factor;

- Design ultimate resistance of the net cross section at holes for fasteners

$$N_{u,Rd} = 0,9 \frac{A_{net} \cdot f_u}{\gamma_{M2}} \quad (2.67)$$

Where:

- A_{net} is the net cross section area;
 f_u is the ultimate strength of steel;
 γ_{M2} is the partial safety factor;

2.3 Numerical modelling

In this section, software used for modelling and different analyses will be presented. The software used in this thesis for different analyses is MIDAS/civil.

2.3.1 Steel composite frame bridge modelling

A three-dimensional computational model of the bridge was created in MIDAS/Civil for static analysis and verification throughout an optimization process in order to obtain the best configuration of the bridge.

The structural elements (girders, piers, cross and transverse beams) for numerical simulation are modelled using 1D fibre beam element since the variation in the section due to the torsional stress is prevented. In the analysis, these elements are connected to each other by a fixed joint with zero degrees of freedom as is done in the practice of such bridges.

Steel piers are directly connected to the girders while rigid links are used to create the appropriate connection between the deck and piers.

The base of the piers is considered fully restrained in rotation and translation since they are supposed to be embedded in a massive concrete foundation at their bases. The end spans of the bridge are connected to the end spans substructure (abutments) with bearings. Abutments were replaced by fixed constraints and elastic links with high vertical stiffness were used as bearing at both bridge end. They were also placed above transversal beam as bearings.

2.3.2 Midas Civil description

To do static analysis of the bridge under permanent and variable loads, MIDAS/civil was used.

The different modules that will be used are presented as follows:

- Properties: this section is meant for definition of material and section properties of different elements (girders, slab, cross beams, piers and transversal beams);
- Boundary: here it is defined boundary restrains, rigid and elastic links of our bridge;
- Loads: loads cases are defined here (self-weight, moving loads, element loads, nodal loads);
- Analysis: to apply the static analysis;
- Results: different results (displacements, stresses, moments, axial, shear forces...) can be displayed.

2.4 Seismic study

Any structure located in a seismic zone is likely to undergo during its live duration a dynamic excitation of a seismic nature. Therefore, determining the seismic response of the structure is essential during the analysis and design of the latter. Thus, the calculation of a bridge subjected to the earthquake aims to assess the loads likely to be generated in the structural system during the earthquake.

Within the framework of our project, the determination of these efforts is carried out by the software Midas Civil.

2.4.1 Response spectrum analysis

The most used current practice consists in defining the seismic loading by a response spectrum. Once the response spectrum has been injected into the data file, the seismic response or demand is obtained under different load combinations (G, Q and E).

The response spectrum analysis is an elastic calculation of the peak dynamic responses of all significant modes of the structure, using the ordinates of the site dependent design spectrum (EN 1998-1:2004).

The ability of structural systems to resist seismic actions in the nonlinear domain generally allows them to be designed to resist forces lower than those corresponding to a linear elastic response. In order to avoid performing an explicit inelastic structural analysis for design purposes, the energy dissipation capacity of the structure, obtained mainly through the ductile behaviour of its elements and/or other mechanisms, is taken into account by performing an elastic analysis based on a reduced response spectrum, hereafter referred to as the "design spectrum". This reduction is by introducing the behaviour factor q .

For the horizontal components of the seismic action, the design spectrum, $S_d(T)$, shall be defined by the following expressions:

$$0 \leq T \leq T_B: S_d(T) = a_g S \left[\frac{2}{3} + \frac{T}{T_B} \left(\frac{2.5}{q} - \frac{2}{3} \right) \right] \quad (2.68)$$

$$T_B \leq T \leq T_C: S_d(T) = a_g S \frac{2.5}{q} \quad (2.69)$$

$$T_C \leq T \leq T_D: S_d(T) = a_g S \frac{2.5}{q} \left[\frac{T_C}{T} \right], \text{ with } \geq \beta \cdot a_g \quad (2.70)$$

$$T_D \leq T: S_d(T) = a_g S \frac{2.5}{q} \left[\frac{T_C T_D}{T^2} \right], \text{ with } \geq \beta \cdot a_g \quad (2.71)$$

Where:

$S_d(T)$ is the design spectrum;

q is the behaviour factor;

β is the coefficient corresponding to the lower limit of the horizontal design spectrum.

Recommended value is 0.2

In order to obtain the demand displacement from the response spectrum analysis in Midas Civil, the following procedures must be applied:

- First obtain the cracked section properties (mostly used for reinforced concrete) by computing the effective moment of inertia as shown in equation 2.76 (EC8).

The mathematical model should represent the stiffness of individual structural elements considering material properties and section dimensions. When an elastic analysis is used to determine the response of an inelastic structure, several assumptions are necessary, of which the most important is that stiffness may be based on an equivalent linearized value. For inelastic columns, common practice is to use cracked section properties for concrete members and full section properties for steel members (the stiffness of structural steel members should be based on elastic properties, that is full section properties). For reinforced concrete piers, stiffness should be based on cracked section properties).

$$J_{eff} = 0.08J_{un} + J_{cr} \quad (2.72)$$

Where:

J_{un} is the moment of inertia of the gross section of the uncracked pier;

is the moment of inertia of the cracked section at the yield point of the tensile reinforcement;
 J_{cr}

J_{cr} may be obtained from the expression

$$J_{cr} = \frac{M_y}{E_c \phi_y} \quad (2.73)$$

In Midas Civil J_{cr} may be estimated based on M-phi analysis in MIDAS GSD.

- Then the response spectrum analysis should be performed. In Midas Civil there is various design codes to implement the response spectrum functions (EC8 will be used). The seismic action should be performed for the major axis of the structure and various damping method is also provided (Model, Mass and stiffness proportional, Strain energy proportional).

Due to damping, modal combination should be specified using either the Square Root of Sum of the Squares (SRSS) or the Complete Quadratic Equation (CQC). SRSS is more useful when the modes shapes are well separated and CQC is more appropriate in the other case and it is recommended for nearly all bridges. Noticed that the useful mode shape for the modal combination will be selected.

For the modal analysis, the eigen value analysis must be performed using the eigen vectors or the ritz vectors which is also useful when a certain direction of the mode must be performed.

2.4.2 Results obtained from Midas Civil

As the results the natural period and frequency of the structure, modal participation masses and eigen vectors could be obtained.

It is important to check the results of the RSA analysis if the behaviour of the bridge has been properly identified. The check is normally done by verifying that the cumulative mass participation is at least 90%. The governing period of the structure should be noted because this value is checked versus project and code requirements.

And then also demand displacement could be obtained. In the Eurocode in order to obtain the design demand displacement, the displacements provided by the results must be known first and the design displacement will be computed as follow:

$$d_E = \pm \eta \mu_d d_{Ee} \quad (2.74)$$

Where:

η is the damping correction factor;

μ_d is the displacement ductility factor;

- If $T \geq T_0 = 1.25T_c$, $\mu_d = q$
- If $T \geq T_0 = 1.25T_c$, then $\mu_d = (q - 1) T_0/T + 1 \leq 5q - 4$

d_{Ee} is the displacement derived from a linear elastic analysis based on the elastic spectrum;

q is the behavior factor.

Either the SRSS or the complete CQC modal combination rules are applicable. The design seismic action effects A_{Ed} should be derived from the most adverse of the combinations from the 100-30 rule (100% seismic effect in one direction plus 30% of seismic action in orthogonal direction).

2.5 Pushover analysis

Pushover analysis is a widely used nonlinear static calculation method for assessing the seismic performance of structures. It compares the demand to the capacity of the structure and help us to obtain the performance point which is the intersection between the demand and the capacity curve.

Demand is the representation of earthquake ground motion or shaking that the bridge is subjected to and it is represented by an estimation deformation that the structure is expected to undergo. Thus, capacity is a representation of the structure ability to resist the seismic demand and the performance point is dependent on the manner that the capacity is able to handle the demand.

At the end of this procedure, the estimation of the sequence and final pattern of the plastic hinge formation, the estimation of the redistribution forces following the plastic hinge formation, the assessment of the capacity curve and of the deformation demand up to the target displacement will be obtained.

This procedure will be completely done in Midas Civil.

2.5.1 Pushover analysis model in Midas Civil

For our analysis, the capacity curve of the structure is determined by performing the following steps:

- Step 1: Definition of the nonlinear behaviour of the elements.
- Step 2: Definition of the loading of the nonlinear static analysis (Pushover).

- Step 3: Nonlinear static analysis and extraction of the capacity curve.

2.5.2 Pushover global control definition

First of all, for the pushover analysis, specify the global control need to be specified. It includes the:

- **Initial load:** enter the initial load (in general the gravity loads) for pushover analysis.
- **Convergence criteria:** specify the maximum number of (iterations) sub-iterations and a tolerance limit for convergence criterion.
- **Stiffness reduction ratio:** specify stiffness reduction ratios after the 1st and 2nd yielding points (1st yielding for bilinear curve, 1st and 2nd yielding for trilinear curve) relative to the elastic stiffness.
- **Reference location for distributed hinge:** specify the reference location for calculating yield strength of beam elements which distributed hinge is assigned.

2.5.3 Pushover Load Cases

The pushover analysis consists in applying to the structure a distribution of the lateral forces gradually incremented until the displacement at the top of the structure reaches a target displacement (analysis in "Controlled displacement" mode).

This type of analysis is carried out when the loads are not known, or when increasing loads during analysis may cause instability of the structure.

In addition to the analysis in "Controlled displacement" mode, the program offers the possibility perform analyses in "Controlled force" mode, this type of analysis is chosen when the loads applied to the structure are known and are unlikely to cause the instability of the structure (e.g., gravity push).

It will be either apply a horizontal force in increment or a horizontal displacement in a form of increment, this will be done accordingly to the procedure detailed in the informative annex H of the Eurocode 8, part 2. Notice that two type of loads pattern will be used to define pushover load cases, which are the loading under static loads (uniform loads, gravity loads) and the horizontal one (mode shape with mass).

2.5.3.1 Horizontal load increment

This is done applying the force node and increasing it step by step. The horizontal load increments $\Delta F_{i,j}$ assumed acting on lumped mass M_i in the direction investigated, at each load loading step j , should be taken as equal to:

$$\Delta F_{i,j} = \Delta \alpha_j g M_i \zeta_i \quad (2.75)$$

Where:

$\Delta \alpha_j$ is the horizontal force increment, normalized to the weight gM_i , applied in step j ;

ζ_i is the shape factor defining the load distribution along the structure;

2.5.3.2 Load distribution method

This is applied following the mode shape obtained from the eigen value analysis. Unless a better approximation is used, both of the following distributions should be investigated:

- Constant along the deck, where:

- For the deck, $\zeta_i = 1$
- For the piers connected to the deck, $\zeta_i = \frac{Z_i}{Z_p}$ (2.76)

Where:

Z_i is the height of point I above the foundation of the individual pier;

Z_p is the total height of pier P (distance from the ground to the centreline of the deck);

- Proportional to the first mode shape, where:

ζ_i is proportional to the component, in the considered horizontal direction, of the modal displacement at point i of the first mode, in the same direction. The mode with the largest participation factor in the considered direction, should be taken as first mode in this direction. Especially for the piers, the following approximation may be used alternatively:

$$\zeta_i = \zeta_{T,P} \frac{Z_i}{Z_p} \quad (2.77)$$

Where:

$\zeta_{T,P}$ is the value of ζ corresponding to the joint connecting the deck and pier;

2.5.4 Nonlinear behaviour definition of the elements

2.5.4.1 Plastic hinge definition and assignation

Generally, for the general shape of a section such as buildings, the hinge properties suggested for the FEMA or the Eurocode can be used, but for the bridge section where the

section is quite irregular and the size of the section is very huge, it will be necessary to separately calculate the hinge primary curve. For this, the Midas GSD (General Section Designer) will be used and linking the properties defined with the pushover model, the hinge length must be defined and express as follow:

$$L_p = 0,10L + 0,015f_{yk}d_{bl} \quad (2.78)$$

Where:

- L is the distance from the plastic hinge section to the section of zero moment, under the seismic action;
- f_{yk} is the characteristic yield stress (in MPa)
- d_{bl} is the bar diameter

After it, the hinge properties could be applied to the steel pier and perform the pushover analysis.

The nonlinear behaviour of the piers is represented by the concentrated attribution of the plastic hinges at the starts and ends of the elements where one assumes that bending yield occurs. The bending characteristics of the piers are defined by moment-rotation relations assigned as moment hinges to the bottom and top of the piers. A three-dimensional interaction surface with five moment interaction equidistant axial-bending force diagrams and a relationship moment-rotation are defined to represent the bending characteristics of the plastics hinges at the ends of the post.

For our calculation model, plastic hinges will be introduced into the pier with behaviour laws defined by default by the software. The properties of the plastic hinges defined by default were used to execute pushover analysis.

Girders and piers are modelled by elements with linear elastic properties.

2.5.4.2 Damage level

The plastic deformation curve is a force-displacement (moment-rotation) curve which gives the value of plasticization and plastic deformation after plasticization and will be used to describe the level of damage of the structure and particularly of the plastic hinges at every step. This curve consists of five points as shown in the figure 2.6.

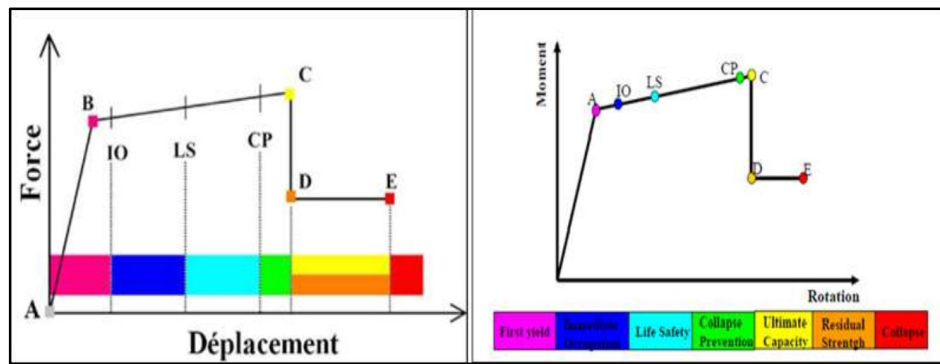


Figure 2.6. Force-displacement or moment-rotation curve for a hinge definition used in Midas Civil (plastic deformation curve)

- Point (A) represents the origin.
- Point (B) represents plasticization, no deformation at the hinge, all elastic deformations are ignored.
- Point (C) represents the ultimate capacity for pushover analysis.
- The point (D) represents the residual resistance for the pushover analysis.
- The point (E) represents the total failure of the elements.

Before reaching point B, the deformation is linear and occurs in the frame member itself, and not in the hinge.

Plastic deformation beyond point B occurs in the hinge in addition to any which elastic deformation may occur in the element, the residual resistance to from D to E allows framing members to support gravity loads.

The user can specify additional strain measurements at points IO, LS and CP, these are informational measures that are reported in the results analysis and used for performance-based design, having no effect on the behaviour of the structure.

According to FEMA-273:

- **The IO (Immediate Occupancy) level:**

Indicates that the state of damage following the earthquake is very limited, the resistance systems of horizontal and vertical forces of the construction retain their strength approximately and pre-earthquake stiffness. The danger to life presented by structural damage is very small, despite this, some simple structural repairs need to take place which are not generally payable before the reuse of the construction.

- **The LS (Life Safety) level:**

Indicates that the state of post-earthquake damage suffered by the structure is significant, but there is a margin against collapse, some structural elements and components are badly damaged, but this does not lead to the fall of significant debris. The damage may occur during the earthquake, but the danger to life resulting from such damage is low, construction use may be prohibited until repaired.

- **The CP (Collapse Prevention) level:**

It indicates that the construction is about to face a partial collapse or total, as it indicates that the great damage suffered by the structural elements and not structural with the probability of a very great degradation in the rigidity of the systems of lateral loading resistance with the presence of a tiny margin against collapse, at this level and in the presence of a great degradation of the resistance systems of the side loading, it is imperative for the main elements of resistance systems to the forces of gravity must continue to resist. There may be a great danger because of the falling structural debris and it is not technically practical to repair the structure. It is to avoid loss of life and property; the structure can cause serious damage during a major earthquake, but it must remain upright after the movement of earth. So, the design of more than one level of seismic attack intensity must be adopted as a basic philosophy of seismic design in terms of displacement, the structural response can be related to a strain limit state, which in turn assumed to be related to some level of damage.

The deformations (IO, LS, CP) define the level of damage to the hinges.

Conclusion

This chapter was about the methodology used in this thesis in order to have the response of a steel composite frame bridge under seismic action. This was started by establishing the procedure of conception of the model to study till material properties. In order to perform analysis, a clear methodology to obtain loads acting on the structure and various load combination was done. The design limit state follows and different verifications were explained. Then seismic analysis approach was presented and it was explained how the collapse prediction, evaluation of the robustness of the bridge and observation of the sequential formation of the plastic hinges due to the non-linearity behaviour of the steel piers will be assess. Finally, software used and bridge modelling were presented and the theories related to seismic loads prediction, modelling and FEM analysis involved. The final chapter will present the results of previous detailed methods and the answer to the main objective of this thesis.

CHAPTER 3: RESULTS AND INTERPRETATIONS

Introduction

This section presents the results obtained from previous detailed methodology outlined in Chapter 2. First, the conceived case study which is a hypothetical steel composite frame bridge inspired from the steel bridge over the highway between Padova and Venezia with the different structural elements will be shown; details on materials will also be given. Secondly, a static analysis and verifications under Ultimate Limit State will be done in order to assess bridge stability. Then a modal analysis will be used to determine the bridge's inherent modes and frequencies as well as all of their dynamic features. Next, prior to a response spectrum analysis to obtain the seismic demand of the structure, nonlinear static analysis commonly called pushover analysis will be performed to outcome effects of seismic load on the bridge. At the end, the performance point of the structure will be checked and some plastic hinges scheme will be analysed to check possible collapse mechanism.

3.1 Presentation of the case study

Elements which allow us to present the conceived case study are geometric data and statistic data.

3.1.1 Bridge geometry and structural solution

The generic bridge under this study is a steel composite frame bridge. The conceived bridge is an integral part of a roadway and connects the road section interrupted by a road highway, it is a first-class bridge commonly for international heavy vehicle traffic.

The bridge is made of a mixed steel-concrete structure, consisting of two "double T" beams with a static scheme of a frame. The elevating structure consists of two piers rigidly connected to the deck and two abutments linked to the deck by a unidirectional pot bearing (low friction bearing) permitting expansion at both end of the bridge only in the longitudinal direction and fixed in the transverse, with a distance between an abutment and a pier of 15 m and a distance between a pier and another pier of 30 m, for a total longitudinal length of 60 m.

The transverse width of the deck is 8 m divided into two 3 m lanes and two 1 m sidewalks. The structural solution proposed for the superstructure is defined by two steel beams with a center distance of 8 m with a collaborating concrete slab of 25 cm thick. The transversal section has been heavily diaphragmed to deal with possible phenomena of loss of shape due to eccentric loads. The crosspieces are transverse beams, composed of H-profiles

(HEA700) coupled with steel plates and placed in the longitudinal direction of the bridge with 3 m interaxis to reduce moments for the easy transmission of loads to the twin girder and directly supporting the deck slab, they also serve as diaphragms to resist lateral forces and transfer loads to supports which are needed for lateral stability during erection and for resisting and transferring earthquake loads. The transverse beams also contribute to the provision of torsional restraint to the bridge deck.

For the analysis of the structure, a tridimensional model with Midas/Civil Software was used. Midas/Civil is a software for the advanced calculation of structures, particularly bridges. It is a very complete tool that allows the modelling of any type of bridge and using different types of materials. The software allows to define the complete constructive process of the bridge and to consider the rheological effects of each element. The modelling is completely parametric, so that any modification that is necessary to introduce, is updated in the whole structure, including in the loads already defined. Figure 3.1, figure 3.2 and figure 3.3 show some representations of the bridge model.

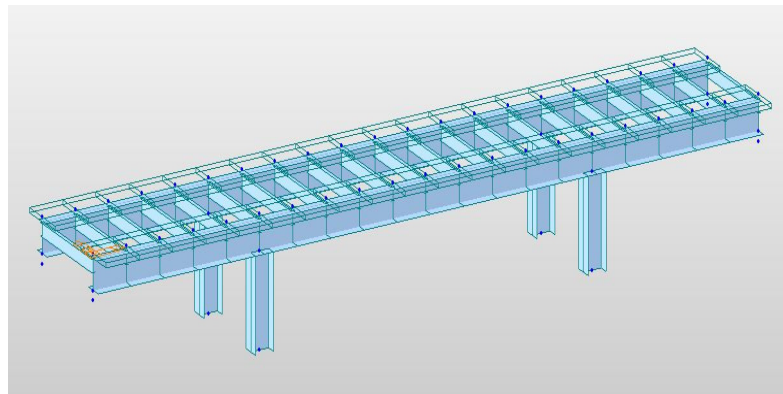


Figure 3.1. Longitudinal view of the bridge model

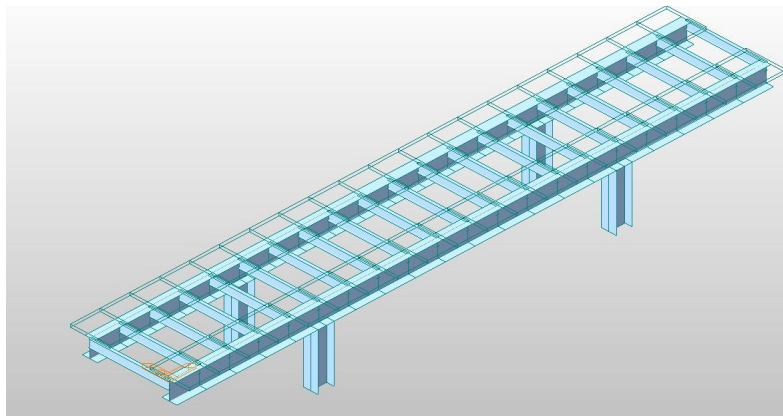


Figure 3.2. Isometric view of the bridge model

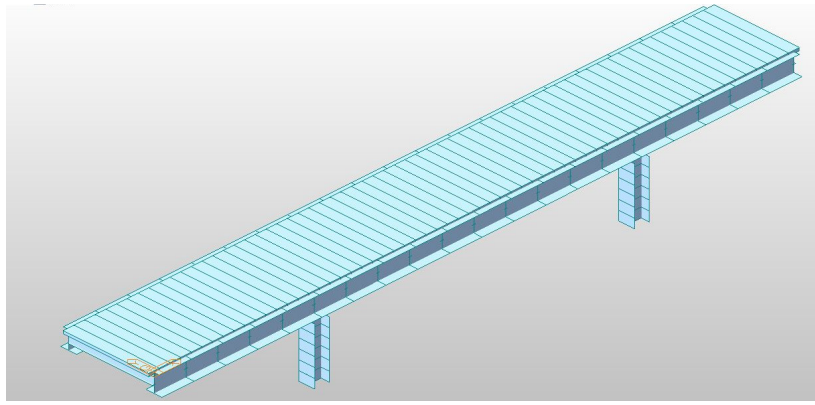


Figure 3.3. Steel frame composite bridge

On these views, the bridge length is along the X direction. Y direction is for transversal width of bridge and Z axis is for height.

As seismic design alternatives, the superstructure-pier connections were defined as a moment-resisting connection. It is a continuous superstructure (continuous deck), with this rigid piers-superstructures connections, longitudinal superstructure movements could be accommodated by flexing of the piers about the transverse axis.

As the final objective of this seismic analysis is to obtain results that refer to the substructure (piers) behaviour, the global model was adopted in this analysis, consisting only of beam elements. This type of model allows not to overload the software with unnecessary information for the effect of this analysis decreasing the calculation time and to obtain viable results.

The nonlinear behaviour between the soil and the structure will not be considered due to lack of geotechnical information and because this would imply having to define the foundations of the bridge in the general model with the corresponding nonlinear behaviour.

Soil structure interaction is not considered in this work and therefore foundations are assumed to be perfectly rigid. The study focuses only on structural aspects with no consideration for soil structure interaction aspects (rigid foundations assumptions).

The connections between the deck and the abutments were modelled using simple supports, which allow displacements in the longitudinal direction and restricts them in the transversal direction.

The piers were modelled using beams elements and the deck is represented by 2 longitudinal beams and cross bars that simulate the transversal stiffness of the deck.

“Shear Lag” effects are not considered in this model because stress analysis of the deck will not be carried out. The modelling in Midas Civil 2022 starts with constructing the section

with its real geometry and the software places the beams in the position of the center of gravity creating rigid bonds between different elements, making the modelling easier.

The transversal section of the deck is shown in figure 3.4 and the longitudinal elevation of the bridge in figure 3.5.

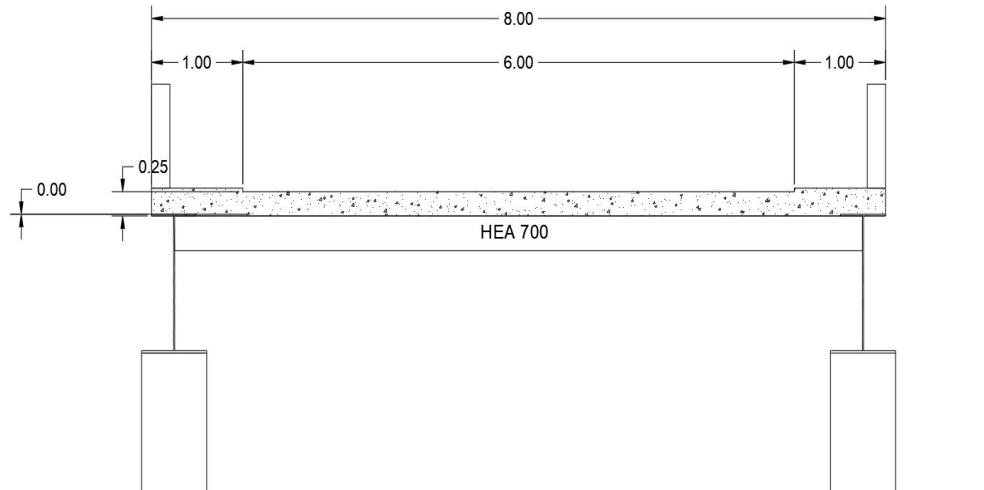


Figure 3.4. Transversal section of the deck

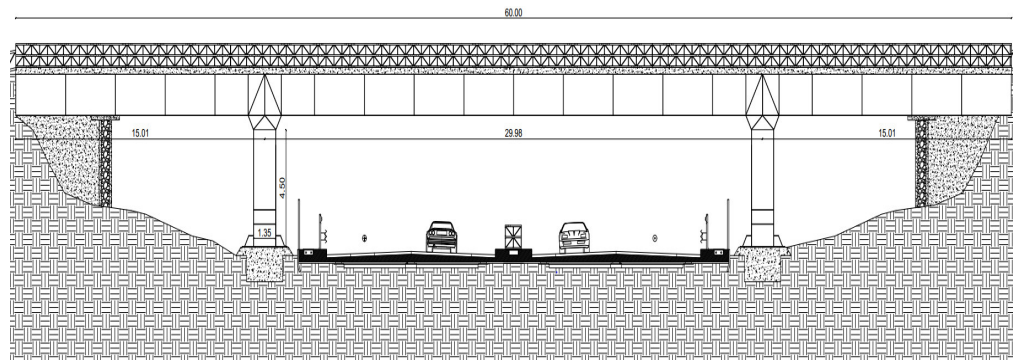


Figure 3.5. Bridge elevation

The preliminary design that permits us to obtain the cross-sections used to model the structural elements will be presented later.

3.1.2 Statistical data

Statistic data will deal with presentation of data link to characteristics of concrete and steel used.

3.1.2.1 Characteristics of slab

The slab concrete belongs to C32/40 resistance class with normal setting (N). For steel reinforcement, B450C was considered. The principal characteristics of concrete and steel reinforcement used in this analysis are reported in tables 3.1 and 3.2 respectively.

Table 3.1. Characteristics of concrete

Designation		C32/40	
Cylindrical Characteristic Strength	f_{ck}	32	MPa
Average Cylindrical Strength	f_{cm}	40	MPa
Average Tensile Strength	f_{ctm}	3.02	MPa
Average Flexural Strength	f_{cfm}	3.63	MPa
Elastic Modulus	E_{cm}	33345.76	MPa
Cracked Elastic Modulus	$E_{cracked}$	16672.88	MPa
Cylindrical Design Strength	f_{cd}	18.13	MPa
Design Tensile Strength	f_{ctd}	1.41	MPa

Table 3.2. Characteristics of steel reinforcement

Designation		B450C	
Characteristic Ultimate Strength	f_{uk}	540	MPa
Characteristic Yield Strength	f_{yk}	450	MPa
Elastic Modulus	E_s	210000	MPa
Design Yield Strength	f_{yd}	391.30	MPa

3.1.2.2 Exposure classes and concrete cover

The design working life of bridge is 100 years. Requirements on concrete cover are established based on the link between the environmental conditions and the protection of reinforcement. Exposure classes of concrete are the following:

- For top of slab: XC3 due to moderate humidity
- For slab bottom: XC3 due to moderate humidity
- For concrete cast-in place: XC4 and XS1 (exposed to airborne salt but not in direct contact with sea water).

In order to ensure the durability of the structure, EC2 indicates the minimum concrete cover value that must be respected depending on the environmental exposure classes.

With reference to a useful service life of 100 years and to a structural class S4, it is decided to assume a cover of 50 mm for all the elements employed in the structure.

3.1.2.3 Shear connectors and structural steel

Stud shear connectors in S235J2G3 steel grade are adopted. Their ultimate strength is $f_u = 450\text{MPa}$.

Materials features of structural elements (steel girders, steel piers, cross beams) are reported in table 3.3.

Table 3.3. Material of structural steels elements

Designation	S 355 NH/NLH		
Characteristic Ultimate Strength	f_{uk}	490	MPa
Characteristic Yield Strength	f_{yk}	355	MPa
Elastic Modulus	E_s	210000	MPa
Design Yield Strength	f_{yd}	338.10	MPa

Plastic properties for S355 are defined following Tresca yield criterion which is suitable for ductile materials such as metals. Plastic materials are defined because of the nonlinear analysis that will be done further.

3.2 Structural analysis of the steel frame bridge

According to some principles enumerated in the second chapter, a preliminary design has been done and modified to find good cross sections. Eurocodes and some physical properties of materials help us to calculate different loads values and assess static analysis verifications.

3.2.1 Preliminary design of structural elements

This part presents preliminary design and shows good sections of structural bridge elements. This case study was inspired from a real existing bridge, which has been transformed to fit geometrical regularity conditions (EC8-2) in terms of spans distributions, piers height and sections, as well as skew and curvature (straight bridge).

3.2.1.1 Span proportions

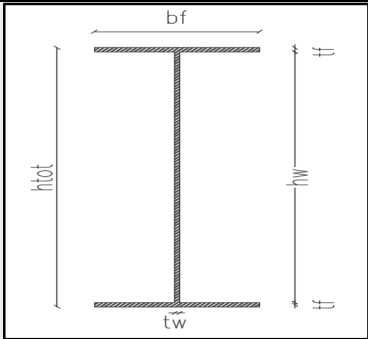
Span ratios for the conventional steel composite frame bridge structure vary according to use. Composite bridges, offers tremendous flexibility in terms of spans distributions. For a bridge crossing a fairly topographic gap featuring major obstructions (waterway, railways, roads or motorways), the ratio between the end span length and standard span length can decrease up to 0.6 without vertical support adjustment and to as little as 0.5 with vertical support adjustment.

It was chosen to round up the ratio to 0.7 and took a bridge that consists of two lateral spans of 15 m long and a main span of 30 m long.

3.2.1.2 Deck cross-section

Characteristics of deck elements are reported in table 3.4.

Table 3.4. Girder geometry

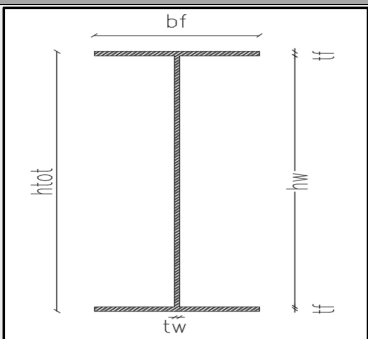
Geometry	Properties	Values	Units
	Total height $htot$	1600	mm
	Flange thickness tf top	30	mm
	Flange thickness tf bottom	50	mm
	Flange width bf	1000	mm
	Web thickness tw	16	mm
	Area	129320	mm ²
	Moment of inertia Iyy	4,79.10 ⁹	mm ⁴

For cross beams, geometrical characteristics are the one provided for HEA 700 hot rolled structural steel sections.

3.2.1.3 Piers sections

For the pier's height and dimensions, it was chosen first the same sections as the main girders, but due to the fact that the sections of the piers must be from class 1 or 2 to develop further a nonlinear analysis, the dimensions were adapted. The piers are 4.5 m high; this was chosen to reduce the buckling effects and thus the second order effects due to the slenderness of steels elements. Tables 3.5 detailed their geometry.

Table 3.5. Pier's geometry

Geometry	Properties	Values	Units
	Total height $htot$	1350	mm
	Flange thickness tf top	100	mm
	Flange thickness tf bottom	100	mm
	Flange width bf	1500	mm
	Web thickness tw	100	mm
	Area	415000	mm ²
	Moment of inertia Iyy	1,32.10 ¹⁰	mm ⁴

3.2.2 Loads computation

Permanent and variable loads values acting on the bridge must be found.

3.2.2.1 Self-weight of structural elements (g_1)

Table 3.6 shows a self-weight estimation concerning structural steel (g_{1a}) and concrete slab (g_{1b}), both expressed as distributive loads. In order to take into account, the weight of the joints, stiffening plates, etc. the weight of the steel box is increased by a 15% factor.

Table 3.6. Self-weight of structural elements

Loads	Weight density [kN/m ³]	g_1 [kN/m]
g_{1a}	76.98	14.87
g_{1b}	25	6.25
Total	/	21.12

3.2.2.2 Self-weight of non-structural elements (g_2)

Self-weights of non-structural elements are summarised in the following table:

Table 3.7. Self-weights of non-structural elements

Elements	Number	Weight density (kN/m ³)	Width (m)	Thickness/height (m)	Characteristic value (kN/m)
Safety barrier	1	/	/	/	2.5
Road pavement	1	24	1.00	0.17	4.08

3.2.2.3 Shrinkage

Values of different coefficients and axial force value obtained for shrinkage figured in table 3.8.

Table 3.8. Shrinkage computation

Relative humidity	RH	0.90	
Perimeter of concrete section exposed to air	u	14500	mm
Area of slab without predalles	A_c	3500000	mm ²
Fictitious dimension of the element	h_0	483	mm
From tables, for $t_0 = 7$ days	$\phi_{(\infty, t_0)}$	2.38	
	kh	0.69	
	$\varepsilon_{d,0}$	-0.24	

Drying shrinkage	$\varepsilon_{d,\infty}$	-0.000167	
Autogenous shrinkage	$\varepsilon_{a,\infty}$	-0.000075	
Total shrinkage	ε_{∞}	-0.000242	
Elastic modulus of concrete reduced	$E_{c,\infty}$	10986.04	MPa
Shrinkage force	R	-9288.26	kN
Shrinkage force on one girder	R_{trav}	-4644.13	kN
Eccentricity	e	1.20	mm
Moment	M_{trav}	-5592.73	kNm

3.2.2.4 Live loads

For traffic distribution, load values of traffic are reported in table 3.9.

Table 3.9. Load values for group 1a

	Lane 1	Lane 2	Residual area
Width of the notional lane [m]	3	3	2
Uniformly distributed load UDL [kN/m²]	9	2,5	2,5
Concentrated load TS [kN] (value of single axle)	300	200	0

3.2.2.5 Wind loads

It is assumed that this bridge faces a terrain of category II ($z_0=0.05$ m and $z_{min}=2$ m). A reference velocity of $V_{b,0}=26$ m/s was chosen. The values of coefficients at height $Z=5$ m used in this process are reported in table 3.10.

Table 3.10. Coefficients of wind

Height	z	5.00	m
Exposure class	II		
Parameter	z_0	0.05	
	z_{min}	2.00	
Characteristic speed of the site	$V_{b,0}$	26.00	m/s
Terrain factor	k_r	0.19	
Exposition coefficient	C_e	1.93	
Dynamic coefficient	C_d	1.00	
Pressure coefficient	C_p	1.40	
Air density	ρ	1.25	kg/m ³
Reference kinetic pressure	q_b	0.42	kN/m ²

Beam to beam distance	d	8.00	m
Beam height	h_{acc}	1.60	m
Ratio	d/h_{acc}	5.00	
From graph, coefficient	m	0.60	
Wind pressure	q	1.14	kN/m ²

For wind force applied in y direction, the computed value figure in table 3.11.

Table 3.11. Wind load computation

Phases	girder	q_i (kN/m ²)	H_i (m)	v_i (kN/m)	Y_g (m)	M_i (kNm/m)	F_v (kN)
Phase 0	girder I	1.14	1.85	2.11	0.53	0.82	0.10
	girder II	0.68	1.85	1.27	0.53	0.49	0.06
Phase 1 (loaded)	girder I	1.14	4.85	5.53	1.22	6.66	0.83
	girder II	0.68	4.85	3.32	1.22	3.99	0.50
Phase 2 (unloaded)	girder I	1.14	3.95	4.51	1.22	3.39	0.42
	girder II	0.68	3.95	2.70	1.22	2.04	0.25

3.2.2.6 Temperature load

Table 3.12 presents temperature load calculation.

Table 3.12. Temperature load calculation

Positive thermal variation	Δt	10.00	°C
Area of slab without predalles	A_c	3.50	m ²
Coefficient	a	0.000012	
Secant modulus of elasticity of concrete	E_{cm}	33346.00	MPa
Axial force at end slab	T_{diff}	14005.32	kN
Axial force at end slab on one girder	$T_{diff, trav}$	7002.66	kN
Eccentricity	e	1.20	m
Moment on one girder	$M_{diff, trav}$	-8433.02	kNm
Negative thermal variation	Δt	-10.00	°C
Area of slab without predalles	A_c	3.50	m ²
Coefficient	a	0.000012	
Secant modulus of elasticity of concrete	E_{cm}	33346	MPa
Axial force at end slab	T_{diff}	-14005.32	kN
Axial force at end slab on one girder	$T_{diff, trav}$	-7002.66	kN
Eccentricity	e	1.20	m
Moment on one girder	$M_{diff, trav}$	8433.02	kNm
Uniform thermal variation	Δt	25.00	°C
Total length of bridge	L_{tot}	130.00	m
Coefficient	a	0.00120	
Change in length	ΔL	3.90	m

3.2.3 Load combinations

The table 3.14 and table 3.13 shows the combination coefficients and load combinations for the ULS.

Table 3.13. Loads combinations

Phase	Combination	G _{1a}	G _{1b}	G ₂	S	W	T+	T-	Q _a	q _a
PHASE 0	COMB 1	1.35	1.35	0	0	1.5				
PHASE 1	COMB 2	1.35	1.35	1.35	0	1.5*0.6	1.5*0.6	0	1.35	1.35
	COMB 3	1.35	1.35	1.35	0	1.5	1.5*0.6	0	1.35*0.75	1.35*0.4
	COMB 4	1.35	1.35	1.35	0	1.5	1.5*0.6	0	0	0
	COMB 5	1.35	1.35	1.35	0	1.5*0.6	1.5	0	1.35*0.75	1.35*0.4
	COMB 6	1.35	1.35	1.35	0	1.5*0.6	0	1.5*0.6	1.35	1.35
	COMB 7	1.35	1.35	1.35	0	1.5	0	1.5*0.6	1.35*0.75	1.35*0.4
	COMB 8	1.35	1.35	1.35	0	1.5	0	1.5*0.6	0	0
	COMB 9	1.35	1.35	1.35	0	1.5*0.6	0	1.5	1.35*0.75	1.35*0.4
PHASE 2	COMB 10	1.35	1.35	1.35	1.2	1.5*0.6	1.5*0.6	0	1.35	1.35
	COMB 11	1.35	1.35	1.35	1.2	1.5	1.5*0.6	0	1.35*0.75	1.35*0.4
	COMB 12	1.35	1.35	1.35	1.2	1.5	1.5*0.6	0	0	0
	COMB 13	1.35	1.35	1.35	1.2	1.5*0.6	1.5	0	1.35*0.75	1.35*0.4
	COMB 14	1.35	1.35	1.35	1.2	1.5*0.6	0	1.5*0.6	1.35	1.35
	COMB 15	1.35	1.35	1.35	1.2	1.5	0	1.5*0.6	1.35*0.75	1.35*0.4
	COMB 16	1.35	1.35	1.35	1.2	1.5	0	1.5*0.6	0	0
	COMB 17	1.35	1.35	1.35	1.2	1.5*0.6	0	1.5	1.35*0.75	1.35*0.4

Table 3.14. Loads description

Loads	Load description
G _{1a}	Steel self-weight
G _{1b}	Slab self-weight
G ₂	Permanent non-structural loads
W	Wind
S	shrinkage
T+	Positive temperature
T-	Negative temperature

Q_a	Tandem loads due to traffic
q_a	Uniform distributed load due to traffic

3.2.4 Verification at Ultimate Limit State

Stresses depend on mixed-section geometrical characteristics. Those characteristics change, they are different at short and long term. Verification will be done at three sections.

3.2.4.1 Geometrical characteristics

To check the sections of the main beams, the stresses deriving from the application of the loads in the various phases must be found. These stresses are calculated considering the geometric and inertia characteristics relating to the analysed phase. The stress state of the subsequent phases consists in the sum of all the stress states acting up to that point.

The following characteristics for short-term was obtained:

Table 3.15. Mixed-section characteristics at t=0

Mixed section t=0		
<i>A_{id}</i>	0.31	m ²
<i>Y_{id}</i>	1.22	m
<i>J_{id}</i>	0.12	m ⁴
<i>W_{low, steel}</i>	0.10	m ³
<i>W_{up, steel}</i>	-0.32	m ³
<i>W_{low, slab}</i>	-1.82	m ³
<i>W_{up, slab}</i>	-1.10	m ³

At long-term loading the data recorded in table 3.16 was obtained.

Table 3.16. Mixed-section characteristics at t=∞

Mixed section t=∞		
<i>A_{id}</i>	0.18	m ²
<i>Y_{id}</i>	0.52	m
<i>J_{id}</i>	0.08	m ⁴
<i>W_{low, steel}</i>	0.16	m ³
<i>W_{up, steel}</i>	-0.08	m ³
<i>W_{low, slab}</i>	-1.49	m ³
<i>W_{up, slab}</i>	-1.21	m ³

3.2.4.2 Stresses

Stresses calculated will be compared to $\sigma_{all} = \frac{355}{1.05} = 338 \text{ MPa}$ for steel and to $f_{cd} = \frac{0.85 \cdot 32}{1.5} = 18.13 \text{ MPa}$ for compressed parts; $f_{cta} = \frac{0.15 \cdot 32}{1.5} = 3.2 \text{ MPa}$ for parts in tension.

The stresses are computed at various locations shown in figure 3.6.

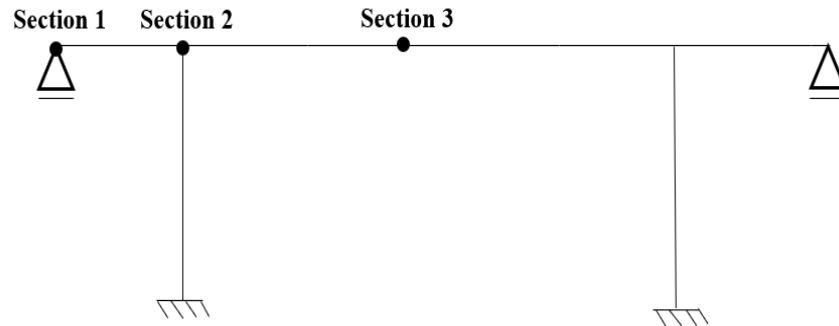


Figure 3.6. Locations of stress computation

The following phases have to be considered.

a) Phase 1

This phase characterises short-term loading.

(i) Section 1

Table 3.17 resumes computed stress values at bridge start.

All stresses in concrete and steel are below the limit fixed previously. Section 1 (near to the abutment) is subjected to bending; the top is compressed and bottom is in tension.

Table 3.17. Stress verification at section 1

Combination	Loads	Results from FEM (MIDAS/CIVIL)			Coefficient γ	Stress parameters			Stress computation			
		N(kN)	M(kNm)	T(kN)		N(MN)	M(MNm)	T(MN)	σ sup,slab (Mpa)	σ inf,slab (Mpa)	σ sup,steel (Mpa)	σ inf,steel (Mpa)
COMB2	G 1a	0.00	0.00	-222.10	1.35	0.00	0.00	-0.30	0.00	0.00	0.00	0.00
	G1b	0.00	0.00	-39.20	1.35	0.00	0.00	-0.05	0.00	0.00	0.00	0.00
	G2	0.00	0.00	-34.40	1.35	0.00	0.00	-0.05	0.00	0.00	0.00	0.00
	W	0.00	0.00	0.50	0.30	0.00	0.00	0.00	0.00	0.00	0.00	0.00
	T+	6995.30	-4621.00	-440.60	0.90	9.44	-4.16	-0.40	10.01	2.79	43.78	-10.91
	Qa	0.00	0.00	0.00	1.35	0.00	0.00	0.00	0.00	0.00	0.00	0.00
	qa	1.20	0.60	734.40	1.35	0.00	0.00	0.99	0.00	0.00	0.00	0.01
total=						9.45	-4.16	0.20	10.01	2.79	43.78	-10.90
COMB3	G 1a	0.00	0.00	-222.10	1.35	0.00	0.00	-0.30	0.00	0.00	0.00	0.00
	G1b	0.00	0.00	-39.20	1.35	0.00	0.00	-0.05	0.00	0.00	0.00	0.00
	G2	0.00	0.00	-34.40	1.35	0.00	0.00	-0.05	0.00	0.00	0.00	0.00
	W	0.00	0.00	0.50	1.50	0.00	0.00	0.00	0.00	0.00	0.00	0.00
	T+	6995.30	-4621.00	-440.60	0.90	9.44	-4.16	-0.40	10.01	2.79	43.78	-10.91
	Qa	0.00	0.00	0.00	1.01	0.00	0.00	0.00	0.00	0.00	0.00	0.00
	qa	1.20	0.60	734.40	0.54	0.00	0.00	0.40	0.00	0.00	0.00	0.01
total=						9.45	-4.16	-0.40	10.01	2.79	43.78	-10.90
COMB4	G 1a	0.00	0.00	-222.10	1.35	0.00	0.00	-0.30	0.00	0.00	0.00	0.00
	G1b	0.00	0.00	-39.20	1.35	0.00	0.00	-0.05	0.00	0.00	0.00	0.00
	G2	0.00	0.00	-34.40	1.35	0.00	0.00	-0.05	0.00	0.00	0.00	0.00
	W	0.00	0.00	0.50	1.50	0.00	0.00	0.00	0.00	0.00	0.00	0.00
	T+	6995.30	-4621.00	-440.60	0.90	9.44	-4.16	-0.40	10.01	2.79	43.78	-10.91
	Qa	0.00	0.00	0.00	0.00	0.00	0.00	0.00	0.00	0.00	0.00	0.00
	qa	1.20	0.60	734.40	0.00	0.00	0.00	0.00	0.00	0.00	0.01	0.01
total=						9.45	-4.16	-0.79	10.01	2.79	43.79	-10.91
COMB5	G 1a	0.00	0.00	-222.10	1.35	0.00	0.00	-0.30	0.00	0.00	0.00	0.00
	G1b	0.00	0.00	-39.20	1.35	0.00	0.00	-0.05	0.00	0.00	0.00	0.00
	G2	0.00	0.00	-34.40	1.35	0.00	0.00	-0.05	0.00	0.00	0.00	0.00
	W	0.00	0.00	0.50	0.90	0.00	0.00	0.00	0.00	0.00	0.00	0.00
	T+	6995.30	-4621.00	-440.60	1.50	9.44	-6.93	-0.66	13.05	4.32	52.40	-38.76
	Qa	0.00	0.00	0.00	0.26	0.00	0.00	0.00	0.00	0.00	0.00	0.00
	qa	1.20	0.60	734.40	0.54	0.00	0.00	0.40	0.00	0.00	0.00	0.01
total=						9.45	-6.93	-0.66	13.05	4.32	52.40	-38.75
COMB6	G 1a	0.00	0.00	-222.10	1.35	0.00	0.00	-0.30	0.00	0.00	0.00	0.00
	G1b	0.00	0.00	-39.20	1.35	0.00	0.00	-0.05	0.00	0.00	0.00	0.00
	G2	0.00	0.00	-34.40	1.35	0.00	0.00	-0.05	0.00	0.00	0.00	0.00
	W	0.00	0.00	0.50	1.50	0.00	0.00	0.00	0.00	0.00	0.00	0.00
	T-	-6973.20	4647.30	709.20	0.90	-9.41	4.18	0.64	-10.02	-2.81	-43.76	11.25
	Qa	0.00	0.00	0.00	1.35	0.00	0.00	0.00	0.00	0.00	0.00	0.00
	qa	1.20	0.60	734.40	1.35	0.00	0.00	0.99	0.00	0.00	0.00	0.01
total=						-9.41	4.18	1.23	-10.02	-2.81	-43.75	11.26
COMB7	G 1a	0.00	0.00	-222.10	1.35	0.00	0.00	-0.30	0.00	0.00	0.00	0.00
	G1b	0.00	0.00	-39.20	1.35	0.00	0.00	-0.05	0.00	0.00	0.00	0.00
	G2	0.00	0.00	-34.40	1.35	0.00	0.00	-0.05	0.00	0.00	0.00	0.00
	W	0.00	0.00	0.50	1.50	0.00	0.00	0.00	0.00	0.00	0.00	0.00
	T-	-6973.20	4647.30	709.20	0.90	-9.41	4.18	0.64	-10.02	-2.81	-43.76	11.25
	Qa	0.00	0.00	0.00	0.26	0.00	0.00	0.00	0.00	0.00	0.00	0.00
	qa	1.20	0.60	734.40	0.54	0.00	0.00	0.40	0.00	0.00	0.00	0.01
total=						-9.41	4.18	0.64	-10.02	-2.81	-43.75	11.25
COMB8	G 1a	0.00	0.00	-222.10	1.35	0.00	0.00	-0.30	0.00	0.00	0.00	0.00
	G1b	0.00	0.00	-39.20	1.35	0.00	0.00	-0.05	0.00	0.00	0.00	0.00
	G2	0.00	0.00	-34.40	1.35	0.00	0.00	-0.05	0.00	0.00	0.00	0.00
	W	0.00	0.00	0.50	1.50	0.00	0.00	0.00	0.00	0.00	0.00	0.00
	T-	-6973.20	4647.30	709.20	0.90	-9.41	4.18	0.64	-10.02	-2.81	-43.76	11.25
	Qa	0.00	0.00	0.00	0.00	0.00	0.00	0.00	0.00	0.00	0.00	0.00
	qa	1.20	0.60	734.40	0.00	0.00	0.00	0.00	0.00	0.00	0.01	0.01
total=						-9.41	4.18	0.24	-10.02	-2.81	-43.75	11.25
COMB9	G 1a	0.00	0.00	-222.10	1.35	0.00	0.00	-0.30	0.00	0.00	0.00	0.00
	G1b	0.00	0.00	-39.20	1.35	0.00	0.00	-0.05	0.00	0.00	0.00	0.00
	G2	0.00	0.00	-34.40	1.35	0.00	0.00	-0.05	0.00	0.00	0.00	0.00
	W	0.00	0.00	0.50	0.90	0.00	0.00	0.00	0.00	0.00	0.00	0.00
	T-	-6973.20	4647.30	709.20	1.50	-9.41	6.97	1.06	-13.08	-4.34	-52.42	39.25
	Qa	0.00	0.00	0.00	0.26	0.00	0.00	0.00	0.00	0.00	0.00	0.00
	qa	1.20	0.60	734.40	0.54	0.00	0.00	0.40	0.00	0.00	0.00	0.01
total=						-9.41	6.97	1.06	-13.08	-4.34	-52.42	39.26

(ii) Section 2

Table 3.18 resumes computed stress values at piers location. All the stresses are lower than design strength for concrete and steel.

Table 3.18. Stress verification at section 2

Combination	Loads	Results from FEM (MIDAS/CIVIL)			Coefficient γ	Stress parameters			Stress computation			
		N(kN)	M(kNm)	T(kN)		N(MN)	M(MNm)	T(MN)	$\sigma_{sup,slab}$ (Mpa)	$\sigma_{inf,slab}$ (Mpa)	$\sigma_{sup,steel}$ (Mpa)	$\sigma_{inf,steel}$ (Mpa)
COMB2	G 1a	-288.80	-3035.50	-644.40	1.35	-0.39	-4.10	-0.87	4.27	2.23	11.46	-42.43
	G1b	-50.00	-526.60	-112.50	1.35	-0.07	-0.71	-0.15	0.74	0.39	1.99	-7.36
	G2	0.00	-462.80	-98.70	1.35	0.00	-0.62	-0.13	0.68	0.34	1.94	-6.27
	W	0.00	3.30	1.10	1.50	0.00	0.00	0.00	-0.01	0.00	-0.02	0.05
	T+	6995.30	1987.80	-440.60	0.90	9.44	1.79	-0.40	3.49	-0.47	25.30	48.83
	Qa	0.00	0.00	0.00	1.35	0.00	0.00	0.00	0.00	0.00	0.00	0.00
	qa	105.00	119.10	861.50	1.35	0.14	0.16	1.16	-0.09	-0.08	-0.04	2.08
	total=					9.13	-3.48	-0.39	9.08	2.40	40.64	-5.11
COMB3	G 1a	-288.80	-3035.50	-644.40	1.35	-0.39	-4.10	-0.87	4.27	2.23	11.46	-42.43
	G1b	-50.00	-526.60	-112.50	1.35	-0.07	-0.71	-0.15	0.74	0.39	1.99	-7.36
	G2	0.00	-462.80	-98.70	1.35	0.00	-0.62	-0.13	0.68	0.34	1.94	-6.27
	W	0.00	3.30	1.10	1.50	0.00	0.00	0.00	-0.01	0.00	-0.02	0.05
	T+	6995.30	1987.80	-440.60	0.90	9.44	1.79	-0.40	3.49	-0.47	25.30	48.83
	Qa	0.00	0.00	0.00	1.01	0.00	0.00	0.00	0.00	0.00	0.00	0.00
	qa	105.00	119.10	861.50	0.54	0.14	0.06	0.47	0.01	-0.03	0.26	1.11
	total=					9.13	-3.58	-1.08	9.19	2.46	40.94	-6.08
COMB4	G 1a	-288.80	-3035.50	-644.40	1.35	-0.39	-4.10	-0.87	4.27	2.23	11.46	-42.43
	G1b	-50.00	-526.60	-112.50	1.35	-0.07	-0.71	-0.15	0.74	0.39	1.99	-7.36
	G2	0.00	-462.80	-98.70	1.35	0.00	-0.62	-0.13	0.68	0.34	1.94	-6.27
	W	0.00	3.30	1.10	1.50	0.00	0.00	0.00	-0.01	0.00	-0.02	0.05
	T+	6995.30	1987.80	-440.60	0.90	9.44	1.79	-0.40	3.49	-0.47	25.30	48.83
	Qa	0.00	0.00	0.00	0.00	0.00	0.00	0.00	0.00	0.00	0.00	0.00
	qa	105.00	119.10	861.50	0.00	0.14	0.00	0.00	0.08	0.01	0.46	0.46
	total=					9.13	-3.64	-1.55	9.26	2.49	41.14	-6.73
COMB5	G 1a	-288.80	-3035.50	-644.40	1.35	-0.39	-4.10	-0.87	4.27	2.23	11.46	-42.43
	G1b	-50.00	-526.60	-112.50	1.35	-0.07	-0.71	-0.15	0.74	0.39	1.99	-7.36
	G2	0.00	-462.80	-98.70	1.35	0.00	-0.62	-0.13	0.68	0.34	1.94	-6.27
	W	0.00	3.30	1.10	0.90	0.00	0.00	0.00	0.00	0.00	-0.01	0.03
	T+	6995.30	1987.80	-440.60	1.50	9.44	2.98	-0.66	2.18	-1.13	21.59	60.80
	Qa	0.00	0.00	0.00	1.01	0.00	0.00	0.00	0.00	0.00	0.00	0.00
	qa	105.00	119.10	861.50	0.54	0.14	0.06	0.47	0.01	-0.03	0.26	1.11
	total=					9.13	-2.38	-1.35	7.88	1.80	37.24	5.88
COMB6	G 1a	-288.80	-3035.50	-644.40	1.35	-0.39	-4.10	-0.87	4.27	2.23	11.46	-42.43
	G1b	-50.00	-526.60	-112.50	1.35	-0.07	-0.71	-0.15	0.74	0.39	1.99	-7.36
	G2	0.00	-462.80	-98.70	1.35	0.00	-0.62	-0.13	0.68	0.34	1.94	-6.27
	W	0.00	3.30	1.10	1.50	0.00	0.00	0.00	-0.01	0.00	-0.02	0.05
	T-	-6973.20	-5990.60	709.20	0.90	-9.41	-5.39	0.64	0.47	2.45	-14.01	-84.91
	Qa	0.00	0.00	0.00	1.35	0.00	0.00	0.00	0.00	0.00	0.00	0.00
	qa	105.00	119.10	861.50	1.35	0.14	0.16	1.16	-0.09	-0.08	-0.04	2.08
	total=					-9.73	-10.66	0.65	6.07	5.33	1.33	-138.85
COMB7	G 1a	-288.80	-3035.50	-644.40	1.35	-0.39	-4.10	-0.87	4.27	2.23	11.46	-42.43
	G1b	-50.00	-526.60	-112.50	1.35	-0.07	-0.71	-0.15	0.74	0.39	1.99	-7.36
	G2	0.00	-462.80	-98.70	1.35	0.00	-0.62	-0.13	0.68	0.34	1.94	-6.27
	W	0.00	3.30	1.10	1.50	0.00	0.00	0.00	-0.01	0.00	-0.02	0.05
	T-	-6973.20	-5990.60	709.20	0.90	-9.41	-5.39	0.64	0.47	2.45	-14.01	-84.91
	Qa	0.00	0.00	0.00	1.01	0.00	0.00	0.00	0.00	0.00	0.00	0.00
	qa	105.00	119.10	861.50	0.54	0.14	0.06	0.47	0.01	-0.03	0.26	1.11
	total=					-9.73	-10.76	-0.05	6.17	5.38	1.63	-139.82
COMB8	G 1a	-288.80	-3035.50	-644.40	1.35	-0.39	-4.10	-0.87	4.27	2.23	11.46	-42.43
	G1b	-50.00	-526.60	-112.50	1.35	-0.07	-0.71	-0.15	0.74	0.39	1.99	-7.36
	G2	0.00	-462.80	-98.70	1.35	0.00	-0.62	-0.13	0.68	0.34	1.94	-6.27
	W	0.00	3.30	1.10	1.50	0.00	0.00	0.00	-0.01	0.00	-0.02	0.05
	T-	-6973.20	-5990.60	709.20	0.90	-9.41	-5.39	0.64	0.47	2.45	-14.01	-84.91
	Qa	0.00	0.00	0.00	0.00	0.00	0.00	0.00	0.00	0.00	0.00	0.00
	qa	105.00	119.10	861.50	0.00	0.14	0.00	0.00	0.08	0.01	0.46	0.46
	total=					-9.73	-10.82	-0.52	6.24	5.42	1.83	-140.46
COMB9	G 1a	-288.80	-3035.50	-644.40	1.35	-0.39	-4.10	-0.87	4.27	2.23	11.46	-42.43
	G1b	-50.00	-526.60	-112.50	1.35	-0.07	-0.71	-0.15	0.74	0.39	1.99	-7.36
	G2	0.00	-462.80	-98.70	1.35	0.00	-0.62	-0.13	0.68	0.34	1.94	-6.27
	W	0.00	3.30	1.10	0.90	0.00	0.00	0.00	0.00	0.00	-0.01	0.03
	T-	-6973.20	-5990.60	709.20	1.50	-9.41	-8.99	1.06	4.41	4.43	-2.84	-121.01
	Qa	0.00	0.00	0.00	1.01	0.00	0.00	0.00	0.00	0.00	0.00	0.00
	qa	105.00	119.10	861.50	0.54	0.14	0.06	0.47	0.01	-0.03	0.26	1.11
	total=					-9.73	-14.35	0.37	10.12	7.35	12.80	-175.93

(iii) Section 3

Stress do not reach the limit; the section is partially subjected to compression and tight at bottom (stresses computed at the mid-span of the second span).

Table 3.19. Stress verification at section 3

Combination	Loads	Results from FEM (MIDAS/CIVIL)			Coefficient	Stress parameters			Stress computation			
		N(kN)	M(kNm)	T(kN)		γ	N(MN)	M(MNm)	T(MN)	σ sup,slab (Mpa)	σ inf,slab (Mpa)	σ sup,steel (Mpa)
COMB2	G 1a	-288.80	1832.10	-134.40	1.35	-0.39	2.47	-0.18	-2.94	-1.38	-8.96	23.57
	G1b	-50.00	317.10	-112.50	1.35	-0.07	0.43	-0.15	-0.51	-0.24	-1.55	4.08
	G2	-43.90	278.20	0.00	1.35	-0.06	0.38	0.00	-0.45	-0.21	-1.36	3.58
	W	0.00	0.50	0.00	1.50	0.00	0.00	0.00	0.00	0.00	0.00	0.01
	T+	6082.30	-403.50	0.00	0.90	8.21	-0.36	0.00	5.14	0.64	27.96	23.18
	Qa	0.00	0.00	0.00	1.35	0.00	0.00	0.00	0.00	0.00	0.00	0.00
	qa	104.80	2462.80	472.90	1.35	0.14	3.32	0.64	-3.56	-1.82	-9.87	33.85
	total=						7.84	6.24	0.31	-2.32	-3.00	6.22
COMB3	G 1a	-288.80	1832.10	-134.40	1.35	-0.39	2.47	-0.18	-2.94	-1.38	-8.96	23.57
	G1b	-50.00	317.10	-112.50	1.35	-0.07	0.43	-0.15	-0.51	-0.24	-1.55	4.08
	G2	-43.90	278.20	0.00	1.35	-0.06	0.38	0.00	-0.45	-0.21	-1.36	3.58
	W	0.00	0.50	0.00	1.50	0.00	0.00	0.00	0.00	0.00	0.00	0.01
	T+	6082.30	-403.50	0.00	0.90	8.21	-0.36	0.00	5.14	0.64	27.96	23.18
	Qa	0.00	0.00	0.00	1.01	0.00	0.00	0.00	0.00	0.00	0.00	0.00
	qa	104.80	2462.80	472.90	0.54	0.14	1.33	0.26	-1.38	-0.72	-3.67	13.82
	total=						7.84	4.24	-0.08	-0.13	-1.91	12.42
COMB4	G 1a	-288.80	1832.10	-134.40	1.35	-0.39	2.47	-0.18	-2.94	-1.38	-8.96	23.57
	G1b	-50.00	317.10	-112.50	1.35	-0.07	0.43	-0.15	-0.51	-0.24	-1.55	4.08
	G2	-43.90	278.20	0.00	1.35	-0.06	0.38	0.00	-0.45	-0.21	-1.36	3.58
	W	0.00	0.50	0.00	1.50	0.00	0.00	0.00	0.00	0.00	0.00	0.01
	T+	6082.30	-403.50	0.00	0.90	8.21	-0.36	0.00	5.14	0.64	27.96	23.18
	Qa	0.00	0.00	0.00	0.00	0.00	0.00	0.00	0.00	0.00	0.00	0.00
	qa	104.80	2462.80	472.90	0.00	0.14	0.00	0.00	0.08	0.01	0.46	0.46
	total=						7.84	2.91	-0.33	1.33	-1.18	16.55
COMB5	G 1a	-288.80	1832.10	-134.40	1.35	-0.39	2.47	-0.18	-2.94	-1.38	-8.96	23.57
	G1b	-50.00	317.10	-112.50	1.35	-0.07	0.43	-0.15	-0.51	-0.24	-1.55	4.08
	G2	-43.90	278.20	0.00	1.35	-0.06	0.38	0.00	-0.45	-0.21	-1.36	3.58
	W	0.00	0.50	0.00	0.90	0.00	0.00	0.00	0.00	0.00	0.00	0.00
	T-	-3452.30	2044.90	0.00	1.50	-4.66	3.07	0.00	-6.05	-1.94	-24.76	15.58
	Qa	0.00	0.00	0.00	1.01	0.00	0.00	0.00	0.00	0.00	0.00	0.00
	qa	104.80	2462.80	472.90	0.54	0.14	1.33	0.26	-1.38	-0.72	-3.67	13.82
	total=						-5.04	7.67	-0.08	-11.32	-4.49	-40.30
COMB6	G 1a	-288.80	1832.10	-134.40	1.35	-0.39	2.47	-0.18	-2.94	-1.38	-8.96	23.57
	G1b	-50.00	317.10	-112.50	1.35	-0.07	0.43	-0.15	-0.51	-0.24	-1.55	4.08
	G2	-43.90	278.20	0.00	1.35	-0.06	0.38	0.00	-0.45	-0.21	-1.36	3.58
	W	0.00	0.50	0.00	1.50	0.00	0.00	0.00	0.00	0.00	0.00	0.01
	T-	-3452.30	2044.90	0.00	0.90	-4.66	1.84	0.00	-4.71	-1.26	-20.95	3.25
	Qa	0.00	0.00	0.00	1.35	0.00	0.00	0.00	0.00	0.00	0.00	0.00
	qa	104.80	2462.80	472.90	1.35	0.14	3.32	0.64	-3.56	-1.82	-9.87	33.85
	total=						-5.04	8.44	0.31	-12.16	-4.91	-42.69
COMB7	G 1a	-288.80	1832.10	-134.40	1.35	-0.39	2.47	-0.18	-2.94	-1.38	-8.96	23.57
	G1b	-50.00	317.10	-112.50	1.35	-0.07	0.43	-0.15	-0.51	-0.24	-1.55	4.08
	G2	-43.90	278.20	0.00	1.35	-0.06	0.38	0.00	-0.45	-0.21	-1.36	3.58
	W	0.00	0.50	0.00	1.50	0.00	0.00	0.00	0.00	0.00	0.00	0.01
	T-	-3452.30	2044.90	0.00	0.90	-4.66	1.84	0.00	-4.71	-1.26	-20.95	3.25
	Qa	0.00	0.00	0.00	1.01	0.00	0.00	0.00	0.00	0.00	0.00	0.00
	qa	104.80	2462.80	472.90	0.54	0.14	1.33	0.26	-1.38	-0.72	-3.67	13.82
	total=						-5.04	6.45	-0.08	-9.98	-3.81	-36.49
COMB8	G 1a	-288.80	1832.10	-134.40	1.35	-0.39	2.47	-0.18	-2.94	-1.38	-8.96	23.57
	G1b	-50.00	317.10	-112.50	1.35	-0.07	0.43	-0.15	-0.51	-0.24	-1.55	4.08
	G2	-43.90	278.20	0.00	1.35	-0.06	0.38	0.00	-0.45	-0.21	-1.36	3.58
	W	0.00	0.50	0.00	1.50	0.00	0.00	0.00	0.00	0.00	0.00	0.01
	T-	-3452.30	2044.90	0.00	0.90	-4.66	1.84	0.00	-4.71	-1.26	-20.95	3.25
	Qa	0.00	0.00	0.00	0.00	0.00	0.00	0.00	0.00	0.00	0.00	0.00
	qa	104.80	2462.80	472.90	0.00	0.14	0.00	0.00	0.08	0.01	0.46	0.46
	total=						-5.04	5.12	-0.33	-8.52	-3.08	-32.36
COMB9	G 1a	-288.80	1832.10	-134.40	1.35	-0.39	2.47	-0.18	-2.94	-1.38	-8.96	23.57
	G1b	-50.00	317.10	-112.50	1.35	-0.07	0.43	-0.15	-0.51	-0.24	-1.55	4.08
	G2	-43.90	278.20	0.00	1.35	-0.06	0.38	0.00	-0.45	-0.21	-1.36	3.58
	W	0.00	0.50	0.00	0.90	0.00	0.00	0.00	0.00	0.00	0.00	0.00
	T-	-3452.30	2044.90	0.00	1.50	-4.66	3.07	0.00	-6.05	-1.94	-24.76	15.58
	Qa	0.00	0.00	0.00	1.01	0.00	0.00	0.00	0.00	0.00	0.00	0.00
	qa	104.80	2462.80	472.90	0.54	0.14	1.33	0.26	-1.38	-0.72	-3.67	13.82
	total=						-5.04	7.67	-0.08	-11.32	-4.49	-40.30

b) Phase 2

Including shrinkage in stress calculation is considering long term effects on elements.

(i) Section 1

Table 3.20. Stress verifications at section 1 (phase 2)

Combination	Loads	Results from FEM (MIDAS/CIVIL)			Coefficient γ	Stress parameters			Stress computation				
		N(kN)	M(kNm)	T(kN)		N(MN)	M(MNm)	T(MN)	$\sigma_{sup,slab}$ (Mpa)	$\sigma_{inf,slab}$ (Mpa)	$\sigma_{sup,steel}$ (Mpa)	$\sigma_{inf,steel}$ (Mpa)	
COMB10	G1a	0.00	0.00	-222.10	1.35	0.00	0.00	-0.30	0.00	0.00	0.00	0.00	0.00
	G1b	0.00	0.00	-39.20	1.35	0.00	0.00	-0.05	0.00	0.00	0.00	0.00	0.00
	G2	0.00	0.00	-34.40	1.35	0.00	0.00	-0.05	0.00	0.00	0.00	0.00	0.00
	S	-4641.00	3065.80	292.30	1.20	-6.27	3.68	0.35	-1.41	-1.99	81.79	57.31	0.00
	W	0.00	0.00	0.40	1.50	0.00	0.00	0.00	0.00	0.00	0.00	0.00	0.00
	T+	6995.30	-4621.00	-440.60	0.90	9.44	-4.16	-0.40	10.01	2.79	43.78	-10.91	0.00
	qa	1.20	0.60	734.40	1.35	0.00	0.00	0.99	0.00	0.00	0.00	0.00	0.01
	total=						3.18	-0.48	0.55	8.60	0.81	125.57	46.42
COMB11	G1a	0.00	0.00	-222.10	1.35	0.00	0.00	-0.30	0.00	0.00	0.00	0.00	0.00
	G1b	0.00	0.00	-39.20	1.35	0.00	0.00	-0.05	0.00	0.00	0.00	0.00	0.00
	G2	0.00	0.00	-34.40	1.35	0.00	0.00	-0.05	0.00	0.00	0.00	0.00	0.00
	S	-4641.00	3065.80	292.30	1.20	-6.27	3.68	0.35	-1.41	-1.99	81.79	57.31	0.00
	W	0.00	0.00	0.40	1.50	0.00	0.00	0.00	0.00	0.00	0.00	0.00	0.00
	T+	6995.30	-4621.00	-440.60	0.90	9.44	-4.16	-0.40	10.01	2.79	43.78	-10.91	0.00
	qa	1.20	0.60	734.40	0.54	0.00	0.00	0.40	0.00	0.00	0.00	0.00	0.01
	total=						3.18	-0.48	-0.05	8.60	0.81	125.57	46.41
COMB12	G1a	0.00	0.00	-222.10	1.35	0.00	0.00	-0.30	0.00	0.00	0.00	0.00	0.00
	G1b	0.00	0.00	-39.20	1.35	0.00	0.00	-0.05	0.00	0.00	0.00	0.00	0.00
	G2	0.00	0.00	-34.40	1.35	0.00	0.00	-0.05	0.00	0.00	0.00	0.00	0.00
	S	-4641.00	3065.80	292.30	1.20	-6.27	3.68	0.35	-1.41	-1.99	81.79	57.31	0.00
	W	0.00	0.00	0.40	1.50	0.00	0.00	0.00	0.00	0.00	0.00	0.00	0.00
	T+	6995.30	-4621.00	-440.60	0.90	9.44	-4.16	-0.40	10.01	2.79	43.78	-10.91	0.00
	qa	1.20	0.60	734.40	0.00	0.00	0.00	0.00	0.00	0.00	0.00	0.01	0.01
	total=						3.18	-0.48	-0.44	8.60	0.81	125.57	46.41
COMB13	G1a	0.00	0.00	-222.10	1.35	0.00	0.00	-0.30	0.00	0.00	0.00	0.00	0.00
	G1b	0.00	0.00	-39.20	1.35	0.00	0.00	-0.05	0.00	0.00	0.00	0.00	0.00
	G2	0.00	0.00	-34.40	1.35	0.00	0.00	-0.05	0.00	0.00	0.00	0.00	0.00
	S	-4641.00	3065.80	292.30	1.20	-6.27	3.68	0.35	0.00	0.00	0.00	0.00	0.00
	W	0.00	0.00	0.40	0.90	0.00	0.00	0.00	-1.41	-1.99	81.79	57.31	0.00
	T+	6995.30	-4621.00	-440.60	1.50	9.44	-6.93	-0.66	13.05	4.32	52.40	-38.76	0.00
	qa	1.20	0.60	734.40	0.54	0.00	0.00	0.40	0.00	0.00	0.00	0.00	0.01
	total=						3.18	-3.25	-0.31	11.64	2.33	134.19	18.57
COMB14	G1a	0.00	0.00	-222.10	1.35	0.00	0.00	-0.30	0.00	0.00	0.00	0.00	0.00
	G1b	0.00	0.00	-39.20	1.35	0.00	0.00	-0.05	0.00	0.00	0.00	0.00	0.00
	G2	0.00	0.00	-34.40	1.35	0.00	0.00	-0.05	0.00	0.00	0.00	0.00	0.00
	S	-4641.00	3065.80	292.30	1.20	-6.27	3.68	0.35	0.00	0.00	0.00	0.00	0.00
	W	0.00	0.00	0.40	1.50	0.00	0.00	0.00	-1.41	-1.99	81.79	57.31	0.00
	T-	-6973.20	4647.30	709.20	0.90	-9.41	4.18	0.64	-10.02	-2.81	-43.76	11.25	0.00
	qa	1.20	0.60	734.40	1.35	0.00	0.00	0.99	0.00	0.00	0.00	0.00	0.01
	total=						-15.68	7.86	1.58	-11.43	-4.79	38.03	68.57
COMB15	G1a	0.00	0.00	-222.10	1.35	0.00	0.00	-0.30	0.00	0.00	0.00	0.00	0.00
	G1b	0.00	0.00	-39.20	1.35	0.00	0.00	-0.05	0.00	0.00	0.00	0.00	0.00
	G2	0.00	0.00	-34.40	1.35	0.00	0.00	-0.05	0.00	0.00	0.00	0.00	0.00
	S	-4641.00	3065.80	292.30	1.20	-6.27	3.68	0.35	0.00	0.00	0.00	0.00	0.00
	W	0.00	0.00	0.40	1.50	0.00	0.00	0.00	-1.41	-1.99	81.79	57.31	0.00
	T-	-6973.20	4647.30	709.20	0.90	-9.41	4.18	0.64	-10.02	-2.81	-43.76	11.25	0.00
	qa	1.20	0.60	734.40	0.54	0.00	0.00	0.40	0.00	0.00	0.00	0.00	0.01
	total=						-15.68	7.86	0.99	-11.43	-4.79	38.04	68.57
COMB16	G1a	0.00	0.00	-222.10	1.35	0.00	0.00	-0.30	0.00	0.00	0.00	0.00	0.00
	G1b	0.00	0.00	-39.20	1.35	0.00	0.00	-0.05	0.00	0.00	0.00	0.00	0.00
	G2	0.00	0.00	-34.40	1.35	0.00	0.00	-0.05	0.00	0.00	0.00	0.00	0.00
	S	-4641.00	3065.80	292.30	1.20	-6.27	3.68	0.35	-1.41	-1.99	81.79	57.31	0.00
	W	0.00	0.00	0.40	1.50	0.00	0.00	0.00	0.00	0.00	0.00	0.00	0.00
	T-	-6973.20	4647.30	709.20	0.90	-9.41	4.18	0.64	-10.02	-2.81	-43.76	11.25	0.00
	qa	1.20	0.60	734.40	0.00	0.00	0.00	0.00	0.00	0.00	0.00	0.01	0.01
	total=						-15.68	7.86	0.59	-11.43	-4.79	38.04	68.56
COMB17	G1a	0.00	0.00	-222.10	1.35	0.00	0.00	-0.30	0.00	0.00	0.00	0.00	0.00
	G1b	0.00	0.00	-39.20	1.35	0.00	0.00	-0.05	0.00	0.00	0.00	0.00	0.00
	G2	0.00	0.00	-34.40	1.35	0.00	0.00	-0.05	0.00	0.00	0.00	0.00	0.00
	S	-4641.00	3065.80	292.30	1.20	-6.27	3.68	0.35	0.00	0.00	0.00	0.00	0.00
	W	0.00	0.00	0.40	0.90	0.00	0.00	0.00	-1.41	-1.99	81.79	57.31	0.00
	T-	-6973.20	4647.30	709.20	1.50	-9.41	6.97	1.06	-13.08	-4.34	-52.42	39.25	0.00
	Qa	0.00	0.00	0.00	1.01	0.00	0.00	0.00	0.00	0.00	0.00	0.00	0.00
	qa	1.2	0.6	734.4	0.54	0.00	0.00	0.40	0.00	0.00	0.00	0.00	0.01
total=						-15.68	10.65	1.41	-14.49	-6.32	29.37	96.57	

(ii) Section 2

All the stresses are lower than design strength for concrete and steel. They are also negative from top of slab to bottom of girder, it means that the section is totally compressed. Buckling resistance will be verified in the following section.

Table 3.21. Stress verifications at section 2 (phase 2)

Combination	Loads	Results from FEM (MIDAS/CIVIL)			Coefficient	Stress parameters			Stress computation			
		N(kN)	M(kNm)	T(kN)		γ	N(MN)	M(MNm)	T(MN)	σ sup,slab (Mpa)	σ inf,slab (Mpa)	σ sup,steel (Mpa)
COMB10	G 1a	-288.80	-3035.50	-644.40	1.35	-0.39	-4.10	-0.87	4.27	2.23	11.46	-42.43
	G1b	-50.00	-526.60	-112.50	1.35	-0.07	-0.71	-0.15	0.74	0.39	1.99	-7.36
	G2	0.00	-462.80	-98.70	1.35	0.00	-0.62	-0.13	0.75	0.93	0.05	-0.10
	S	-6973.20	-5990.60	709.20	1.20	-9.41	-7.19	0.85	-12.66	-11.54	-40.58	7.24
	W	0.00	2.70	0.90	1.50	0.00	0.00	0.00	0.00	0.00	-0.01	0.04
	T+	6995.30	1987.80	-440.60	0.90	9.44	1.79	-0.40	3.49	-0.47	25.30	48.83
	qa	105.00	119.10	861.50	1.35	0.14	0.16	1.16	-0.09	-0.08	-0.04	2.08
	total=						-0.29	-10.67	0.46	-3.50	-8.55	-1.84
COMB11	G 1a	-288.80	-3035.50	-644.40	1.35	-0.39	-4.10	-0.87	4.27	2.23	11.46	-42.43
	G1b	-50.00	-526.60	-112.50	1.35	-0.07	-0.71	-0.15	0.74	0.39	1.99	-7.36
	G2	0.00	-462.80	-98.70	1.35	0.00	-0.62	-0.13	0.75	0.93	0.05	-0.10
	S	-6973.20	-5990.60	709.20	1.20	-9.41	-7.19	0.85	-12.66	-11.54	-40.58	7.24
	W	0.00	2.70	0.90	1.50	0.00	0.00	0.00	0.00	0.00	-0.01	0.04
	T+	6995.30	1987.80	-440.60	0.90	9.44	1.79	-0.40	3.49	-0.47	25.30	48.83
	qa	105.00	119.10	861.50	0.54	0.14	0.06	0.47	0.01	-0.03	0.26	1.11
	total=						-0.29	-10.76	-0.23	-3.40	-8.49	-1.54
COMB12	G 1a	-288.80	-3035.50	-644.40	1.35	-0.39	-4.10	-0.87	4.27	2.23	11.46	-42.43
	G1b	-50.00	-526.60	-112.50	1.35	-0.07	-0.71	-0.15	0.74	0.39	1.99	-7.36
	G2	0.00	-462.80	-98.70	1.35	0.00	-0.62	-0.13	0.75	0.93	0.05	-0.10
	S	-6973.20	-5990.60	709.20	1.20	-9.41	-7.19	0.85	-12.66	-11.54	-40.58	7.24
	W	0.00	2.70	0.90	1.50	0.00	0.00	0.00	0.00	0.00	-0.01	0.04
	T+	6995.30	1987.80	-440.60	0.90	9.44	1.79	-0.40	3.49	-0.47	25.30	48.83
	qa	105.00	119.10	861.50	0.00	0.14	0.00	0.00	0.08	0.01	0.46	0.46
	total=						-0.29	-10.83	-0.70	-3.33	-8.46	-1.34
COMB13	G 1a	-288.80	-3035.50	-644.40	1.35	-0.39	-4.10	-0.87	4.27	2.23	11.46	-42.43
	G1b	-50.00	-526.60	-112.50	1.35	-0.07	-0.71	-0.15	0.74	0.39	1.99	-7.36
	G2	0.00	-462.80	-98.70	1.35	0.00	-0.62	-0.13	0.68	0.34	1.94	-6.27
	S	-6973.20	-5990.60	709.20	1.20	-9.41	-7.19	0.85	0.75	0.93	0.05	-0.10
	W	0.00	2.70	0.90	0.90	0.00	0.00	0.00	-12.66	-11.54	-40.58	7.24
	T+	6995.30	1987.80	-440.60	1.50	9.44	2.98	-0.66	2.18	-1.13	21.59	60.80
	qa	105.00	119.10	861.50	0.54	0.14	0.06	0.47	0.01	-0.03	0.26	1.11
	total=						-0.29	-9.57	-0.50	-4.01	-8.80	-3.29
COMB14	G 1a	-288.80	-3035.50	-644.40	1.35	-0.39	-4.10	-0.87	4.27	2.23	11.46	-42.43
	G1b	-50.00	-526.60	-112.50	1.35	-0.07	-0.71	-0.15	0.74	0.39	1.99	-7.36
	G2	0.00	-462.80	-98.70	1.35	0.00	-0.62	-0.13	0.68	0.34	1.94	-6.27
	S	-6973.20	-5990.60	709.20	1.20	-9.41	-7.19	0.85	0.75	0.93	0.05	-0.10
	W	0.00	2.70	0.90	1.50	0.00	0.00	0.00	-12.66	-11.54	-40.58	7.24
	T-	-6973.20	-5990.60	709.20	0.90	-9.41	-5.39	0.64	0.47	2.45	-14.01	-84.91
	qa	105.00	119.10	861.50	1.35	0.14	0.16	1.16	-0.09	-0.08	-0.04	2.08
	total=						-19.14	-17.85	1.50	-5.83	-5.28	-39.19
COMB15	G 1a	-288.80	-3035.50	-644.40	1.35	-0.39	-4.10	-0.87	4.27	2.23	11.46	-42.43
	G1b	-50.00	-526.60	-112.50	1.35	-0.07	-0.71	-0.15	0.74	0.39	1.99	-7.36
	G2	0.00	-462.80	-98.70	1.35	0.00	-0.62	-0.13	0.68	0.34	1.94	-6.27
	S	-6973.20	-5990.60	709.20	1.20	-9.41	-7.19	0.85	0.75	0.93	0.05	-0.10
	W	0.00	2.70	0.90	1.50	0.00	0.00	0.00	-12.66	-11.54	-40.58	7.24
	T-	-6973.20	-5990.60	709.20	0.90	-9.41	-5.39	0.64	0.47	2.45	-14.01	-84.91
	qa	105.00	119.10	861.50	0.54	0.14	0.06	0.47	0.01	-0.03	0.26	1.11
	total=						-19.14	-17.95	0.80	-5.72	-5.23	-38.89
COMB16	G 1a	-288.80	-3035.50	-644.40	1.35	-0.39	-4.10	-0.87	4.27	2.23	11.46	-42.43
	G1b	-50.00	-526.60	-112.50	1.35	-0.07	-0.71	-0.15	0.74	0.39	1.99	-7.36
	G2	0.00	-462.80	-98.70	1.35	0.00	-0.62	-0.13	0.75	0.93	0.05	-0.10
	S	-6973.20	-5990.60	709.20	1.20	-9.41	-7.19	0.85	-12.66	-11.54	-40.58	7.24
	W	0.00	2.70	0.90	1.50	0.00	0.00	0.00	0.00	0.00	-0.01	0.04
	T-	-6973.20	-5990.60	709.20	0.90	-9.41	-5.39	0.64	0.47	2.45	-14.01	-84.91
	qa	105.00	119.10	861.50	0.00	0.14	0.00	0.00	0.08	0.01	0.46	0.46
	total=						-19.14	-18.01	0.34	-6.34	-5.54	-40.64
COMB17	G 1a	-288.80	-3035.50	-644.40	1.35	-0.39	-4.10	-0.87	4.27	2.23	11.46	-42.43
	G1b	-50.00	-526.60	-112.50	1.35	-0.07	-0.71	-0.15	0.74	0.39	1.99	-7.36
	G2	0.00	-462.80	-98.70	1.35	0.00	-0.62	-0.13	0.68	0.34	1.94	-6.27
	S	-6973.20	-5990.60	709.20	1.20	-9.41	-7.19	0.85	0.75	0.93	0.05	-0.10
	W	0.00	2.70	0.90	0.90	0.00	0.00	0.00	-12.66	-11.54	-40.58	7.24
	T-	-6973.20	-5990.60	709.20	1.50	-9.41	-8.99	1.06	4.41	4.43	-2.84	-121.01
	Qa	0.00	0.00	0.00	1.01	0.00	0.00	0.00	0.00	0.00	0.00	0.00
	qa	105.00	119.10	861.50	0.54	0.14	0.06	0.47	0.01	-0.03	0.26	1.11
total=						-19.14	-21.54	1.23	-1.78	-3.25	-27.72	-168.82

(iii) Section 3

Beam and slab stresses under different load combination in table 3.22 are lower than maximum allowable stress for steel and concrete.

Table 3.22. Stress verifications at section 2 (phase 2)

Combination	Loads	Results from FEM (MIDAS/CIVIL)			Coefficient γ	Stress parameters			Stress computation			
		N(kN)	M(kNm)	T(kN)		N(MN)	M(MNm)	T(MN)	σ sup,slab (Mpa)	σ inf,slab (Mpa)	σ sup,steel (Mpa)	σ inf,steel (Mpa)
COMB10	G1a	-288.80	1832.10	-134.40	1.35	-0.39	2.47	-0.18	-2.94	-1.38	-8.96	23.57
	G1b	-50.00	317.10	-112.50	1.35	-0.07	0.43	-0.15	-0.51	-0.24	-1.55	4.08
	G2	-43.90	278.20	0.00	1.35	-0.06	0.38	0.00	-0.47	-0.58	-0.36	-0.27
	S	-4035.30	267.70	0.00	1.20	-5.45	0.32	0.00	-3.61	-3.66	34.12	31.98
	W	0.00	-0.40	0.00	1.50	0.00	0.00	0.00	0.00	0.00	0.00	-0.01
	T+	6082.30	-403.50	0.00	0.90	8.21	-0.36	0.00	5.14	0.64	27.96	23.18
	qa	104.80	2462.80	472.90	1.35	0.14	3.32	0.64	-3.56	-1.82	-9.87	33.85
	total=					2.39	6.56	0.31	-5.95	-7.03	41.35	116.40
COMB11	G1a	-288.80	1832.10	-134.40	1.35	-0.39	2.47	-0.18	-2.94	-1.38	-8.96	23.57
	G1b	-50.00	317.10	-112.50	1.35	-0.07	0.43	-0.15	-0.51	-0.24	-1.55	4.08
	G2	-43.90	278.20	0.00	1.35	-0.06	0.38	0.00	-0.47	-0.58	-0.36	-0.27
	S	-4035.30	267.70	0.00	1.20	-5.45	0.32	0.00	-3.61	-3.66	34.12	31.98
	W	0.00	-0.40	0.00	1.50	0.00	0.00	0.00	0.00	0.00	0.00	-0.01
	T+	6082.30	-403.50	0.00	0.90	8.21	-0.36	0.00	5.14	0.64	27.96	23.18
	qa	104.80	2462.80	472.90	0.54	0.14	1.33	0.26	-1.38	-0.72	-3.67	13.82
	total=					2.39	4.56	-0.08	-3.76	-5.93	47.55	96.36
COMB12	G1a	-288.80	1832.10	-134.40	1.35	-0.39	2.47	-0.18	-2.94	-1.38	-8.96	23.57
	G1b	-50.00	317.10	-112.50	1.35	-0.07	0.43	-0.15	-0.51	-0.24	-1.55	4.08
	G2	-43.90	278.20	0.00	1.35	-0.06	0.38	0.00	-0.47	-0.58	-0.36	-0.27
	S	-4035.30	267.70	0.00	1.20	-5.45	0.32	0.00	-3.61	-3.66	34.12	31.98
	W	0.00	-0.40	0.00	1.50	0.00	0.00	0.00	0.00	0.00	0.00	-0.01
	T+	6082.30	-403.50	0.00	0.90	8.21	-0.36	0.00	5.14	0.64	27.96	23.18
	qa	104.80	2462.80	472.90	0.00	0.14	0.00	0.00	0.08	0.01	0.46	0.46
	total=					2.39	3.23	-0.33	-2.31	-5.20	51.68	83.00
COMB13	G1a	-288.80	1832.10	-134.40	1.35	-0.39	2.47	-0.18	-2.94	-1.38	-8.96	23.57
	G1b	-50.00	317.10	-112.50	1.35	-0.07	0.43	-0.15	-0.51	-0.24	-1.55	4.08
	G2	-43.90	278.20	0.00	1.35	-0.06	0.38	0.00	-0.45	-0.21	-1.36	3.58
	S	-4035.30	267.70	0.00	1.20	-5.45	0.32	0.00	-0.47	-0.58	-0.36	-0.27
	W	0.00	-0.40	0.00	0.90	0.00	0.00	0.00	-3.61	-3.66	34.12	31.98
	T+	6082.30	-403.50	0.00	1.50	8.21	-0.61	0.00	5.40	0.78	28.71	20.75
	qa	104.80	2462.80	472.90	0.54	0.14	1.33	0.26	-1.38	-0.72	-3.67	13.82
	total=					2.39	4.32	-0.08	-3.95	-6.01	46.94	97.51
COMB14	G1a	-288.80	1832.10	-134.40	1.35	-0.39	2.47	-0.18	-2.94	-1.38	-8.96	23.57
	G1b	-50.00	317.10	-112.50	1.35	-0.07	0.43	-0.15	-0.51	-0.24	-1.55	4.08
	G2	-43.90	278.20	0.00	1.35	-0.06	0.38	0.00	-0.45	-0.21	-1.36	3.58
	S	-4035.30	267.70	0.00	1.20	-5.45	0.32	0.00	-0.47	-0.58	-0.36	-0.27
	W	0.00	-0.40	0.00	1.50	0.00	0.00	0.00	-3.61	-3.66	34.12	31.98
	T-	-3452.30	2044.90	0.00	0.90	-4.66	1.84	0.00	-4.71	-1.26	-20.95	3.25
	qa	104.80	2462.80	472.90	1.35	0.14	3.32	0.64	-3.56	-1.82	-9.87	33.85
	total=					-10.48	8.76	0.31	-16.25	-9.15	-8.92	100.05
COMB15	G1a	-288.80	1832.10	-134.40	1.35	-0.39	2.47	-0.18	-2.94	-1.38	-8.96	23.57
	G1b	-50.00	317.10	-112.50	1.35	-0.07	0.43	-0.15	-0.51	-0.24	-1.55	4.08
	G2	-43.90	278.20	0.00	1.35	-0.06	0.38	0.00	-0.45	-0.21	-1.36	3.58
	S	-4035.30	267.70	0.00	1.20	-5.45	0.32	0.00	-0.47	-0.58	-0.36	-0.27
	W	0.00	-0.40	0.00	1.50	0.00	0.00	0.00	-3.61	-3.66	34.12	31.98
	T-	-3452.30	2044.90	0.00	0.90	-4.66	1.84	0.00	-4.71	-1.26	-20.95	3.25
	qa	104.80	2462.80	472.90	0.54	0.14	1.33	0.26	-1.38	-0.72	-3.67	13.82
	total=					-10.48	6.77	-0.08	-14.06	-8.05	-2.72	80.02
COMB16	G1a	-288.80	1832.10	-134.40	1.35	-0.39	2.47	-0.18	-2.94	-1.38	-8.96	23.57
	G1b	-50.00	317.10	-112.50	1.35	-0.07	0.43	-0.15	-0.51	-0.24	-1.55	4.08
	G2	-43.90	278.20	0.00	1.35	-0.06	0.38	0.00	-0.47	-0.58	-0.36	-0.27
	S	-4035.30	267.70	0.00	1.20	-5.45	0.32	0.00	-3.61	-3.66	34.12	31.98
	W	0.00	-0.40	0.00	1.50	0.00	0.00	0.00	0.00	0.00	0.00	-0.01
	T-	-3452.30	2044.90	0.00	0.90	-4.66	1.84	0.00	-4.71	-1.26	-20.95	3.25
	qa	104.80	2462.80	472.90	0.00	0.14	0.00	0.00	0.08	0.01	0.46	0.46
	total=					-10.48	5.44	-0.33	-12.15	-7.11	2.77	63.08
COMB17	G1a	-288.80	1832.10	-134.40	1.35	-0.39	2.47	-0.18	-2.94	-1.38	-8.96	23.57
	G1b	-50.00	317.10	-112.50	1.35	-0.07	0.43	-0.15	-0.51	-0.24	-1.55	4.08
	G2	-43.90	278.20	0.00	1.35	-0.06	0.38	0.00	-0.45	-0.21	-1.36	3.58
	S	-4035.30	267.70	0.00	1.20	-5.45	0.32	0.00	-0.47	-0.58	-0.36	-0.27
	W	0.00	-0.40	0.00	0.90	0.00	0.00	0.00	-3.61	-3.66	34.12	31.98
	T-	-3452.30	2044.90	0.00	1.50	-4.66	3.07	0.00	-6.05	-1.94	-24.76	15.58
	qa	104.80	2462.80	472.90	0.54	0.14	1.33	0.26	-1.38	-0.72	-3.67	13.82
	total=					-10.48	8.00	-0.08	-15.40	-8.72	-6.53	92.34

3.2.4.3 Verifications of girder

a) Classification of section

Classes of different parts of main beam are presented in tables 3.23 and 3.24. It concerns web classification and next table is for flanges.

Table 3.23. Web classification

Web classification	Sections 1 and 3
c [mm]	1520
t [mm]	16
c/t	95
ϵ	0,81
124ϵ	100,44
→Class 3	
Web classification	Section 2
c [mm]	2420
t [mm]	40
c/t	95
ϵ	0,81
42ϵ	34,02
→Class 4	

Table 3.24. Flanges classification

Upper Flange classification	Sections 1,2,3
c [mm]	492
t [mm]	30
c/t	16,4
ϵ	0,81
14ϵ	11,34
→Class 4	
Lower Flange classification	Sections 1,2,3
c [mm]	742
t [mm]	16
c/t	46,375
ϵ	0,81
14ϵ	11,34
→Class 4	

b) Shear verifications

The maximum shear found in previous load combinations is at section 1 with a value of 1580 kN.

The verification of shear has been done in two steps and table 3.25 presents it.

Table 3.25. Verification of shear resistance

Shear force	$V_{Ed} = 1580 \text{ kN}$
Plastic resistance	$V_{Ed} < V_{pl,Rd} = 14306.162 \text{ kN}$
Interaction between shear and moment	$V_{Ed} < \frac{V_{b,Rd}}{2} = 7153.081 \text{ kN}$

c) Buckling verification

Looking at the results of stresses at ULS, it can be testified that section 2 at bridge pier is compressed. Buckling resistance must be checked.

Table 3.26. Buckling resistance of section 2

Axial force	$N_{Ed} = 19140 \text{ kN}$
Slenderness	$\bar{\lambda} = 0.28$
Reduction factor	$\chi = 0.98$
Buckling resistance	$N_{b,Rd} = 147\,475.2 \text{ kN}$

3.2.4.4 Pier verification

This section concerns different verifications done on pier sections which are section classification, bending, compression and buckling resistance. Also, in order to proceed with a nonlinear analysis, it is necessary to classify the sections and verify that they can develop their plastic capacity that is to say if they are of class 1 or 2 (according to EC formulation).

a) Classification of section

Classification of pier cross sections is shown in table 3.27.

Table 3.27. Pier section classification

Web classification	Pier section
c [mm]	1350
t [mm]	100
c/t	13.50
ε	0,81
33ε	26.73

→Class 1	
Flange classification	Pier section
c [mm]	710
t [mm]	100
c/t	7.10
ε	0,81
9ε	7.29
→Class 1	

The conclusion is that pier sections are from class 1.

b) Bending Verification

Bending resistance of the pier is presented in table 3.28:

Table 3.28. Bending resistance of the piers

Bending moment	$M_{Ed} = 23163,50 \text{ kN.m}$
Plastic resistance	$M_{Ed} < M_{pl,Rd} = 24015,81 \text{ kN.m}$

c) Compression verification

The table 3.29 shows the resistance of the piers to the axial force (compression).

Table 3.29. Resistance to compression

Compression force	$N_{Ed} = 3561,50 \text{ kN}$
Plastic resistance	$N_{Ed} < N_{pl,Rd} = 147 \text{ 325 kN}$

d) Buckling verification

Pier buckling resistance is presented in table 3.30.

Table 3.30. Buckling resistance verification

Axial force	$N_{Ed} = 3561.50 \text{ kN}$
Slenderness	$\bar{\lambda} = 0.054$
Reduction factor	$\chi = 1$
Buckling resistance	$N_{b,Rd} = 147 \text{ 325 kN}$

e) Shear verification

Shear resistance of the pier is presented in the table 3.31:

Table 3.31. Shear verifications

Shear force	$V_{Ed} = 5266.40 \text{ kN}$
Plastic resistance	$V_{Ed} < V_{pl,Rd} = 61 \text{ 487.80 kN}$

3.2.4.5 Transverse cross beams verification

This section concerns different verifications done on cross beams sections (HEA 700) which are classifications and bending resistance.

a) Classification of section

Classification of cross beam cross sections is shown in table 3.32.

Table 3.32. Classification of transversal cross beam sections

Web classification	Cross beams section
c [mm]	582
t [mm]	14.50
c/t	40.14
ϵ	0,81
72ϵ	58.32
→Class 1	
Flange classification	Cross beams section
c [mm]	142.75
t [mm]	27
c/t	5.287
ϵ	0,81
9ϵ	7.29
→Class 1	

b) Bending verification

Bending resistance of the cross beams is presented in the following table:

Table 3.33. Bending resistance of the cross beams

Bending moment	$M_{Ed} = 2371 \text{ kN.m}$
Plastic resistance	$M_{Ed} < M_{pl,Rd} = 2496,72 \text{ kN.m}$

3.3 Eigen-value analysis

Having defined the mass of the structure which is 172.30 kN/g (dead loads), a modal analysis was performed in the software Midas Civil 2022. This analysis is done in order to obtain the fundamental information about the dynamic characteristics of the bridge structure. In the table 3.34 and table 3.35 it is possible to find the periods and effective mass ratios of the first 15 modes. Mode 1 is the fundamental mode in the transverse direction with an effective mass ratio of 62.75% and period of 0.11 s, and mode 5 is fundamental in the longitudinal direction with 89.32% of effective mass ratio and period of 0.06 s. It can be

noticed from these results that the numerical model was well represented because of the convergence of the following periods.

Table 3.34. Frequency and periods of the first 15 modes

Mode No	Frequency		Period
	(rad/sec)	(cycle/sec)	(sec)
1	55.89	8.89	0.11
2	78.27	12.46	0.08
3	79.48	12.65	0.08
4	97.87	15.58	0.06
5	110.45	17.58	0.06
6	111.55	17.75	0.06
7	117.21	18.65	0.05
8	153.44	24.42	0.04
9	179.55	28.58	0.03
10	179.62	28.59	0.03
11	181.09	28.82	0.03
12	182.56	29.06	0.03
13	184.48	29.36	0.03
14	185.43	29.51	0.03
15	207.88	33.08	0.03

Table 3.35. Modal participation ratios

MODAL PARTICIPATION MASSES PRINTOUT						
Mode No	TRAN-X		TRAN-Y		TRAN-Z	
	MASS (%)	SUM (%)	MASS (%)	SUM (%)	MASS (%)	SUM (%)

1	0	0	62.75	62.75	0	0
2	0	0	0	62.75	33.77	33.77
3	0	0	2.98	65.73	0	33.77
4	0	0	0	65.73	0	33.77
5	89.32	89.32	0	65.73	0	33.77
6	0	89.32	0	65.73	0	33.77
7	0	89.32	31	96.72	0	33.77
8	0	89.32	0	96.72	0	33.77
9	0	89.32	0	96.72	41.28	75.05
10	9.87	99.19	0	96.72	0	75.05
11	0	99.19	0.48	97.21	0	75.05
12	0	99.19	0	97.21	0	75.05
13	0	99.19	0	97.21	0	75.05
14	0	99.19	0	97.21	0	75.05
15	0	99.19	0.28	97.49	0	75.05

The figure 3.7, 3.8, show the deflection of the structure when subjected to the first mode and the figure 3.9, 3.10, for the fifth mode.

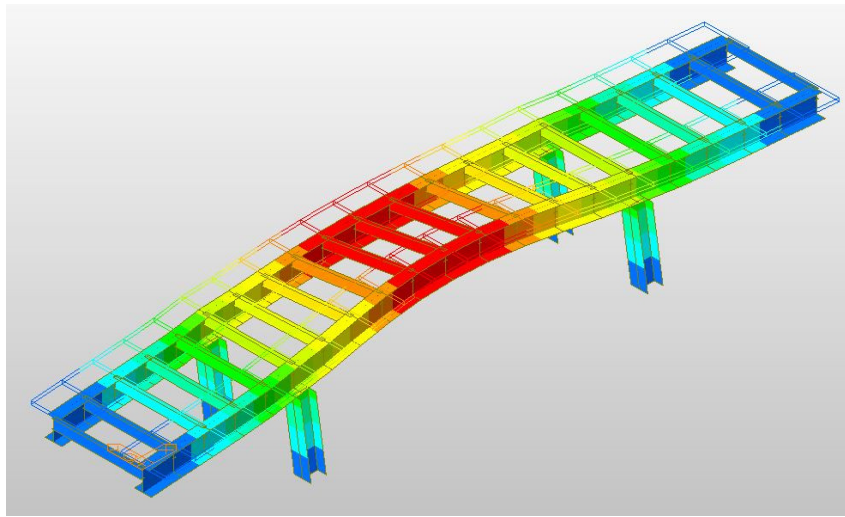


Figure 3.7. Isometric view (Mode 1)

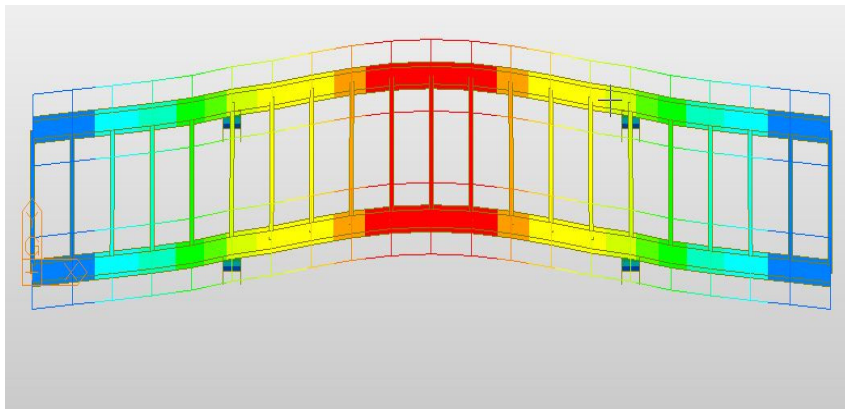


Figure 3.8. Plan View (Mode 1)

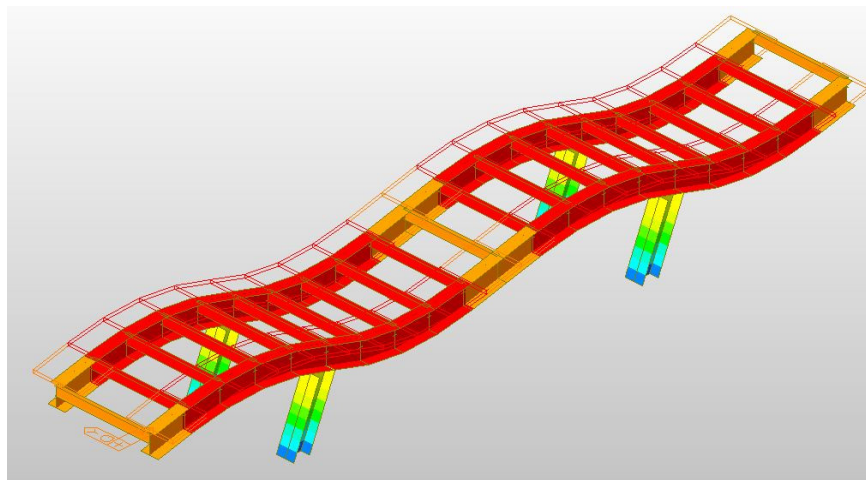


Figure 3.9. Isometric view (Mode 5)

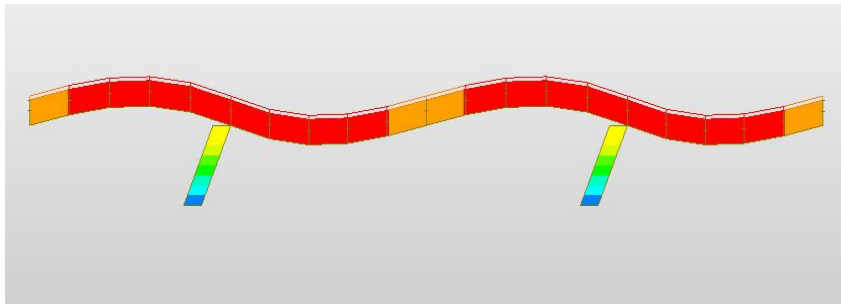


Figure 3.10. Elevation view (Mode 5)

3.4 Seismic analysis

These analyses were performed with the software Midas/Civil. First a response spectrum analysis was applied to obtain the demand displacement and then a nonlinear static analysis commonly call pushover analysis to obtain the capacity of the bridge.

In order to proceed with the analysis, it is necessary to mention some simplifications adopted in the modelling:

- Since, the bridge is not located within an active fault, the response in the vertical direction will be ignored and not combined with the horizontal response. Also, the vertical seismic component effects on the piers could be neglected in regions of low to moderate seismicity, in case of high seismicity regions, the vertical component effects must be analysed only in some exceptional cases where the piers are subjected to important bending due to the permanent actions of the deck (EC8-2).
- The monotonic nonlinear behaviour of the materials should be known in the form of a tensile-strain relationships, the laws of material behaviour which contain the variation of the rigidity of the constituent materials as a function of the tensions and deformations to which they are subjected. In this bridge there is only one considered structural material which is steel.
- The deck was considered to perform elastically, given that, in order to properly consider its nonlinear behaviour a detailed definition of all longitudinal and transverse elements, distribution or detailing of steel reinforcement would be required. Usually, in steel frame bridges, hinges form firstly in the substructure due to transverse seismic action. Also, it is due to the fact that the analysis of a ductile substructure with an essentially elastic superstructure is considered.
- In the preliminary study, the possibility of pushing the deck alone has been investigated, the choice of pushing just the deck was considered observing that at

least for the considered case study, the superstructure is the physical location where the vast majority of the inertia mass is found.

- Geometric imperfections are not considered.

Notice that monolithic or rigid connection of the deck to the piers tops also affects the bridge performance under non-seismic actions. The effect may be favourable (the performance under braking or centrifugal traffic action in railway bridges), or negative (the restraint of thermal or shrinkage deformations in a long deck on stiff piers, which may even be prohibitive for the bridge).

3.4.1 Response spectrum analysis

3.4.1.1 Response spectrum functions

A spectrum is an envelope of the maximum values recorded so it reproduces the worst-case scenario in terms of maximum seismic accelerations experienced for a given structure considering a given return period.

The seismic load applied in this work will be applied as a ground acceleration corresponding to the horizontal component of the design response spectrum.

Since the structure achieved a dissipative structural behaviour, that is to say that the seismic actions do take in account the nonlinear material and geometric behaviour, then, it was chosen a behaviour factor q of 1.5 (for Ultimate Limit States-ULS).

The bridge has been classified as an importance class III, which comprises bridges of critical importance for maintaining communications, especially in the immediate post-earthquake periods, bridges failure of which is associated a large number of probable fatalities and major bridges where a design life greater than normal is required (EC 8-2).

For maximum ground acceleration (peak ground acceleration-PGA), the values from the reference horizontal peak ground acceleration according to the seismic zone map of Italy was taken (see figure 3.11). The table 3.36 gives the different PGA's values.

Table 3.36. Seismic zonation criteria and reference horizontal peak ground acceleration (Conference & Engineering, 2004)

Zone	Horizontal peak ground acceleration with 10% exceedance probability in 50 years [a_g/g]	Reference horizontal peak ground acceleration [a_g/g]
1	> 0.25	0.35
2	0.15 - 0.25	0.25
3	0.05 - 0.15	0.15
4	< 0.05	0.05

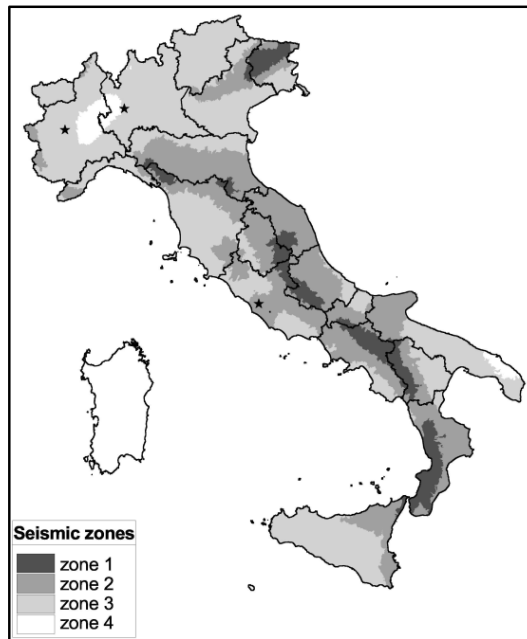


Figure 3.11. Seismic zonation of Italy (Conference & Engineering, 2004)

It is important to know that:

- Zone 1 stands for high seismicity;
- Zone 2 stands for medium-high intensity;
- Zone 3 stands for medium-low seismicity;
- Zone 4 stands for low seismicity.

In addition to it others PGA’s values were obtained from the modified Mercalli intensity scale.

The properties of the different spectrum are defined in table 3.37.

Table 3.37. Seismic parameters

Soil classes	B
Importance class III	1.2
Damping ratio	4%
Peak ground acceleration (a_{gR})	<ul style="list-style-type: none"> • Zone 1 : 0.35g • Zone 2 : 0.25g • Zone 3 : 0.15g • Zone 4: 0.05g • Very strong: 0.401g

	<ul style="list-style-type: none"> • Severe: 0.747g • Violent: 1.39g
Horizontal response spectrum	<ul style="list-style-type: none"> • Type 1 for zone 1 to 2 and very strong to violent • Type 2 for zone 3 to 4
Lower limit of the horizontal design spectrum	0.2
Behaviour factor	1.5

Design response spectrums according to EC-8 regulations and formulations (equation 2.72 to 2.75) to obtained it, are illustrated on figure 3.12.

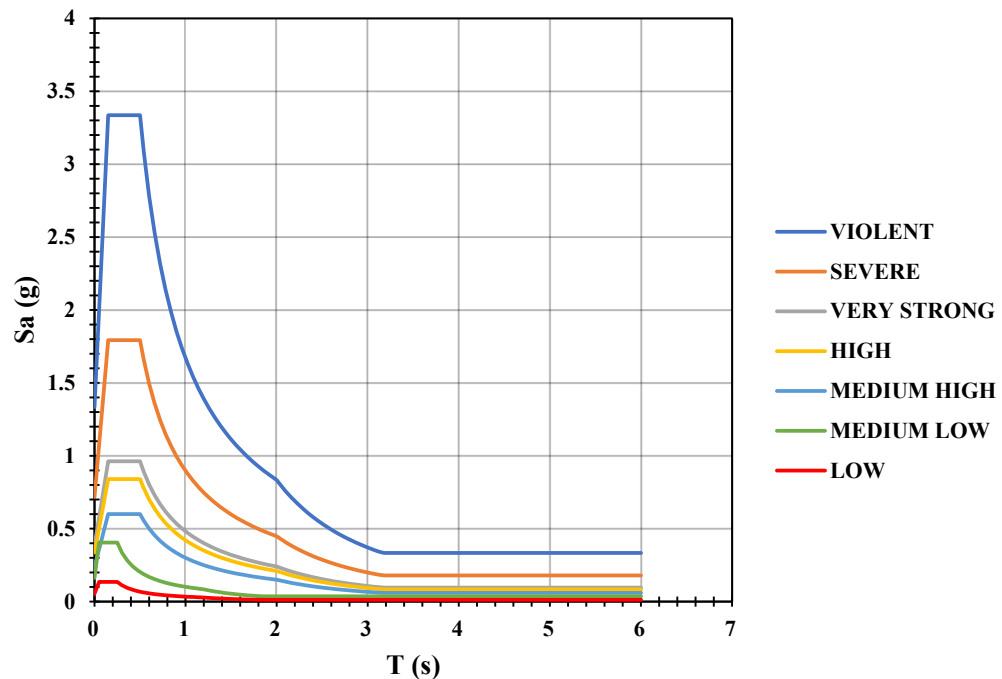


Figure 3.12. Design response spectrums

3.4.1.2 Demand displacement

From the response spectrum analysis, the various demand displacement in both horizontal directions for the seven response spectrum functions was obtained and from these results, the design seismic displacements were obtained.

The 100:30 rule was applied as the following:

- First case: seismic demand displacements along each of the principal axes of a member shall be obtained by adding 100% of the absolute value of the member seismic displacements resulting from the analysis in one of the perpendicular (longitudinal) direction to 30% of the absolute value of the corresponding member seismic displacements resulting from the analysis in the second perpendicular direction (transverse).
- Second case: seismic demand displacements along each of the principal axes of a member shall be obtained by adding 100% of the absolute value of the member seismic displacements resulting from the analysis in one of the perpendicular (transverse) direction to 30% of the absolute value of the corresponding member seismic displacements resulting from the analysis in the first perpendicular direction (longitudinal).

A damping correction factor of 1.4 was obtained and a displacement ductility factor of 3.5.

Using the equation 2.78, it was obtained the following results presented in the table 3.38.

Table 3.38. Design seismic displacement

Response spectrum functions	Demand displacements (m)	Displacement magnification (m)	Design seismic displacements (m)
Violent intensity	$d_{EeX} = 0.008$ $d_{EeY} = 0.053$	$D_{eX} = 0.026$ $D_{eY} = 0.185$	$D_X = 0.082$ $D_Y = 0.193$
Severe intensity	$d_{EeX} = 0.004$ $d_{EeY} = 0.028$	$D_{eX} = 0.014$ $D_{eY} = 0.099$	$D_X = 0.044$ $D_Y = 0.104$
Very strong intensity	$d_{EeX} = 0.002$ $d_{EeY} = 0.015$	$D_{eX} = 0.008$ $D_{eY} = 0.053$	$D_X = 0.024$ $D_Y = 0.056$
High intensity	$d_{EeX} = 0.002$ $d_{EeY} = 0.013$	$D_{eX} = 0.007$ $D_{eY} = 0.047$	$D_X = 0.021$ $D_Y = 0.049$
Medium-high intensity	$d_{EeX} = 0.001$ $d_{EeY} = 0.010$	$D_{eX} = 0.005$ $D_{eY} = 0.033$	$D_X = 0.015$ $D_Y = 0.035$

Medium-low intensity	$d_{EeX} = 0.001$	$D_{eX} = 0.004$	$D_X = 0.011$
	$d_{Eey} = 0.006$	$D_{eY} = 0.022$	$D_Y = 0.024$
Low intensity	$d_{EeX} = 0.002$	$D_{eX} = 0.008$	$D_X = 0.024$
	$d_{EeY} = 0.015$	$D_{eY} = 0.053$	$D_Y = 0.056$

3.4.2 Pushover analysis

Pushover analysis allows, for a given seismic action, to estimate the structure performance and check if it meets the desired one. In order to perform the pushover analysis, it is necessary to know all the elements of the structure and the behaviour curve of the materials.

3.4.2.1 Nonlinear behaviour of the elements

The nonlinear behaviour is defined by the definition of the plastic hinges. In fact, the piers are modelled with elements having linear elastic properties. Therefore, the nonlinearity due to seismic aspects must be assign.

The plastic hinges properties were defined by default to execute the pushover analysis. For our calculation model, plastic hinges will be introduced in the piers with behaviour laws defined by default by the software as follows and the properties will be automatically computed:

- Bilinear type hinge: linear, 1st yielding strength, 2nd yielding strength (moment-curvature curve, distributed plasticity type with degree of freedom: D_x, R_y, R_z), where:
 - D_x : axial component in the element's local x-direction;
 - D_y : shear component in the element's local y-direction;
 - D_z : shear component in the element's local z-direction;
 - R_x : torsional component about the element's local x-axis;
 - R_y : bending moment component about the element's local y-axis;
 - R_z : bending moment component about the element's local z-axis;
 - 1st yield strength represents the member force a structural steel member at the time the top or bottom fiber starts yielding;
 - 2nd yield strength represents the member force at which an entire member starts yielding.

The figure 3.13 illustrates the bilinear model.

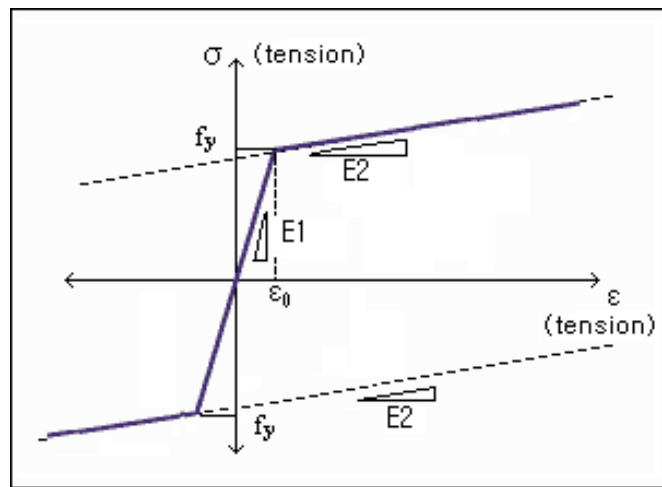


Figure 3.13. Steel bilinear model

- Trilinear: linear, 1st yielding strength, 2nd yielding strength, 3rd yielding strength (moment-curvature curve, distributed plasticity type with degree of freedom: Dx, Ry, Rz). The figure 3.14 illustrates the trilinear model.

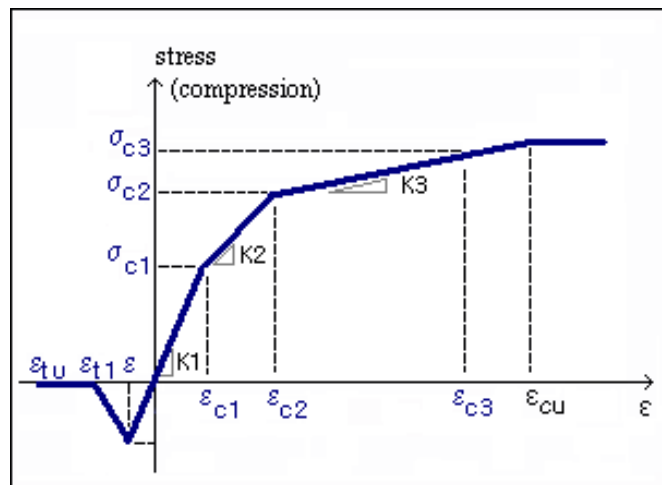


Figure 3.14. Steel trilinear model

- FEMA type hinge (moment-rotation curve, concentrated plasticity, hinge status is classified based on three levels of FEMA functionality which are: linear, IO (Immediate Occupancy), LS (Life Safety), CP (Collapse Prevention)). This hinge will be used to assess the status of yielding. Figure 3.15 illustrates the FEMA type hinge model.

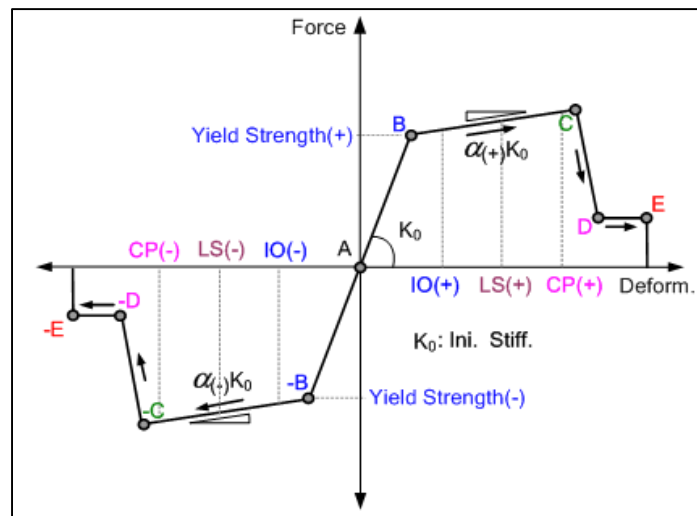


Figure 3.15. FEMA hinge model

- Point (A) represents the origin.
- Point (B) represents plasticization, no deformation at the hinges, all elastic deformations are ignored.
- Point (C) represents the ultimate capacity for pushover analysis.
- Point (D) represents the residual strength for the pushover analysis.
- Point (E) represents the total failure of the elements.

Before reaching point B, the deformation is linear and occurs in the element itself, not in the hinge.

Plastic deformation beyond point B occurs in the hinge in addition to any elastic deformation that may occur in the member, the residual strength from D to E allows the members to support gravity loads.

The status of yielding, capacity curve and performance due to bilinear and trilinear hinge type will be presented in the annex part.

3.4.2.2 Load pattern

According to FEMA and EC8, at least two patterns should be used:

- Uniform pattern with lateral forces proportional to mass, independent of their elevation (uniform response acceleration).
- Modal pattern with lateral forces proportional to the modal lateral force distribution according to elastic analysis in the direction under consideration.

In this approach two types of distribution are considered for the representation of the earthquake loading:

- The modal shape distribution of the major mode in the considered direction (in the longitudinal direction it is mode 5 with 89% of the mass and in the transverse direction it is mode 1 with 63% of the mass involved).
- Inertia force distribution or uniform acceleration (in which for the both directions 100% of the mass is involve).

3.4.2.3 Capacity curve

The capacity curve of the structure represents the horizontal force (in kN) at the base of the bridge as a function of displacement (in m), and is formed by a phase of linear elasticity, followed by a nonlinear phase corresponding to the formation of flexural plastic hinges, until the moment of failure.

With the two types of loads defined above, it is possible to obtain the respective capacity curve for both load patterns that are represented in the following figures (200 steps was applied with a maximum global displacement of 0.8 m largely higher compare to the demand displacement), figure 3.16, figure 3.17, figure 3.18 and figure 3.19 illustrate the different capacity curves obtained:

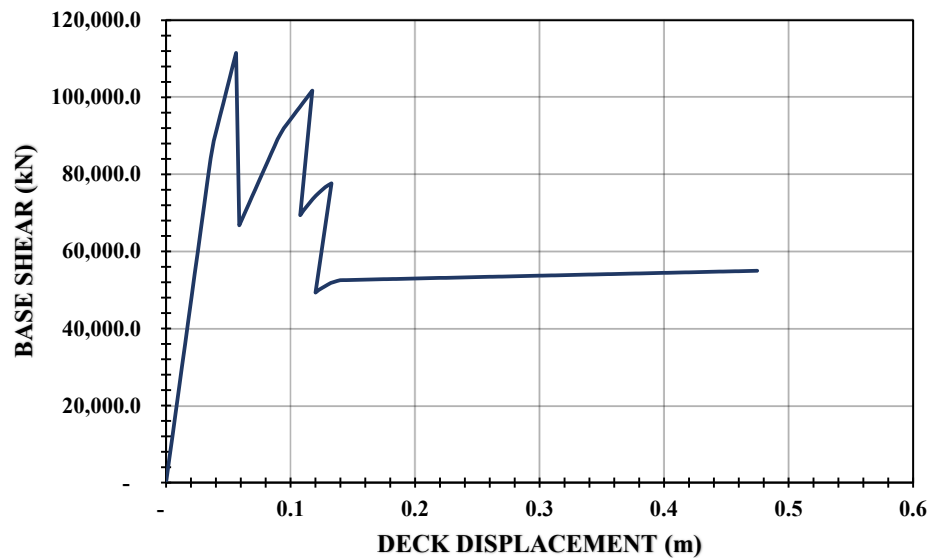


Figure 3.16. Capacity curve obtained for the uniform shape distribution in the longitudinal direction (FEMA)

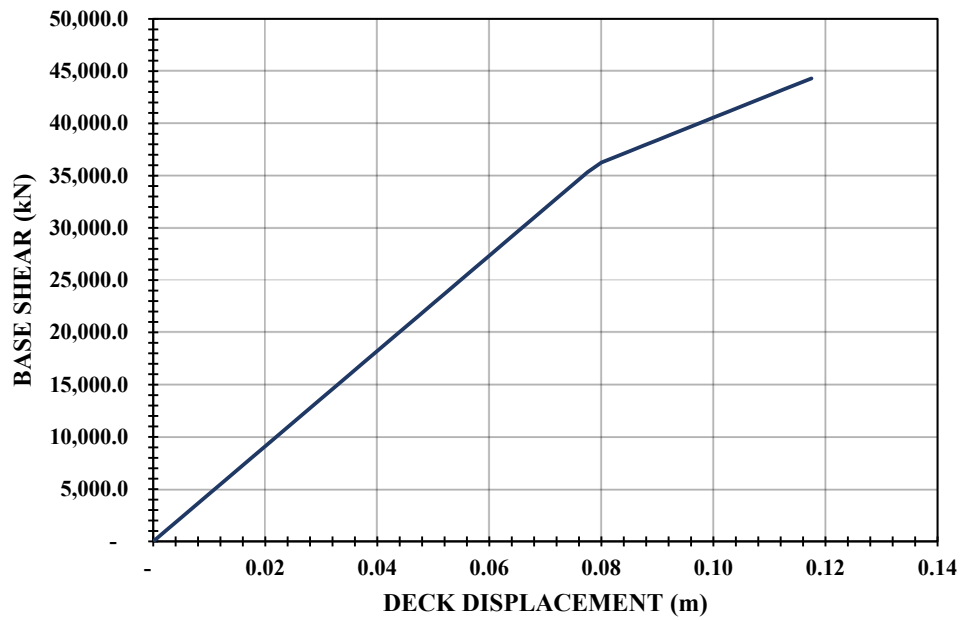


Figure 3.17. Capacity curve obtained for the uniform shape distribution in the transverse direction (FEMA)

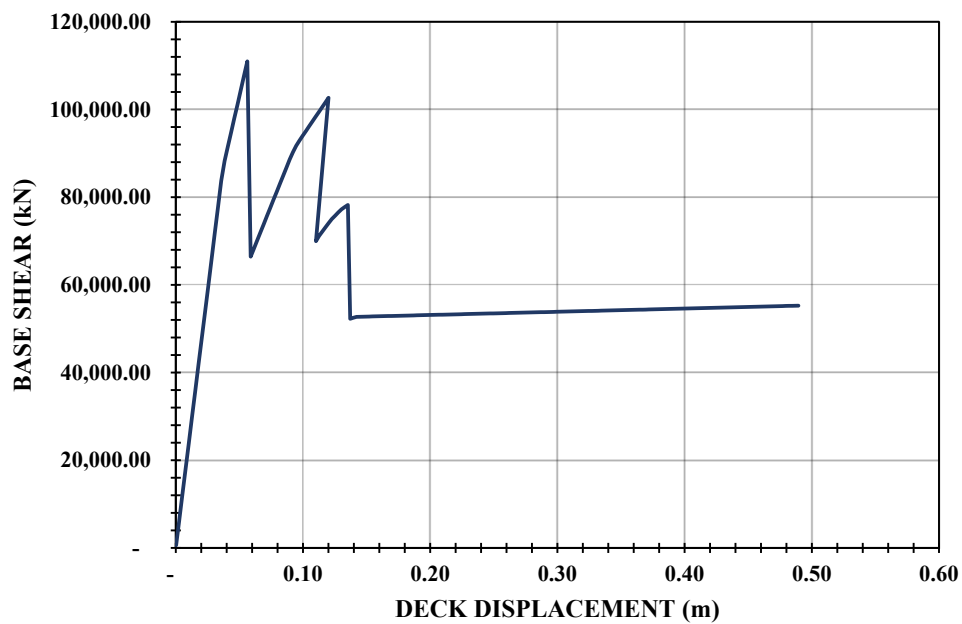


Figure 3.18. Capacity curve obtained for the modal shape distribution in the longitudinal direction (FEMA)

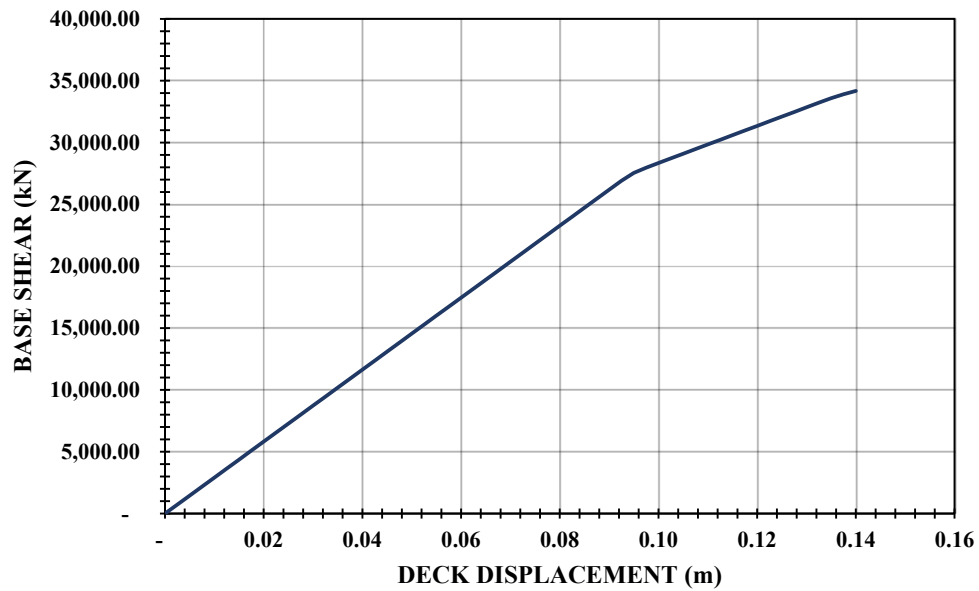


Figure 3.19. Capacity curve obtained for the uniform shape distribution in the transverse direction (FEMA)

It is possible to verify from the figures that the capacity curves in the considered directions are quite similar. Maximum displacement of equivalent SDOF system subjected to modal is 0.14 m in the transverse direction and 0.49 m in the longitudinal direction and for the uniform loading, it is 0.11 m for the transverse direction and 0.48 m in the longitudinal direction.

In the longitudinal direction, the capacity displacement is 0.06 m for the uniform and modal loading which is greater than the design seismic displacement for severe intensity (0.04 m) and less than for the violent intensity (0.08). It is also the case for the transverse direction where the capacity displacement in the both load patterns are greater than the seismic demand displacement of severe earthquake (0.10 m) but less than the violent intensity (0.19 m).

As for the maximum base shear force it is 34175 kN (step 56) in the transverse direction and 111000 kN (step 22) in the longitudinal direction for the modal loading and 44303.4 kN (step 47) in the transverse direction and 111519 kN (step 22) in the longitudinal direction for the uniform loading.

The curves obtained, using the default hinge characteristics consist of eleven parts for the longitudinal direction and two parts for the transverse.

For the longitudinal direction, the first part is an ascending straight line, its slope represents the initial stiffness of the structure, the second part of the curve is a straight line with a small slope, which represents the phase after, the beginning of plasticization of the

structure, in this phase the resistance capacity increases due to the phenomenon of steel work hardening, until the point that represents the displacement capacity of the structure, which corresponds to the beginning of the degradation of the shear strength at the base of the bridge piers. After this point, the curves begin their descent, where the deformation increases with the degradation of the shear strength at the base of the structure, then the same process is repeated two times due to residual stiffness of the structure, until the total failure of the structure.

For the transverse direction, the first part is an ascending straight line, its slope represents the initial stiffness of the structure, the second part of the curve is a straight line with a small slope, which represents the phase after, the beginning of plasticization of the structure, in this phase the resistance capacity increases due to the phenomenon of steel work hardening, until the point that represents the displacement capacity of the structure.

It should be noticed that in the transverse direction 56 steps was obtained that is to say 56 increments of loads in the modal loading and 47 steps in the uniform loading.

3.4.2.4 Status of yielding – damage level

The damage level according to FEMA regulations will be analysed which implies that for a good explanation of the yielding mechanism, the FEMA hinge type will be used as previously said before. The mechanisms are quite the same for modal and uniform loading, the focus will be only on the uniform loading involving 100% of the mass.

a) Longitudinal direction

After the distribution of the plastic hinges in the structure, and after each step of the pushover analysis loading, it was noticed that the first plastic hinges of type B were formed at the base (bottom) of the piers exactly in step 15 (figure 3.20) then it becomes a plastic hinge of type IO at step 17 (figure 3.21), until here it indicates that the state of damage up to step 17 is very limited, no deformation in the hinges. The horizontal and vertical force-resisting systems of the bridge retain their pre-earthquake strength and rigidity. The danger to life from structural damage is very low, despite this, some simple structural repairs must take place which are not generally required before the bridge can be re-used.

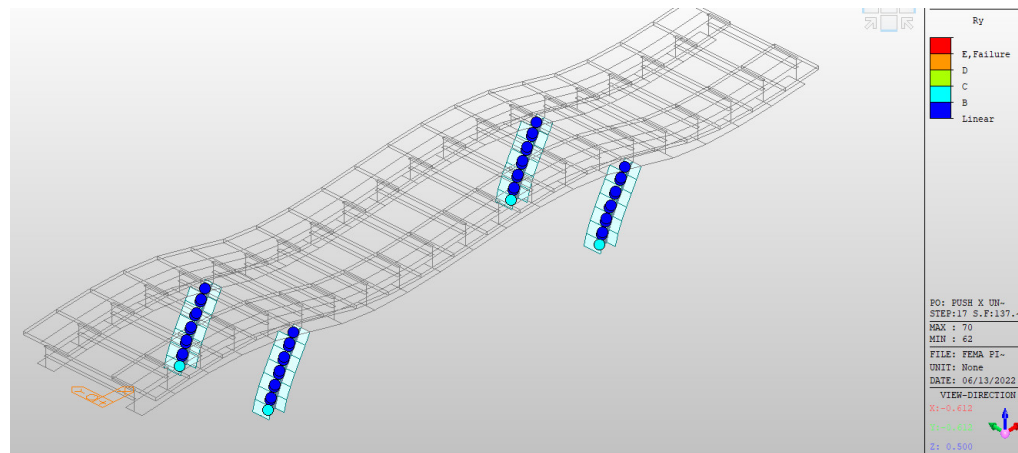


Figure 3.20. Plastic hinges at step 15

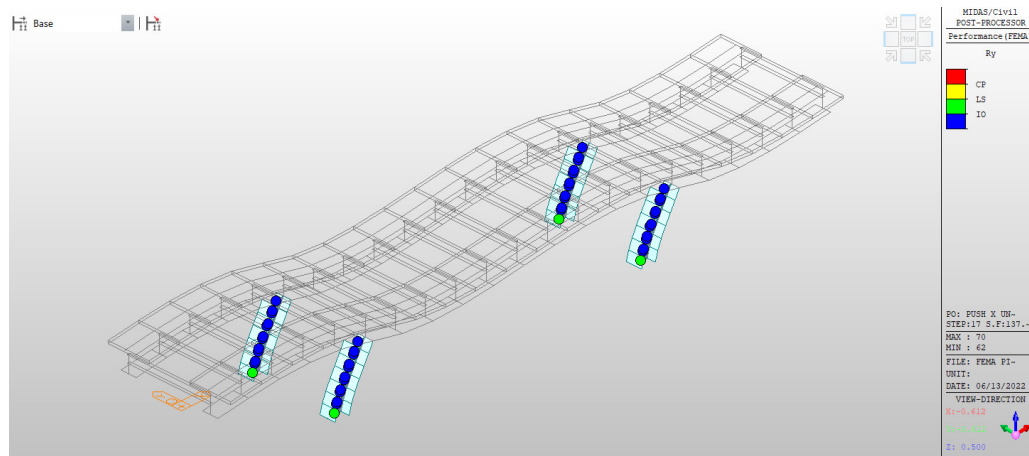


Figure 3.21. Plastic hinges at step 17

When the load is increased incrementally, plastic hinges of type LS are formed at the base of the piers at step 21. This indicates that, the post-earthquake damage to the structure is significant, but there is a margin against collapse, some structural elements and components are badly damaged, but this does not result in the fall of important debris. The damage may occur during the earthquake, but the danger to life resulting from this damage is low, the use of the bridge can be prohibited until it is repaired.

At step 23, the appearance (figure 3.22) of ruin plastic hinges type is observed and the structure is facing collapse at this level. There can be a great danger from falling structural debris and it is not practical to repair the structure is technically unusable.

At step 36, plastic hinges of type B are observed at the top of two piers (figure 3.23), then in all the top of the piers at step 37.

In step 58 (figure 3.24), ruin plastic hinges type has also been formed in the others top of the piers.

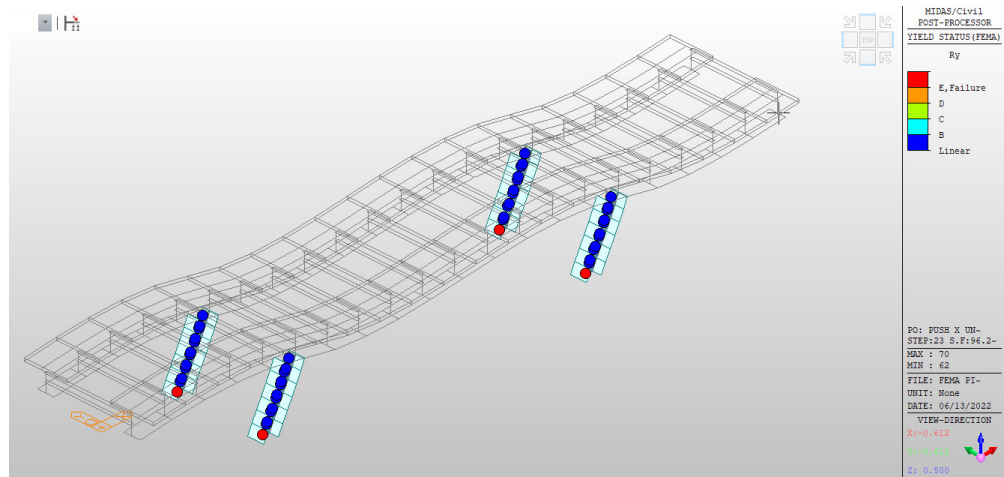


Figure 3.22. Plastic hinges at step 23

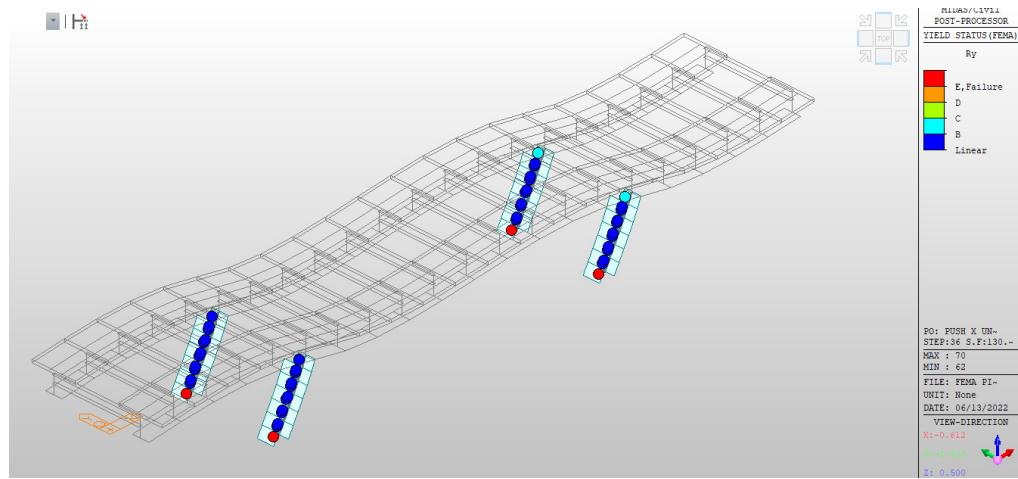


Figure 3.23. Plastic hinges at step 36

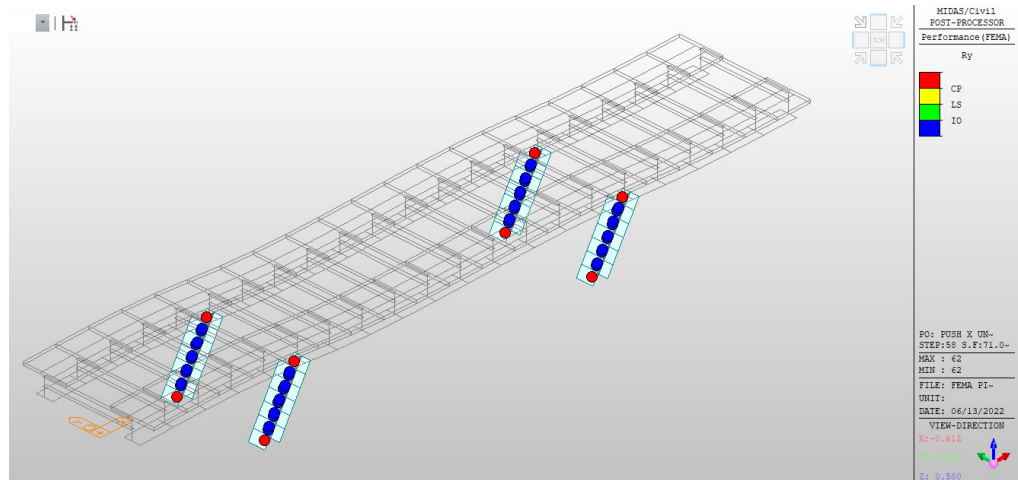


Figure 3.24. Plastic hinges at step 36

Step 36 shows the final plastic hinges pattern for the longitudinal direction and any increment of the load will not change it, the structure is totally facing collapse since in the top

and the bottom of the piers the plastic hinges have reach their ultimate strength. It should be noticed that before reaching it, plastic hinges of type IO and LS (figure 3.25) have been formed successively when loading the structure.

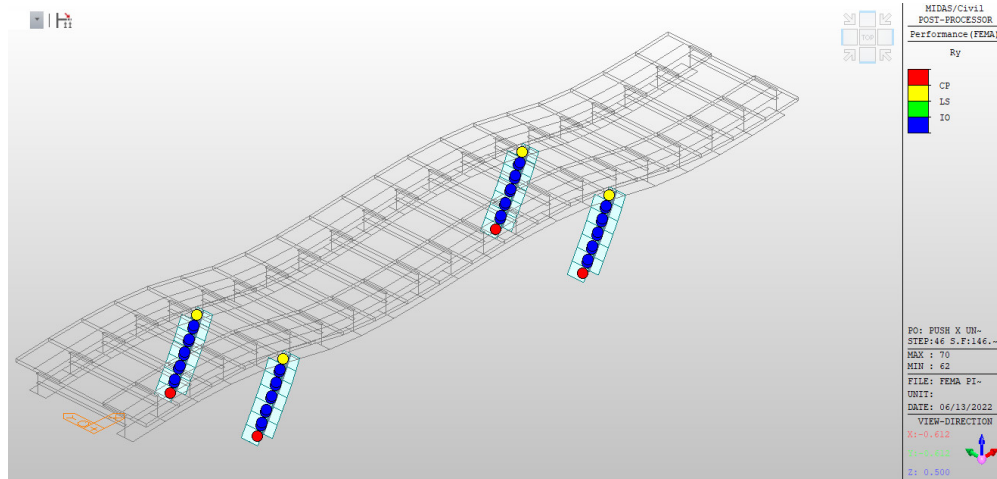


Figure 3.25. Plastic hinges at step 45

b) Transverse direction

After the distribution of the plastic hinges in the structure, and after each step of the pushover analysis loading, it was noticed that the first plastic hinges of type (B) are formed at the two back piers in step 32 (figure 3.26), and type B and IO plastic hinges appear progressively on the piers up to step 8 (figure 3.27 and figure 3.28).

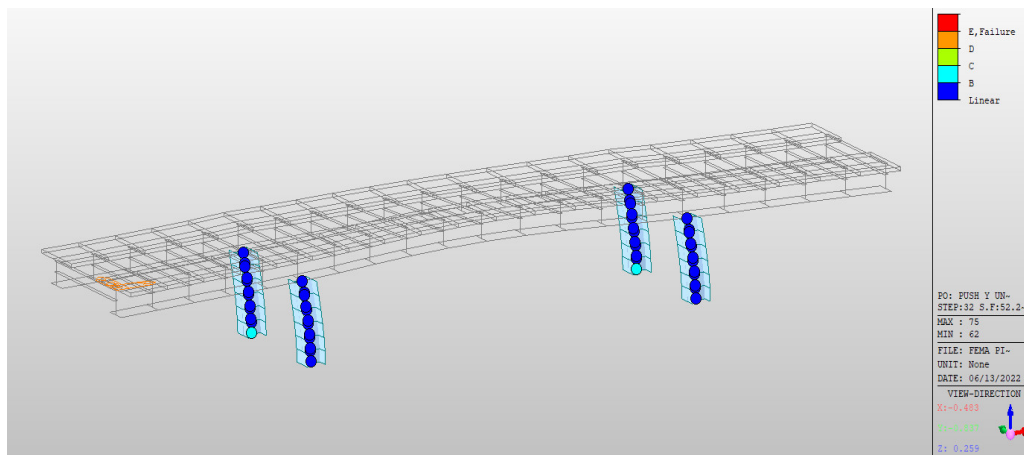


Figure 3.26. Plastic hinges at step 32

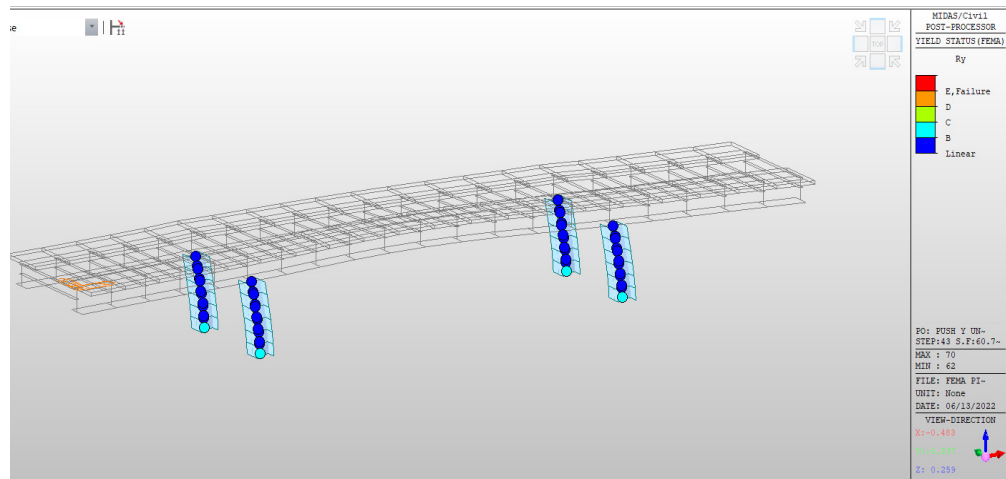


Figure 3.27. Plastic hinges at step 43, type B

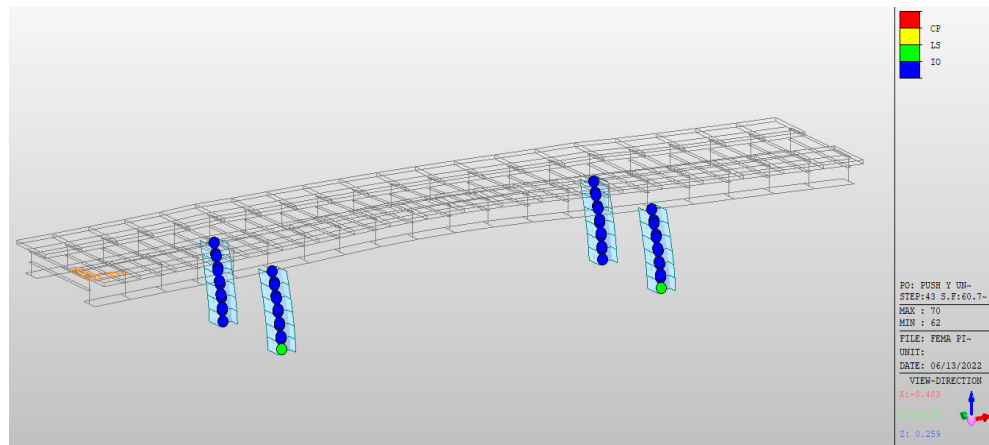


Figure 3.28. Plastic hinges at step 43, type IO

After step 43 till the end of the loading, it is observed the formation of the ruin plastic hinges in the side front piers (figure 3.29).

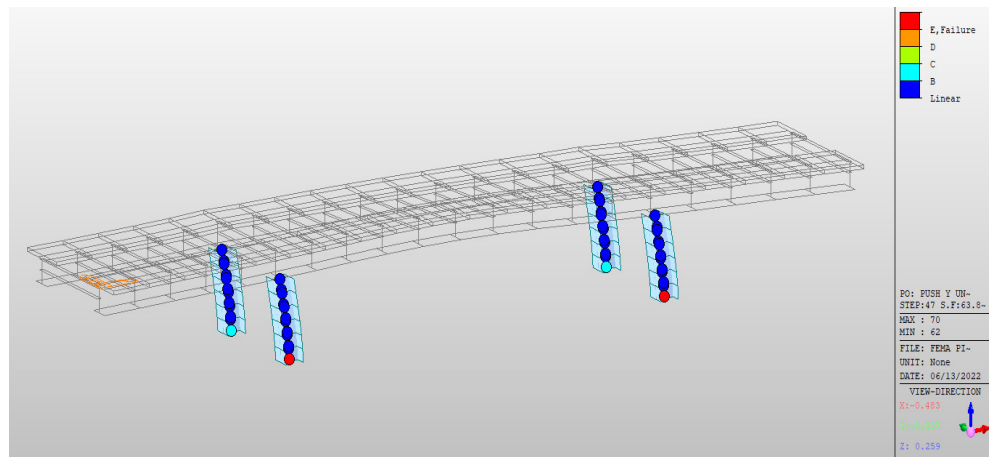


Figure 3.29. Final plastic hinges pattern

The use of pushover analysis allows the determination of the location of probable weak points and likely failure modes in the structure exposed to an earthquake. For the longitudinal direction, the plastic hinges were formed at the top and bottom of the piers but for the transverse direction, they appear only at the bottom of the structure.

3.4.3 Performance point

The capacity spectrum method is a method that allows a graphical comparison between the capacity of the structure and the earthquake demand. The lateral resistance capacity of the structure is represented by a force-displacement curve obtained from the pushover analysis, and the earthquake demand is represented by these response spectra curves.

The curves are plotted on a graph, using the same coordinates in the (ADRS) format (Acceleration Displacement Response Spectrum), where Sa is the Pseudo Acceleration Spectrum and Sd is the Displacement Spectrum.

The intersection of the capacity curve with the demand curves brings the predicted performance and the maximum responses of the structure under a given earthquake. This graphical method shows the relationship between bridge capacity and seismic demand.

The shear force values at the base and the displacement values at the top are converted to pseudo-spectral acceleration values Sa and spectral displacement values Sd , respectively, by using certain factors determined from the dynamic characteristics of the structure, whose responses are assumed to be dominated by a single eigenmode.

The demand curves are represented by the earthquake response spectrum. Typically, the response spectrum of 5% percent damping is used to represent the demand curves when the structure has an elastic response. The response spectra for 10%, 15% and 20% damping are used to represent the reduced demand in the inelastic domain to explain hysteretic damping and nonlinear effects.

In the (ADRS) format, the natural vibration periods are represented by radial lines. This spectral capacity curve (FEMA 440) is used to evaluate the performance level of the structure.

To obtain the performance point, the severe intensity with PGA equal to 1.39g was taken as the seismic demand and the performance point were obtained for each loading pattern. The following figures (figure 3.30, figure 3.31, figure 3.32 and figure 3.33) and tables (table 3.39, table 3.40, table 3.41 and table 3.42) relate information about the performance point for each loading using FEMA 440, procedure A approach.

Table 3.39. Performance point for uniform loading in the longitudinal direction

Step	2
Shear, displacement (V, D)	Elastic ($1,55.10^4$ kN, 0.006591 m)
Spectral acceleration, spectral displacement (Sa, Sd)	Elastic (2.66g, 0.007g)
Effective period, effective damping (T_{eff}, D_{eff})	0.11 sec, 5%

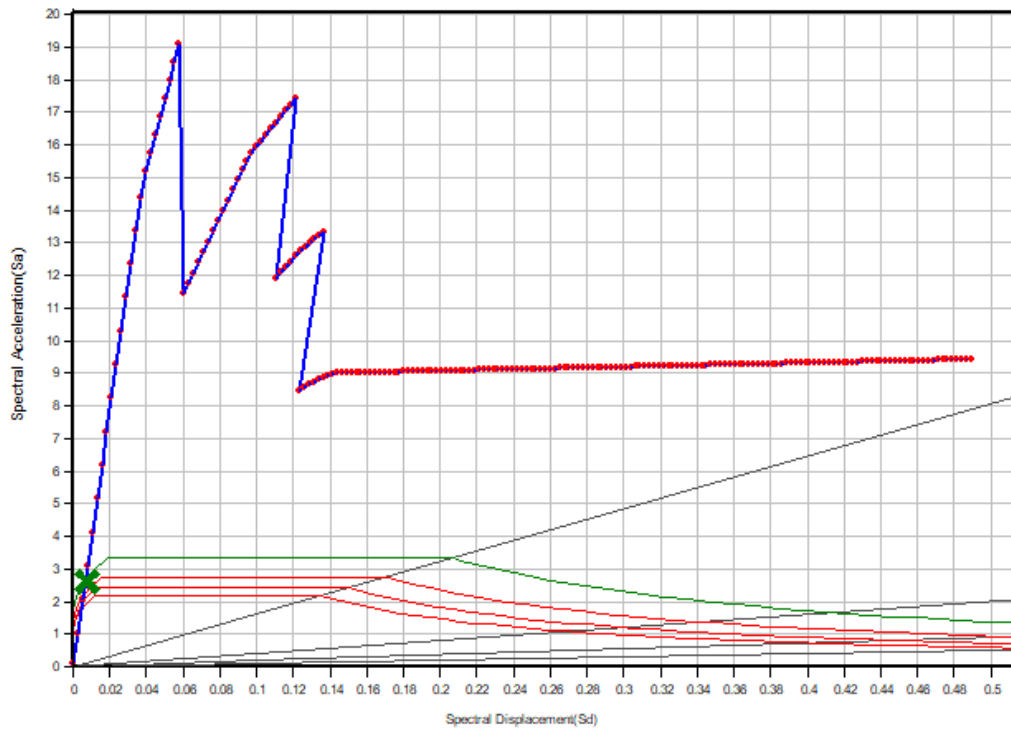


Figure 3.30. Performance point for uniform loading in the longitudinal direction

Table 3.40. Performance point for uniform loading in the transverse direction

Step	12
Shear, displacement (V, D)	Elastic ($1,371.10^4$ kN, 0.03 m)
Spectral acceleration, spectral displacement (Sa, Sd)	Elastic (3.328g, 0.022g)
Effective period, effective damping (T_{eff}, D_{eff})	0.22 sec, 5%

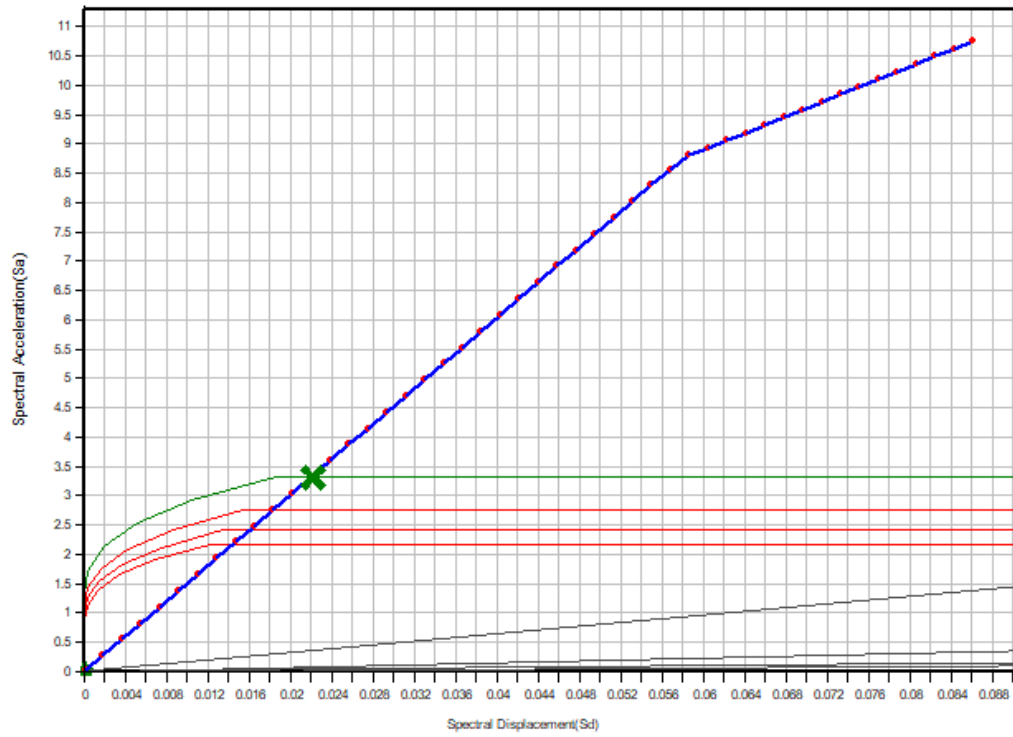


Figure 3.31. Performance point for uniform loading in the transverse direction

Table 3.41. Performance point for modal loading in the longitudinal direction

Step	2
Shear, displacement (V, D)	Elastic ($1,552 \cdot 10^4$ kN, 0.006625 m)
Spectral acceleration, spectral displacement (Sa, Sd)	Elastic (2.658g, 0.006828g)
Effective period, effective damping (T_{eff} , D_{eff})	0.11 sec, 5%

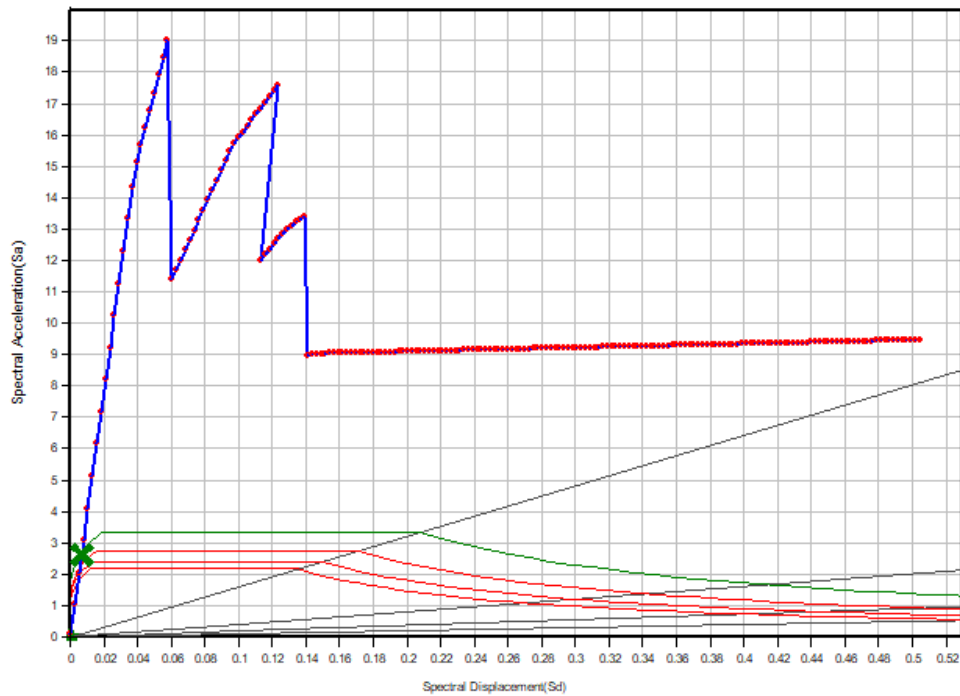


Figure 3.32. Performance point for modal loading in the longitudinal direction

Table 3.42. Performance point for modal loading in the transverse direction

Step	18
Shear, displacement (V, D)	Elastic ($1,371.10^4$ kN, 0.04712 m)
Spectral acceleration, spectral displacement (Sa, Sd)	Elastic (3.328g, 0.03456g)
Effective period, effective damping (T_{eff} , D_{eff})	0.22 sec, 5%

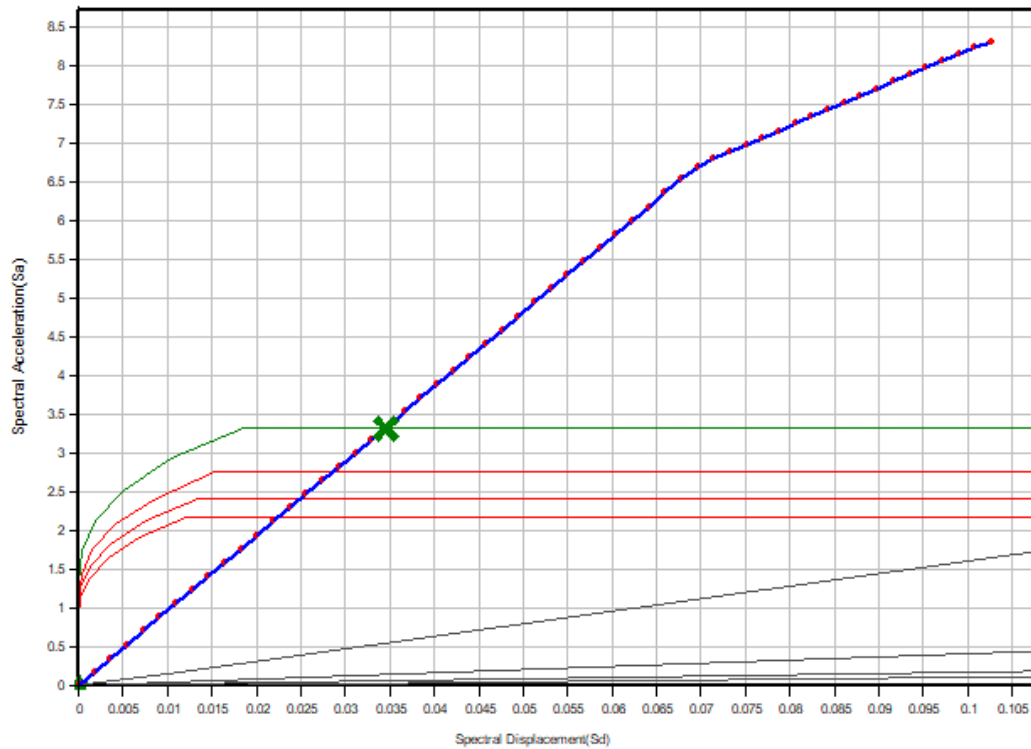


Figure 3.33. Performance point for modal loading in the transverse direction

According to these results, the equivalent viscous damping starts at 5% up to 20%, and for a PGA value of 1.39g, it was obtained:

- For the uniform loading in the longitudinal direction, the performance point is equal to 0.66 cm under a lateral force equal to 15500 kN is the target displacement of our structure which is at step 2, after step 2 the ultimate capacity of the structure has been exceeded, so the construction is on the verge to face a partial or total collapse.
- For the uniform loading in the transverse direction, the performance point is equal to 3 cm under a lateral force equal to 13710 kN is the target displacement of our structure which is at step 12, after step 12 the ultimate capacity of the structure has been exceeded, so the construction is on the verge to face a partial or total collapse.
- For the modal loading in the longitudinal direction, the performance point is equal to 0.66 cm under a lateral force equal to 15520 kN is the target displacement of our structure which is at step 2, after step 2 the ultimate capacity of the structure has been exceeded, so the construction is on the verge to face a partial or total collapse.

- For the modal loading in the transverse direction, the performance point is equal to 4.71 cm under a lateral force equal to 13710 kN is the target displacement of our structure which is at step 18, after step 18 the ultimate capacity of the structure has been exceeded, so the construction is on the verge to face a partial or total collapse.

It can be observed that the different results obtained in modal or uniform loading are quite similar. Also, the bridge strength against the seismic actions is higher in the longitudinal direction than the transversal direction which could be due to a high stiffness of the elements in the longitudinal directions compare to the transverse.

The subsequent analysis showed that for the different earthquake; the structure is almost entirely in the elastic branch at the performance point and that the dimensions of some elements, based on the seismic analysis, could be optimized in the detailed design stage (It is possible to perceive that the structure is over dimensioned because for the design earthquake event, according to its target displacement, the structure behaviour is located in the elastic response zone).

Pushover analysis is a very useful tool in the design of structures, allowing to meet specific performance criteria required by codes or owner of the future project. In this case, the structure would be in the operational performance level (figure 3.34).

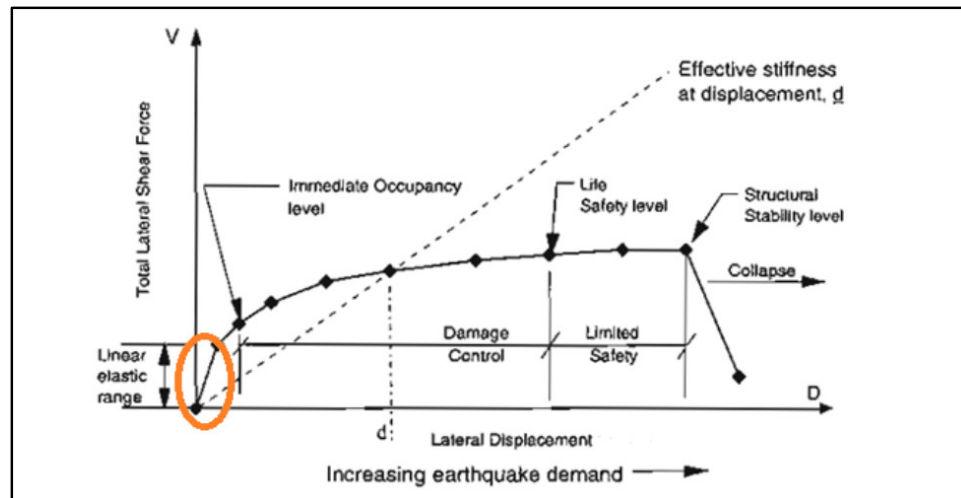


Figure 3.34. Localization of the performance point (case study) accordingly to performance level (ATC-40, 1996)

3.4.4 Analysis of the bridge considering the ductile superstructure

The use of a ductile superstructure is a relatively new strategy for design of bridges, and it was developed first as a retrofit strategy for existing bridges. The idea behind this strategy, which is effective mostly in the transverse direction and for steel I-girder

superstructures, is that cross bracing and cross beams between the girders can be detailed to be sufficiently ductile to dissipate earthquake-induced kinetic energy and with such a strategy only the cross frames at the piers and abutments are considered as yielding elements. Cross frames in the span do not experience significant inelastic action in these systems. The design requirements for such systems are not yet fully developed, and therefore are not as detailed because it is an emerging technology (AASHTO LRFD Guide Specification, 2014).

Here it is assumed to consider the structure globally ductile, that is to say that a ductile substructure was associate to a ductile superstructure. The goal is to illustrate the plastic hinge mechanism in the girders (in the case it was assumed the superstructure able to develop ductile mechanisms) especially the one coming from the loading (uniform or modal) in the longitudinal direction since for the transverse direction, the plastic hinge appears only in the pier's bottom.

It should be noticed that since it is a composite section (mixed steel concrete section) for the superstructure, plastic mechanisms could not in reality develop at this location but the goal is neglecting the presence of the concrete deck to show how the girders could collapse if for one reason the superstructure were supposed to be ductile and develop plasticity due to seismic actions.

3.4.4.1 Status of yielding

After the distribution of the plastic hinges in the structure, and after each step of the pushover analysis loading, it was noticed that the first plastic hinges of type (B) are formed at the piers in step 10 (figure 3.35), and type B, IO and LS plastic hinges appear progressively on the piers up to step 15 (figure 3.36).

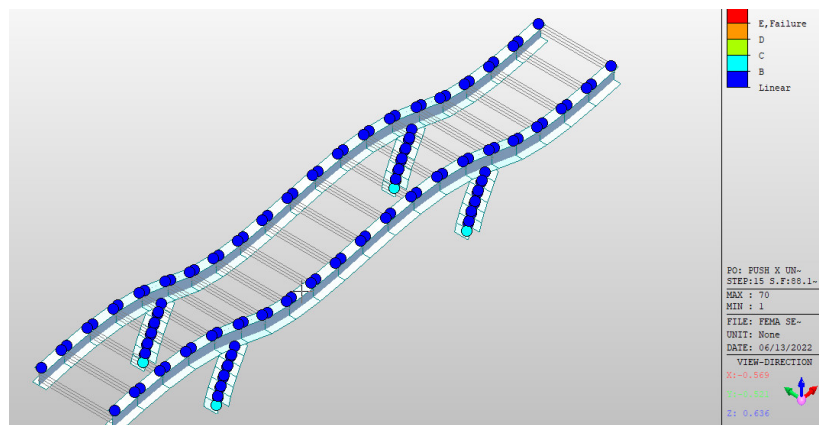


Figure 3.35. Plastic hinges at step 10

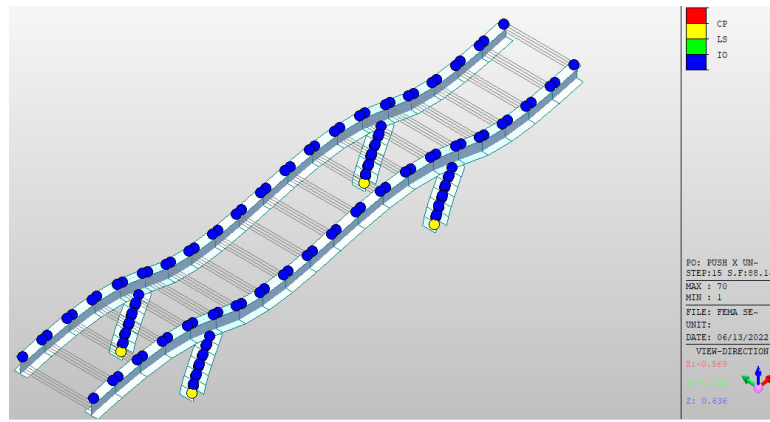


Figure 3.36. Plastic hinges at step 15

At step 16, ruin plastic hinges form at the bottom of the piers (figure 3.37), then loading progressively, it is observed the formation of the first plastic hinges of type B at the step 18 in the girders at the pier's top location that continue to progress till the step 29 (figure 3.38). After the step 29, the ruin plastic hinges started to form (figure 3.39).

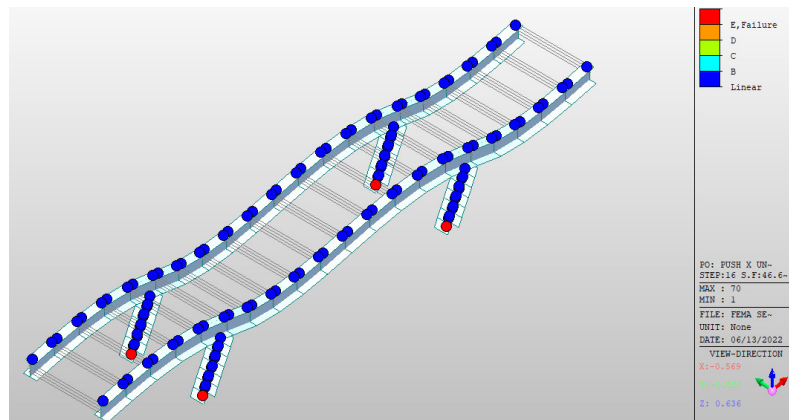


Figure 3.37. Plastic hinges at step 16

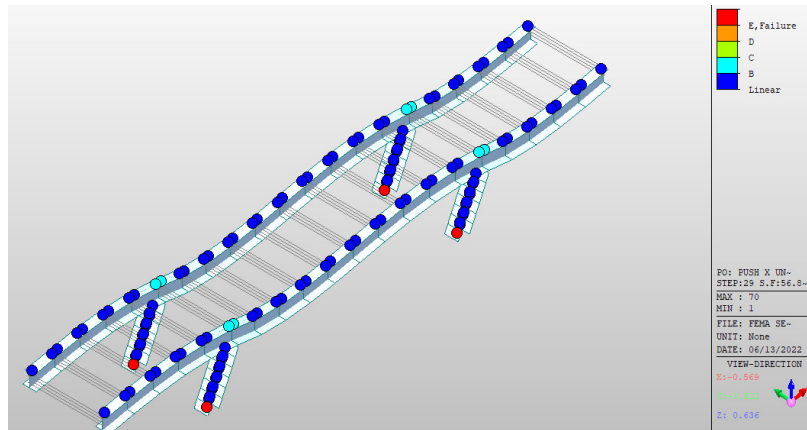


Figure 3.38. Plastic hinges at step 29

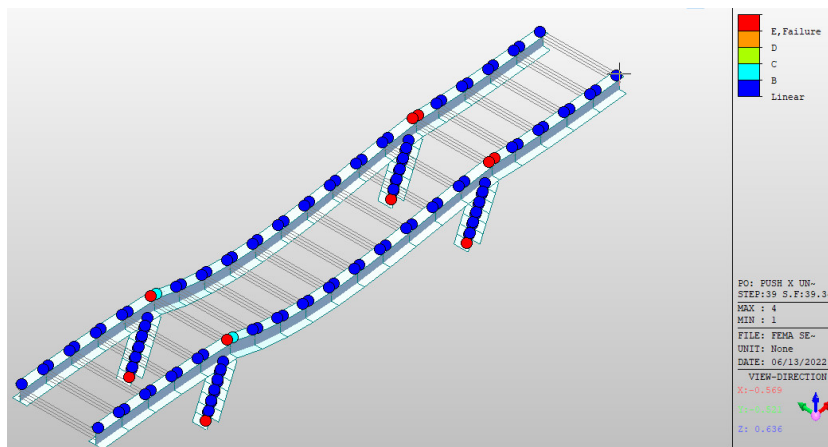


Figure 3.39. Plastic hinges at step 39

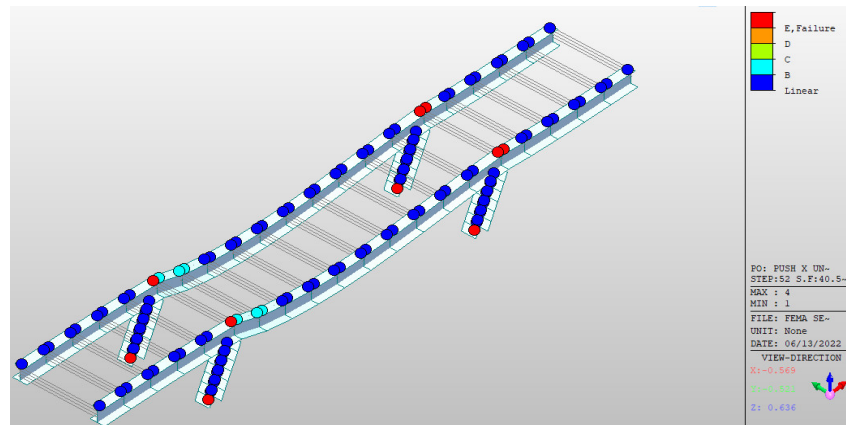


Figure 3.40. Final plastic hinge pattern

This observed distribution of plastic hinges formation indicates that the hinges characteristics used in this study define that girder are weaker than pier. After that, and at the ultimate displacement, the hinges increase in propagation in the girders.

When using the default plastic hinges, the structure collapsed after the failure of the girders, which indicates that the structure is designed according to the strong piers – weak girders principles. The girders collapsed before the piers, even though their strength was higher, due to the residual strength of the columns after the structure reached the capacity displacement.

3.4.4.2 Capacity curve

The following capacity curves (figure 3.41 and figure 3.42) in uniform loading and modal loading for the longitudinal direction was obtained:

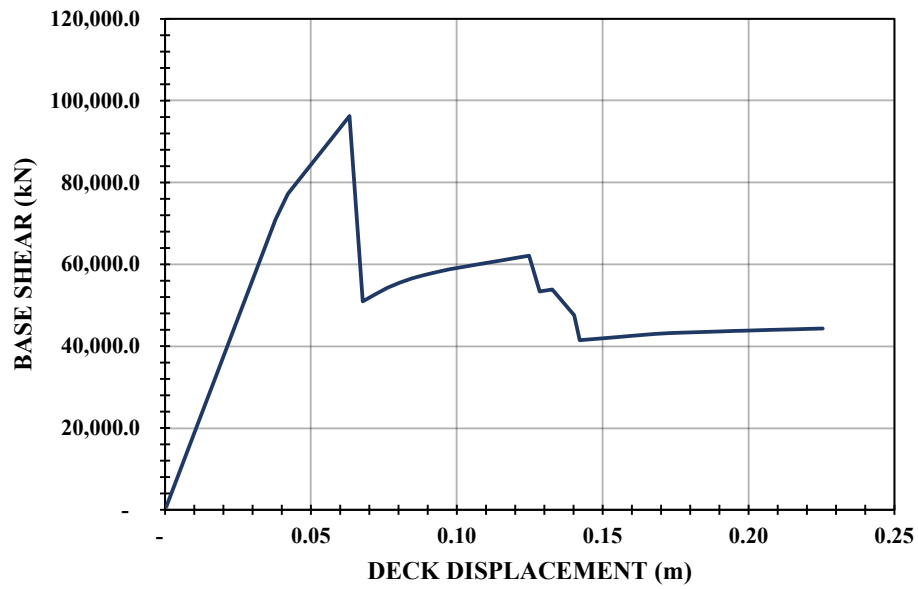


Figure 3.41. Capacity curve for the uniform loading

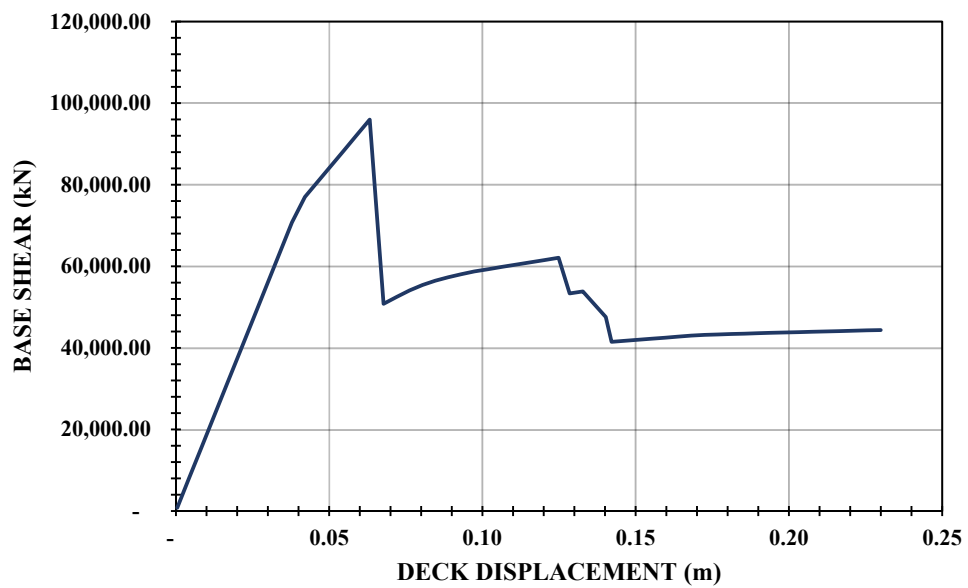


Figure 3.42. Capacity curve for the modal loading

It is possible to verify from the figures that the capacity curves in the considered direction are quite similar. Maximum displacement of equivalent SDOF system subjected to modal loading is 0.23 m and for the uniform loading, it is 0.225 m.

The capacity displacement is 0.063 m for the uniform and modal loading which is greater than the design seismic displacement for severe intensity (0.044 m) and less than for

the violent intensity (0.082 m). Also, this value is more or less similar to the one obtained when the superstructure was considered essentially elastic (0.06 m).

As for the maximum base shear force it is 95971.2 kN (step 15) for the modal loading and 96257.6 kN (step 15) for the uniform loading.

It is observed that after the capacity displacement, there is still some resistance coming from the girders and the residual stiffness of the piers but it will decrease with the increasing load until the collapse will be achieved.

It should be noticed that 53 steps were obtained that is to say 53 increments of loads in the modal loading and 52 steps in the uniform loading.

3.4.4.3 Performance point

The following capacity spectrum (figure 3.43 and figure 3.44) in the longitudinal direction considering modal and uniform loading was obtained:

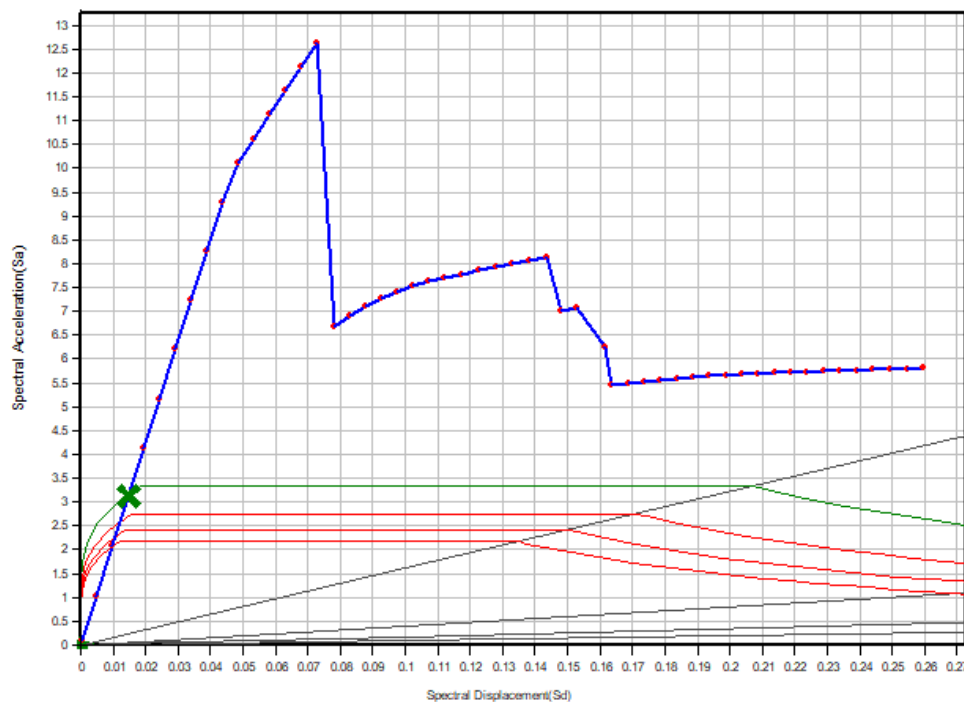


Figure 3.43. Performance point for the uniform loading

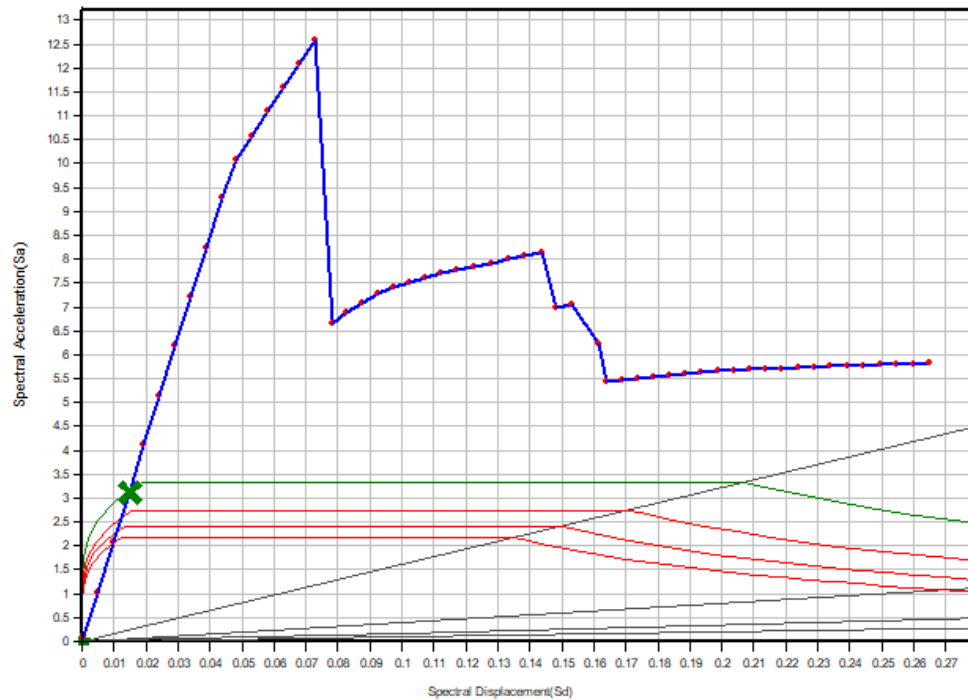


Figure 3.44. Performance point for the modal loading

According to these results, the equivalent viscous damping starts at 5% up to 20%, and for a PGA value of 1.39g, it was obtained:

- For the uniform loading in the longitudinal direction, the performance point is equal to 1.277 cm under a lateral force equal to 23950 kN is the target displacement of our structure which is at step 3, after step 3 the ultimate capacity of the structure has been exceeded, so the construction is on the verge to face a partial or total collapse.
- For the modal loading in the longitudinal direction, the performance point is equal to 1.282 cm under a lateral force equal to 23950 kN is the target displacement of our structure which is at step 2, after step 2 the ultimate capacity of the structure has been exceeded, so the construction is on the verge to face a partial or total collapse.

Conclusion

The key point of this chapter was to show the results of seismic analysis investigated on steel composite frame bridge. It started with presentation of details on the case study. After a static analysis was made to ensure bridge stability. Followed by the modal analysis, the main mode in the considered directions and information on the dynamic properties of bridges was obtained. Then, it was assessed a seismic analysis, where the response and performance of the

structure against a given seismic actions was studied. The results showed that the bridge strength against the seismic actions in the longitudinal direction were strong compared to the transverse direction, the longitudinal direction capacity provided additional location for energy dissipation (plastic hinges in the top) compared to the transverse direction capacity. Also, the subsequent analysis showed that for the earthquake in question the structure is almost entirely in the elastic branch at the performance point and that the dimensions of some elements, based on the seismic analysis, could be optimized in the detailed design stage. As for the application of load, which in this study was applied as a modal and uniform load pattern, it was verified that the results were quite similar. An analysis considering a ductile superstructure was performed and it was noticed that in the longitudinal direction, the bridge collapsed due to the failure of the girders, the piers was still having a residual stiffness to sustain actions after the capacity displacement was reached. The plastic hinges were formed in the top and bottom of the piers and when considering the superstructure, the plastic hinges were formed at the connection between the piers and girders, which illustrates the different critical regions of the bridge where a sensible design must be done to ensure the resistance of the bridge.

GENERAL CONCLUSION

From the previous analysis, it has been attempted to explore the concept of steel composite frame bridges with focus on seismic analysis to evaluate the response of the structure. In order to reach this goal, the work was divided in three main parts which are: for the first part, a presentation of an overview of the bridge structural typologies and the seismic aspects analysis techniques with a particular attention to pushover analysis; the second part was focused on the methodology used in this work and finally the results of our investigation were exposed. Following the above, this methodology has been implemented to achieve the principal objective. The static design of a three spans steel frame bridge was done manually on an excel sheet. Using MIDAS/civil, a static analysis was performed to obtain the solicitations. Verifications have been done with respect to recommendations in Eurocodes 1, 2, 3 and 4. After ensuring that the structure is stable, the seismic analysis was applied. MIDAS/civil was used in order to obtain the dynamic properties of the bridge which was useful for the seismic analysis.

Results of analysis revealed that the longitudinal direction provide additional location for energy dissipation (plastic hinges in the top) compared to the transverse direction. For the earthquake in question (violent, PGA of 1.39g) the structure is almost entirely in the elastic branch at the performance point and therefore the dimensions of some elements, based on the seismic analysis, could be optimized in the detailed design stage. When considering the superstructure ductile, it was noticed that in the longitudinal direction, the bridge collapsed due to the failure of the girders (step 39), the piers still having a residual stiffness to sustain actions after the capacity displacement was reached. The plastic hinges were formed in the top and bottom of the piers and when the superstructure was defined ductile, the plastic hinges were formed at the connection between the piers and girders, which illustrates the different critical regions of the bridge where a sensible design must be done to ensure the resistance of the bridge.

Concerning the frame scheme, it is possible to illustrate some aspects. The rigid substructure and superstructure connection is most appropriate for comparatively slender piers or short bridges. The moment-resisting capacity of the connection creates the potential for additional redundancy in the lateral force resisting path, particularly for longitudinal response rather than classical ones where the girders only resist the seismic action in the longitudinal direction. Considering the moment fixity at the pier's base, the plastic hinge at the top of the pier creates an additional location for energy dissipation during seismic attack, compared with

the bearing supported alternative. The rigid connection is insensitive to levels of seismic displacements, except insofar as larger displacements may affect the strength of the connection and the rotational capacity of the column-top plastic hinge and the steel piers provide more ductility than the reinforced concrete piers.

The subject dealt with is very vast and it was necessary to limit the field of research for this work. However, this work cannot be without imperfections due to the failure to carry out certain analyses and that should be taken into account in future developments such as:

- The comparison of the obtained results with those from a time-history analysis, where interaction with higher vibration modes is accurately captured;
- The modelling of the deck considering its nonlinear behaviour;
- The consideration of the soil-structure nonlinear behaviour to capture the effect of soil-structure interaction in the global response of the bridge;
- The variations of the geometry of the bridges (span's length and pier's height), to assess different response scenarios. More tests and investigations should be performed to extrapolate these conclusions to other type of bridges or other configurations including irregular geometries, other types of bearings, or critical soil-structure interaction;
- The local analysis and specific design of the critical regions.

BIBLIOGRAPHY

- Aboubakr, M. (2018). *Application de La méthode d'analyse statique non-linéaire (Pushover) sur un bâtiment R+3*. Université L'Arbi Ben M'hidi Oum El Bouaghi Faculté.
- Applied Technology Council. (1996). ATC 40 Seismic Evaluation and Retrofit of Concrete Buildings Redwood City California. In *Seismic safety commission* (Vol. 1, Issue November 1996).
- Applied Technology Council, A.-55. (2005). Improvement of Nonlinear Static Seismic Analysis Procedures. In *FEMA 440, Federal Emergency Management Agency, Washington DC* (Issue June).
- ATC-40. (1996). Seismic evaluation and retrofit of concrete buildings volume 1 ATC-40. In *ATC 40, Applied Technology Council* (Vol. 1).
- BRANKO E., G., RON, T., & ARUN A., S. (2012). *STEEL DESIGNERS' HANDBOOK*.
- BSCA Limited. (2010). *Steel Bridges A Practical Approach to Design for Efficient Fabrication and Construction* (BCSA Publi, Issue 51).
- Carr, A. J. (1994). Dynamic analysis of structures. *Bulletin of the New Zealand National Society for Earthquake Engineering*, 27(2), 129–146. <https://doi.org/10.5459/bnzsee.27.2.129-146>
- Conference, W., & Engineering, E. (2004). *13 th World Conference on Earthquake Engineering SEISMIC ZONATION CRITERIA IN ITALY: ANALYSIS ON METHODOLOGIES AND PARAMETERS*. 3322.
- Craig D., C., Richard W., N., & Christopher, R. (1996). *ATC-40 Seismic Evaluation and Retrofit of Concrete Buildings by APPLIED TECHNOLOGY COUNCIL (z-lib.org)*.
- Dai, P., Xu, P., Lu, J., Zhao, G., & Mao, D. (2019). Research on the characteristic of seismic damage and seismic design of reinforced concrete simply-supported girder bridge. *IOP Conference Series: Materials Science and Engineering*, 592(1). <https://doi.org/10.1088/1757-899X/592/1/012118>
- Davi, D. (2014). Seismic analysis and design of bridges according to EC8-2 : comparison of different analysis methods on a theoretical case-study. *Second European Conference on Earthquake Engineering and Seismology, Aug*, 1–10.
- Dong, P., Carr, A. J., & Moss, P. J. (2004). *Earthquake scaling for inelastic dynamic analysis of reinforced concrete ductile framed structures*. 16.
- EN 1991-1-4 (Vol. 1, Issue 2005). (2011).
- EN 1991-1-5. (2011). *Bases de calcul et actions sur les structures - Partie 2-5: Actions sur les*

structures - Actions thermiques.

EN 1991-2. (2003). *Eurocode 1 : Bases de calcul et actions sur les structures, Partie 3 : Charges sur les ponts dues au trafic.*

EN 1993-2 (Vol. 1, Issue 2005). (2011).

ENSTP. (2021). *Module XI : Seismic issues related to bridge capacity design.*

Eurocode 8. (2000). *Conception et dimensionnement des structures pour leur résistance aux séismes. Partie 2 : Ponts.*

F. Naeim and J. M. Kelly. (1999). Design of Seismic Isolated Structures: From Theory to Practice. In *Earthquake Spectra* (Vol. 16, Issue 3). <http://earthquakespectra.org/doi/abs/10.1193/1.1586135>

FEMA-450. (2003). *RECOMMENDED PROVISIONS FOR SEISMIC REGULATIONS FOR NEW BUILDINGS AND OTHER STRUCTURES (FEMA 450). Fema 450.*

Giuseppe, F., Aldo, G., & Marco, M. (2004). DEFINITION OF SUITABLE BILINEAR PUSHOVER CURVES IN NONLINEAR STATIC ANALYSES. *Analysis*, 3213.

Kolias, B., Denco, S. a, Ave, K., & Summary, I. (2008). Eurocode 8 - Part 2. In *Eurocode 8* (Issue see 6).

Li, H. (2020). The seismic design suggestions of girder bridge. *E3S Web of Conferences*, 165, 163–166. <https://doi.org/10.1051/e3sconf/202016504034>

MICHAEL N., F., Kolias, B., & ALAIN, P. (2012). Designers' Guide to Eurocode 8: Design of bridges for earthquake resistance. In *Designers' Guide to Eurocode 8: Design of bridges for earthquake resistance*. <https://doi.org/10.1680/dber.57357>

Monteiro, R., Ribeiro, R., Marques, M., Delgado, R., & Costa, A. (2008). Pushover Analysis of Rc Bridges Using Fiber Models or Plastic Hinges. *The 14th World Conference on Earthquake Engineering*.

Ray W., C., & Joseph, P. (2002). Dynamics of structures. In *Earthquake Engineering Handbook (Computers)*. <https://doi.org/10.1201/9781003095699-8>

Sarraf, R. El, R, D. I., & A, M. (2013). *Steel-concrete composite bridge design guide September 2013* (Issue September).

SETRA. (2010). *Steel – Concrete Composite Bridges – Sustainable Design Guide.*

Smith, D. A., Norman, J. B., & Dykman, P. T. (1986). *Historic Highway Bridges of Oregon.*

WEBOGRAPHY

Direct-info. (2021). *Route Batchenga – Ntui / Pont sur la Sanaga – Le temps des inaugurations*. [Consulted in February 2022]. <https://direct-info.net/2021/01/26/route-batchenga-ntui-pont-sur-la-sanaga-le-temps-des-inaugurations/>

Google maps. (2021). *Aerian view of the highway between Padova and Venezia*. [Consulted in February 2022].

<https://www.google.com/maps/place/35020+Autostrada+PD/@45.4459391,12.069544,261a,35y,80.38h,45t/data=!3m1!1e3!4m5!3m4!1s0x477ee75002841109:0x16782718cb6a0007!8m2!3d45.2828416!4d11.7973214>

Google maps. (2021). *Highway between Padova and Venezia*. [Consulted in February 2022].

<https://www.google.com/maps/@45.4459134,12.0728891,3a,60y,80.38h,90t/data=!3m6!1e1!3m4!1st89-cJVtDndGoYsitzDQng!2e0!7i16384!8i8192>

Midas Bridge. (2021). *Concepts of Plastic Hinging and Pushover Analysis with Midas Civil*. [Consulted in February 2022].

https://www.google.com/amp/s/www.midasbridge.com/en/blog/casestudy/concepts-of-plastic-hinging-and-pushover-analysis-with-midas-civil%3Fhs_amp=true

Midas manual. (2022). *Eigenvalue Analysis Control*. [Consulted in May 2022].

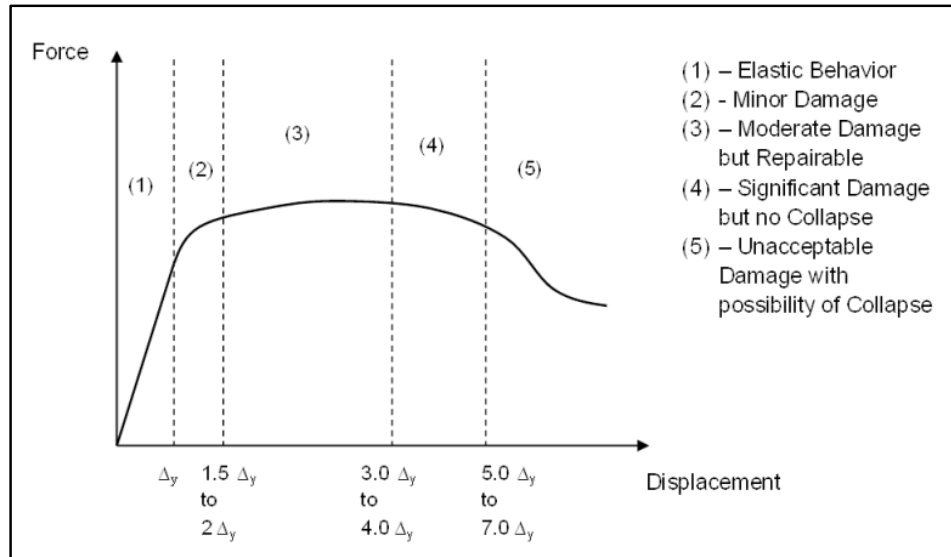
http://manual.midasuser.com/EN_Common/Civil/895/Start/06_Analysis/Eigenvalue_Analysis_Control.htm#:~:text=Eigenvalue%20analysis%20provides%20dynamic%20properties,frequencies

SteelConstruction.info. (2021). *Multi-girder composite bridges*. [Consulted in February 2022]. https://www.steelconstruction.info/Multi-girder_composite_bridges

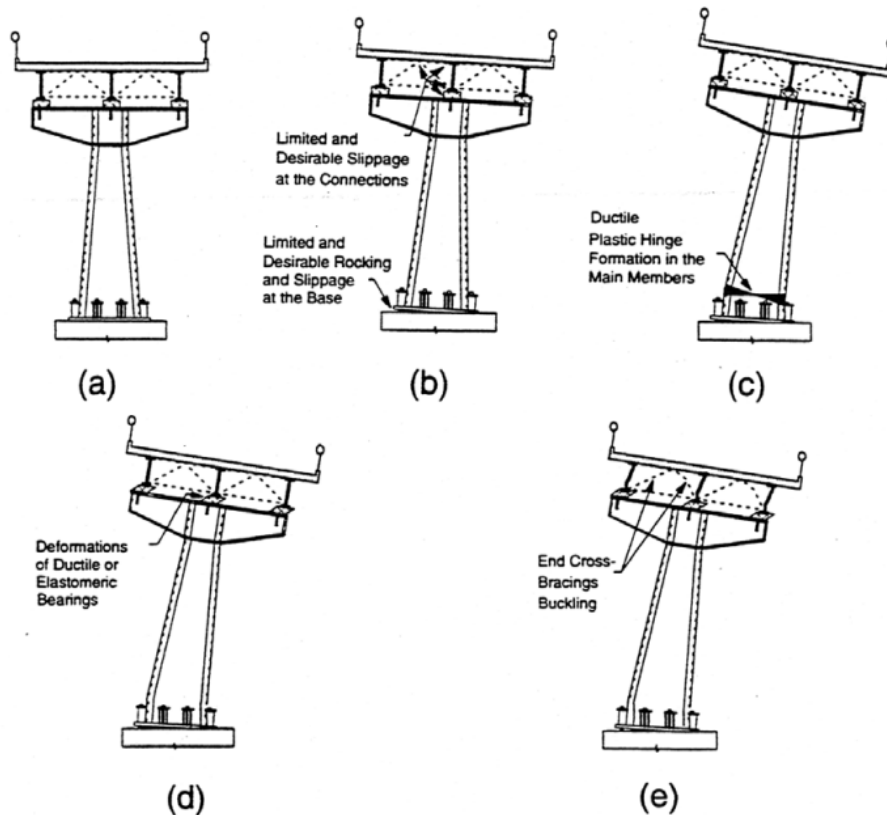
ANNEXES

ANNEX A: System deformation capacity of steel substructures (AASHTO GUIDE)

Annex A.1 Five regions of expected performance and damage for steel

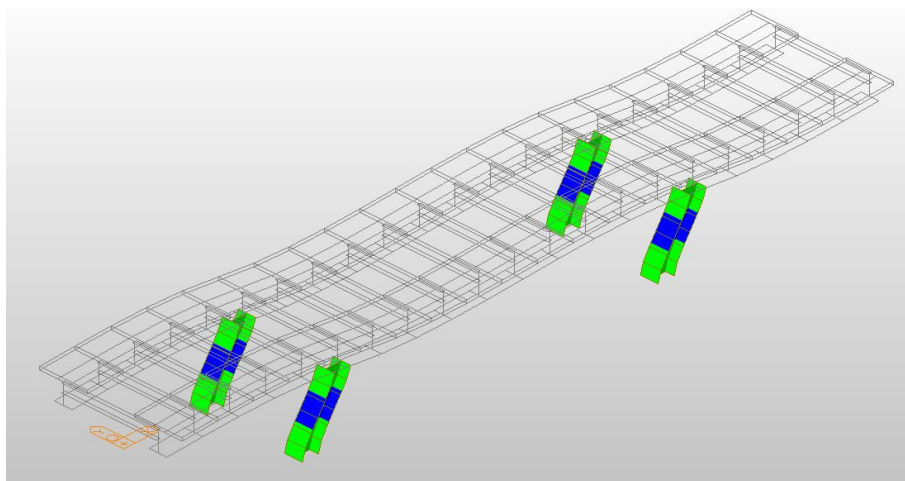
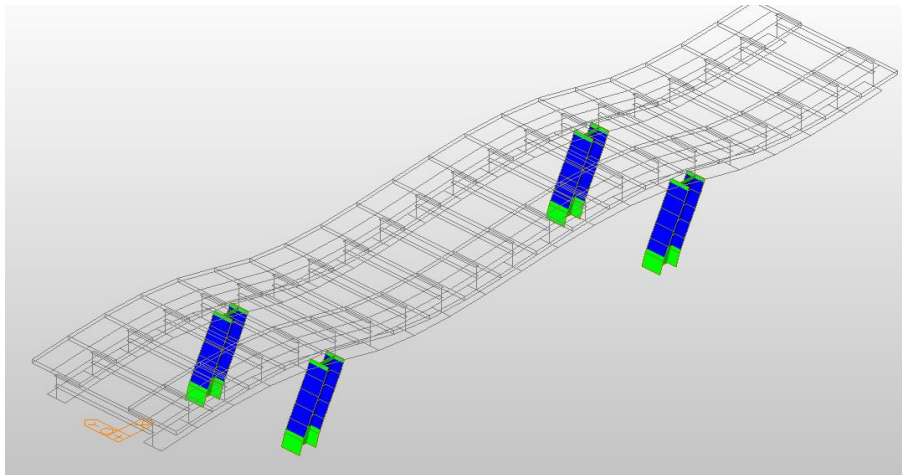
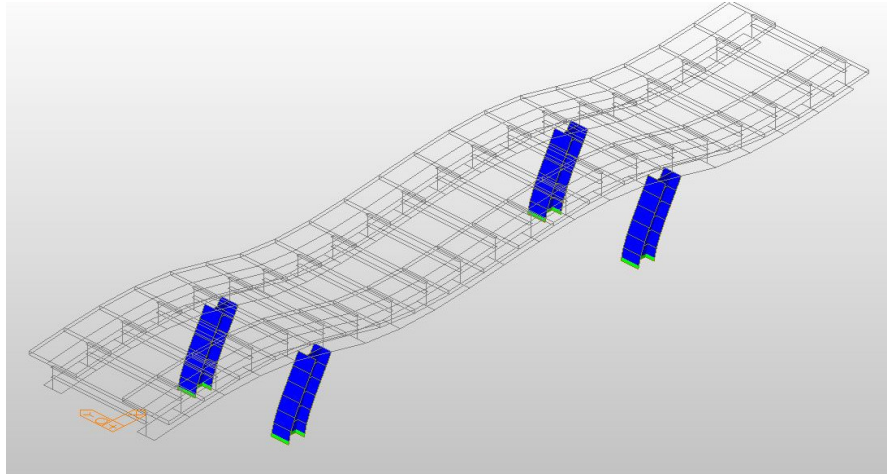


Annex A.2 Areas of potential inelastic deformations in steel substructure

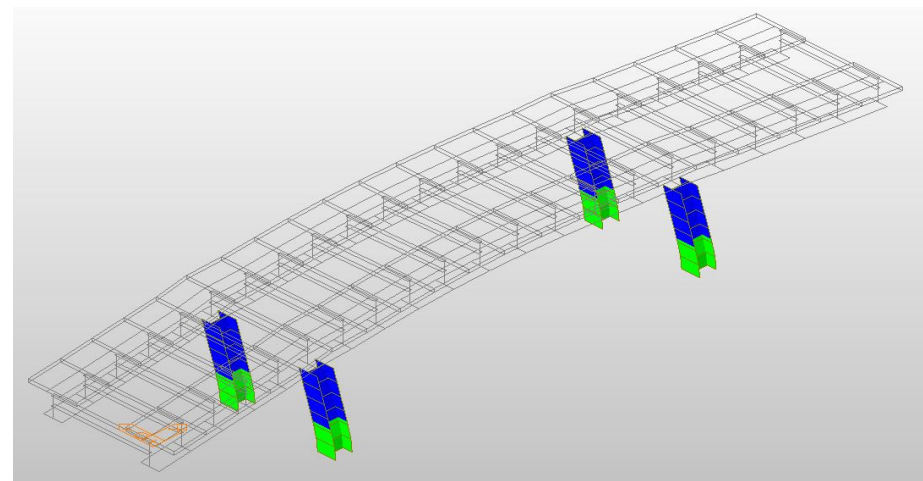
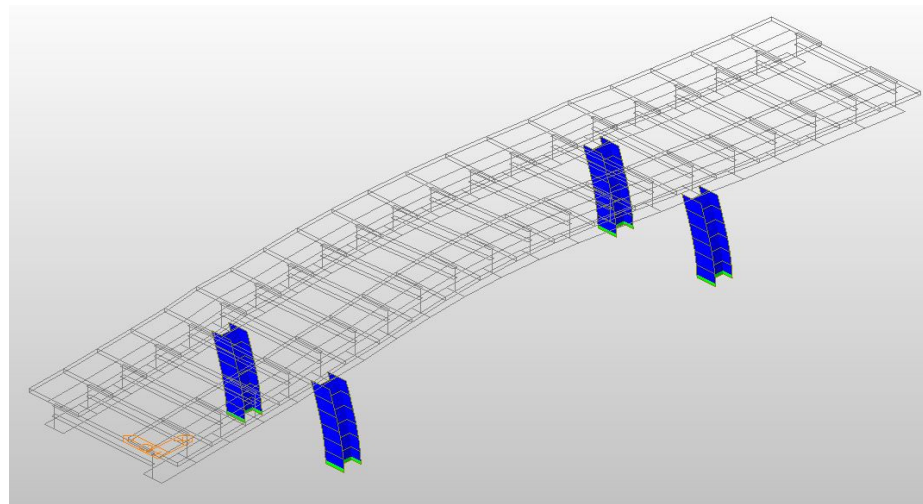
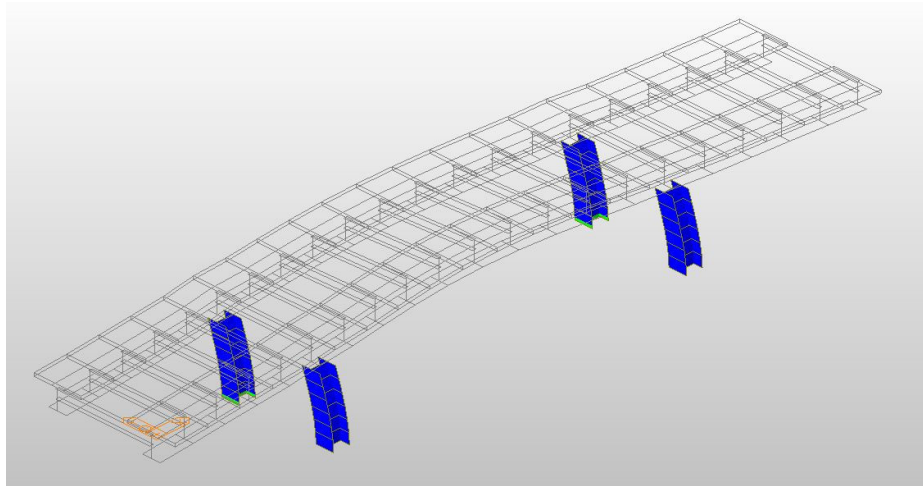


ANNEX B: Seismic response with bilinear hinge type

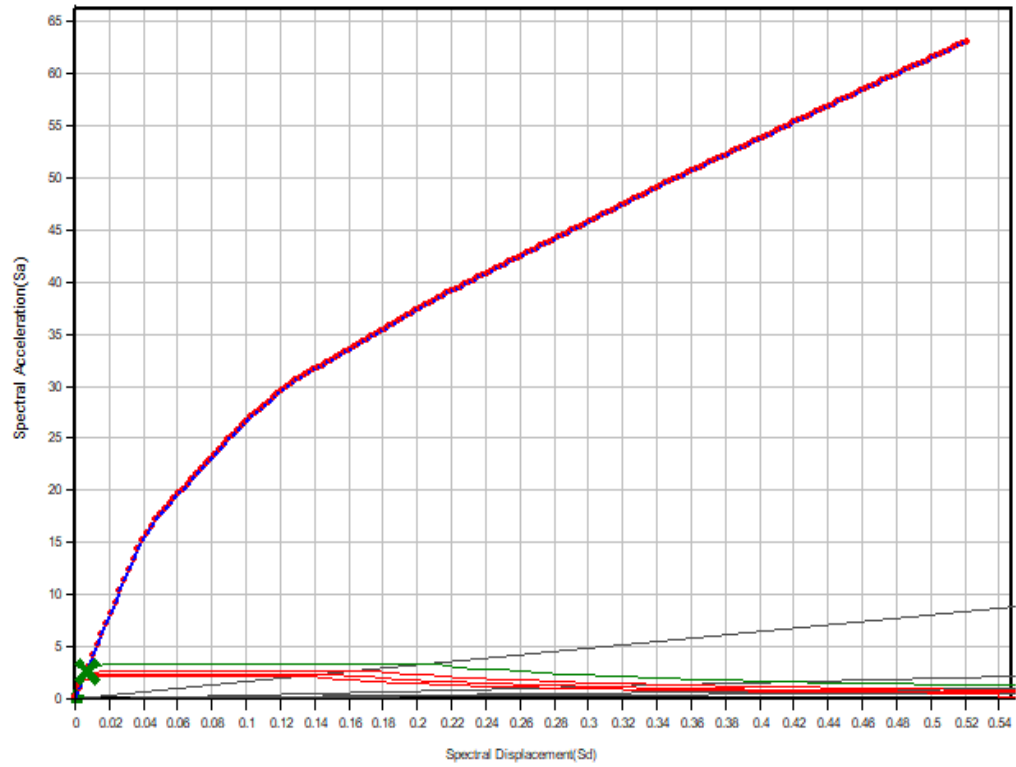
Annex B.1 Sequential plastic hinge formation in the longitudinal direction



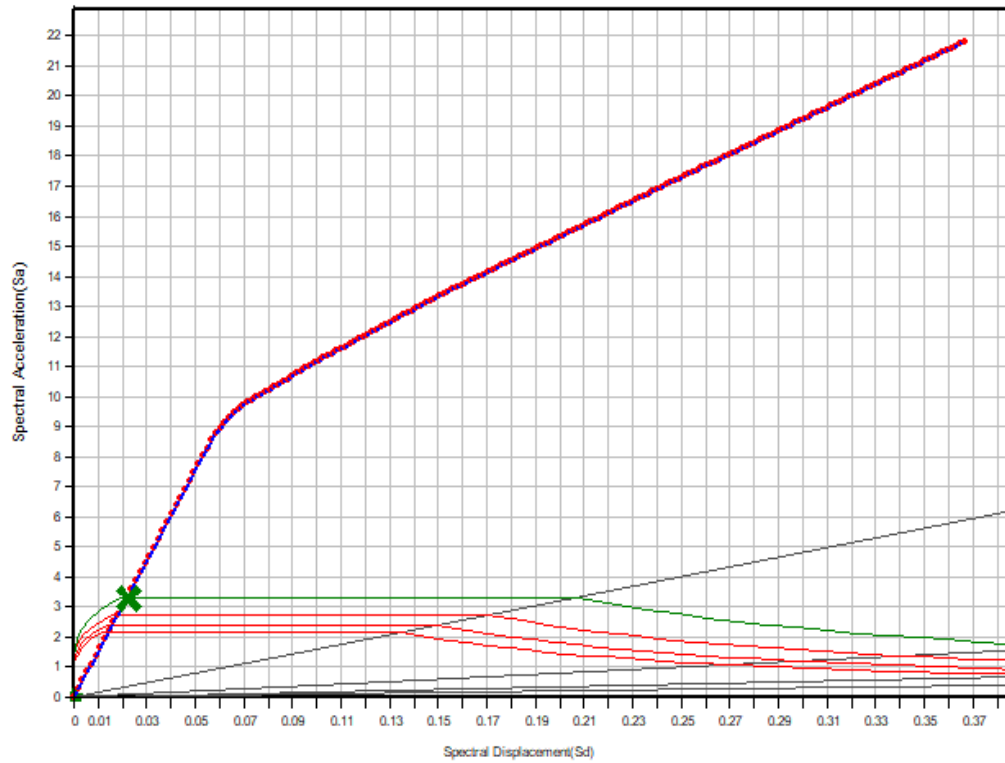
Annex B.2 Sequential plastic hinge formation in the transverse direction



Annex B.5 Performance point in the longitudinal direction

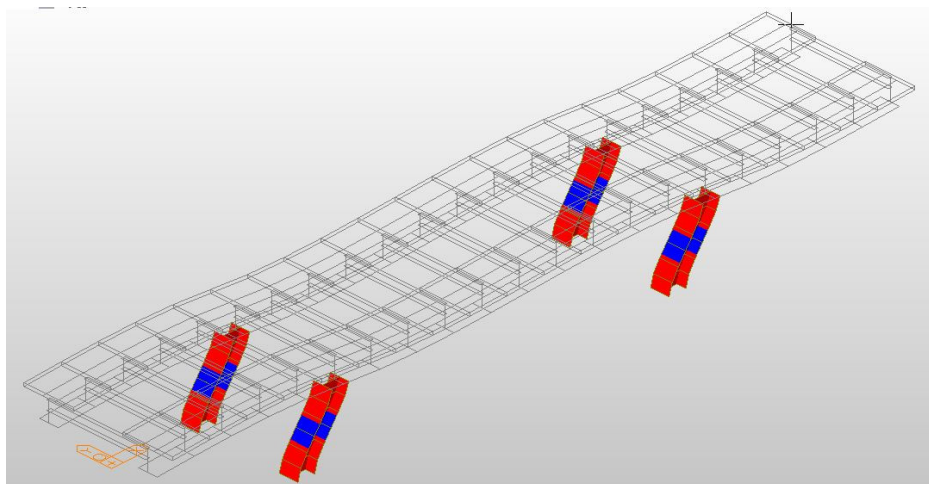
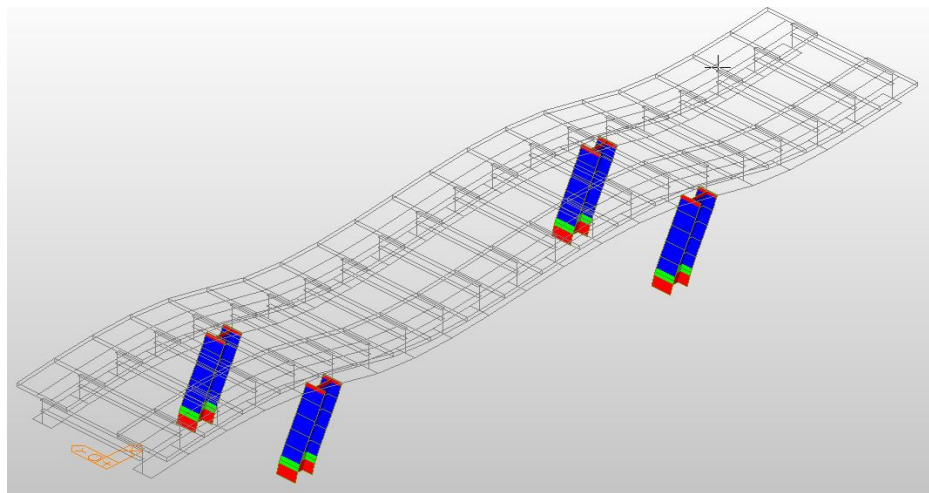
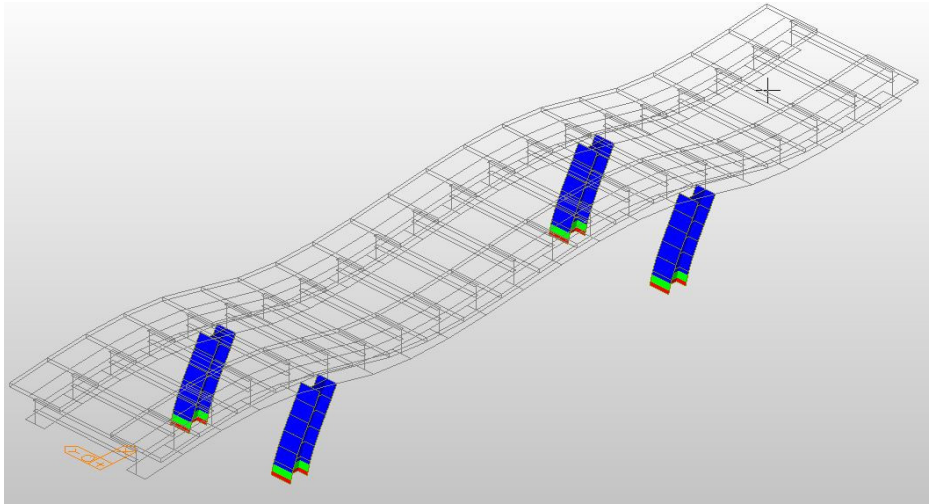


Annex B.6 Performance point in the transverse direction

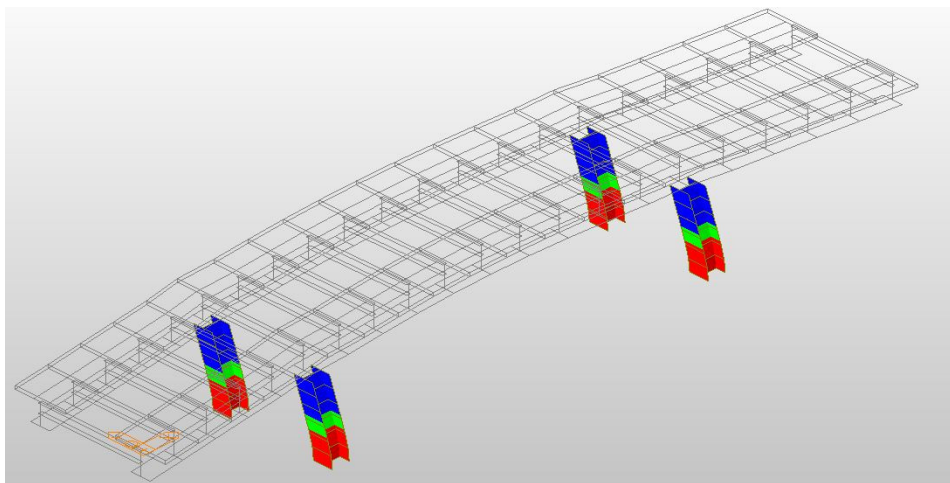
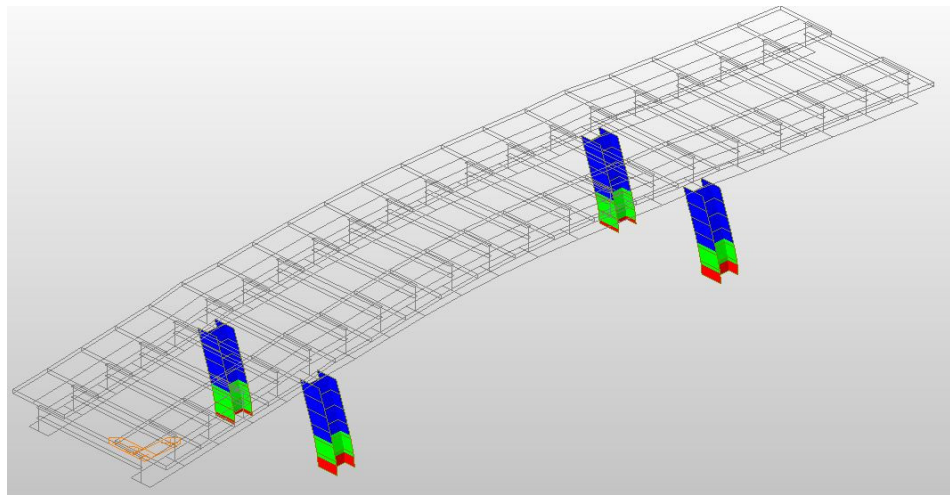
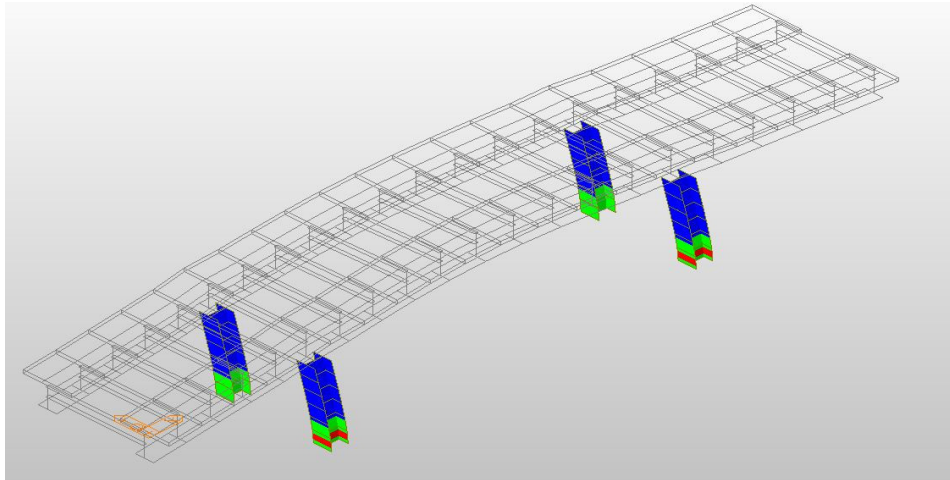


ANNEX C: Seismic response with trilinear hinge type

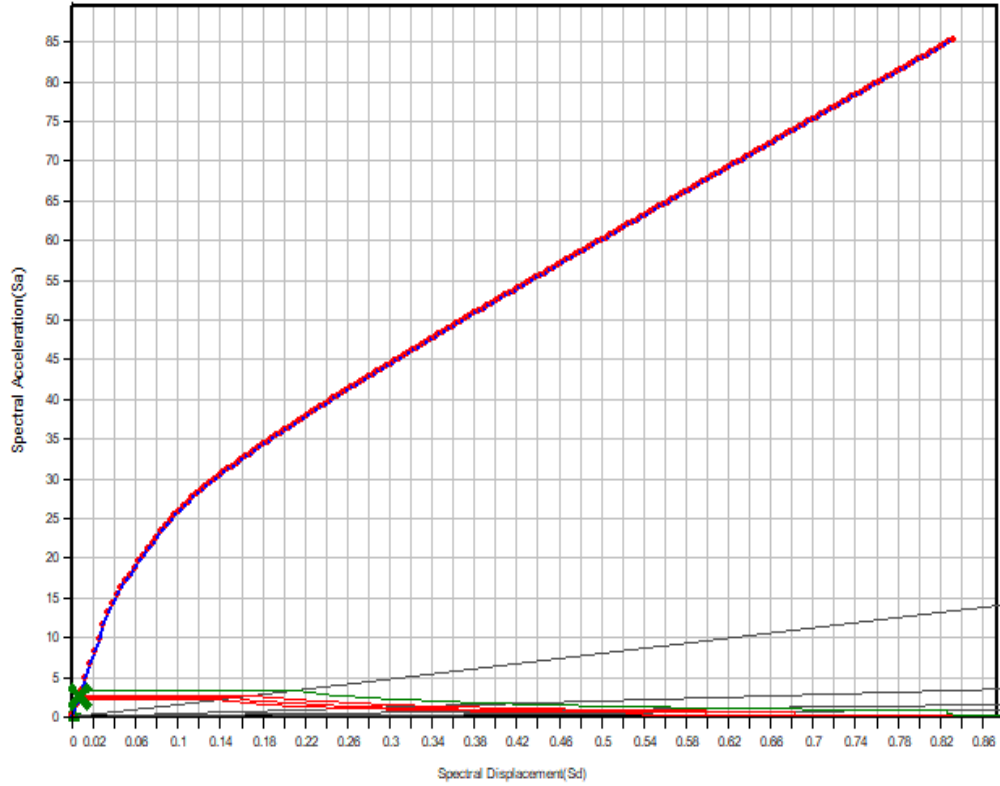
Annex C.1 Sequential plastic hinge formation in the longitudinal direction



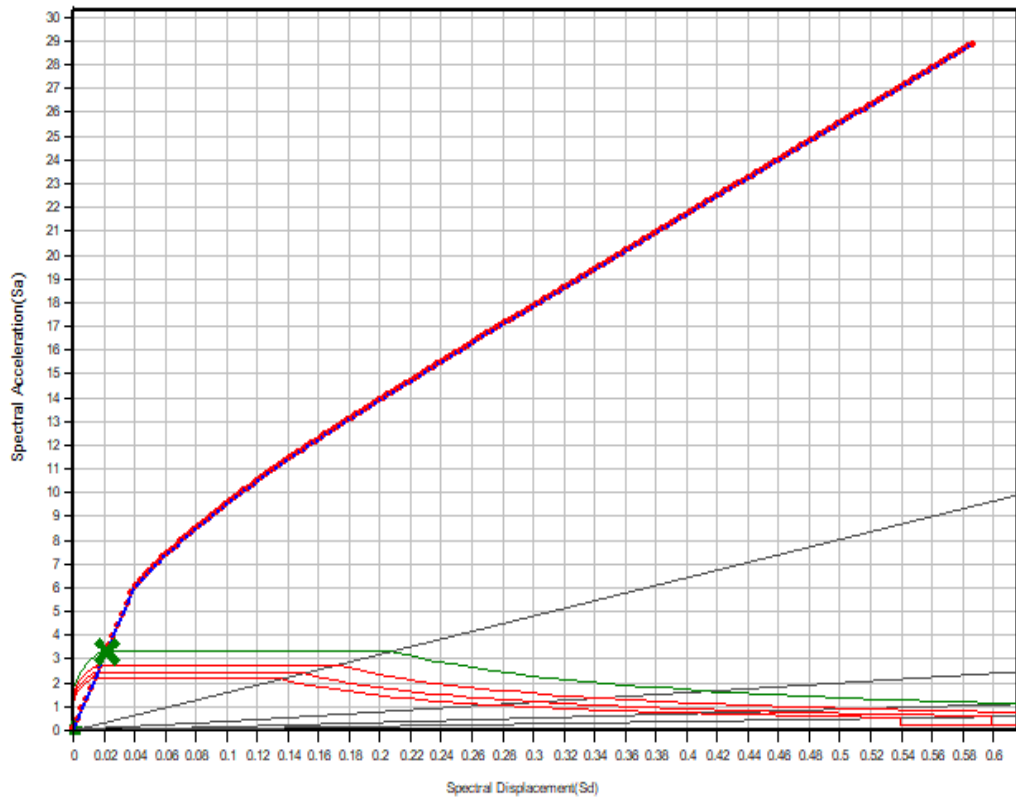
Annex C.2 Sequential plastic hinge formation in the longitudinal direction



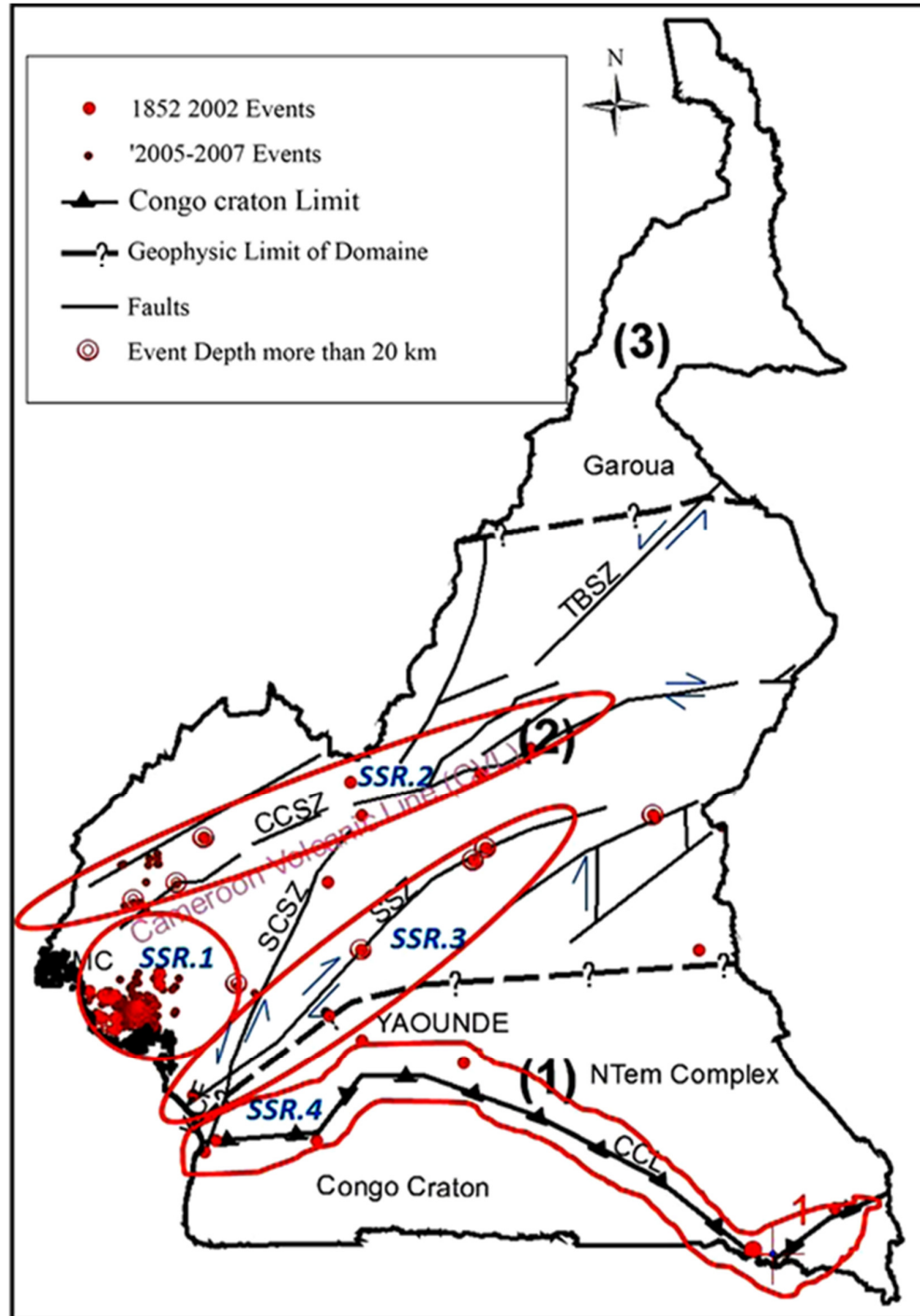
Annex C.5 Performance point in the longitudinal direction



Annex C.6 Performance point in the transverse direction



ANNEX D: Seismic source regions in Cameroon (Open Journal of Earthquake Research, 2014)



- Seismic Source Region I (SSR.1): It corresponds to the area of “Mount Cameroon” volcano, in South-West Cameroon. From data recorded by temporary seismic network, 93.4 % of events are located in this Region. Mostly events are shallow with depth inferior to 25 km. The “Mount Cameroon Source Region” is related to

the magmatic activity, probably related to small-scale mantle convection. The maximum magnitude recorded in the source region is 4.4 Mb; this suggests a weak seismicity.

- Seismic Source Region II (SSR.2): It is also located in the South West region, in the North of mount Cameroon. In contrary to the “Seismic Source Region I”, “Source Region II” is affected by southern segments faults of “Central Cameroon Shear Zone” (CCSZ). Shallow and very shallow events are found, but clusters have few events compared to Source Region I. The maximum magnitude recorded is 5.1 Mb; this might suggest a weak to moderate seismicity.
- Seismic Source Region III (SSR.3): Central Cameroon, along Fault called “Sanaga Shear Zone” (SSZ). Despite the seeming diffuseness in seismicity, the epicenters of some events appear to be aligned along the Sanaga Shear Zone. Events occurring on the Sanaga Shear Zone (Seismic Source Region III) have their focal depth at 33 km. The maximum magnitude recorded in this source region was 5.8 Mb. Although this might suggest a moderate seismicity.
- Seismic Source Region IV(SSR.4) follows the northern boundary of Congo Craton. One characteristic event has focal depth at 33 km and magnitude of 6 M. Although most events are shallow and have weak magnitude, this characteristic event shows that segment faults of this source region can generate large earthquakes.